

**Rod ejection simulation on VVER 1000/320 core
using PARCS/TRACE.**

by

Marek Ruscak

B.S., University of Hradec Kralove (2014)

Submitted to the Department of Nuclear Engineering
in partial fulfillment of the requirements for the degree of

Master in Nuclear Engineering

at the

POLYTECHNIC UNIVERSITY OF CATALONIA

July 2016

© Marek Ruscak, MMXVI. All rights reserved.

The author hereby grants to UPC permission to reproduce and to
distribute publicly paper and electronic copies of this thesis document
in whole or in part in any medium now known or hereafter created.

Author.....
Department of Nuclear Engineering
July 20, 2016

Certified by.....
Dr. Ing. Guido Mazzini
Senior Researcher at Research Centre Rez
Thesis Supervisor

Accepted by.....
Prof. Dr. Francesc Reventos
Supervisor, Department of Nuclear Engineering

Rod ejection simulation on VVER 1000/320 core using PARCS/TRACE.

by

Marek Ruscak

Submitted to the Department of Nuclear Engineering
on July 20, 2016, in partial fulfillment of the
requirements for the degree of
Master in Nuclear Engineering

Abstract

The rod ejection (RE) is a design basis accident in accordance with NUREG-0800 and usually studied using point kinetics. In this thesis a 3D kinetic model is prepared and coupled with a thermal hydraulic system code for simulating this accident scenario for general VVER 1000 technology. This topic has been defined by the Research Centre Rez of the Czech Republic as a part of a larger project concerning beyond design basis accident focused on the Station Black Out (SBO) and a Loss of Ultimate Heat Sink (LOUHS). Because of this, the simulation conditions will be considered under SBO scenario.

Initially the state of the art is discussed, followed by the general information on the major documentation needed for the analysis (10-CFR, NUREG-0800). This thesis shows the complete coupling methodology from a cross section generation to transient coupled calculation.

Thesis Supervisor: Dr. Ing. Guido Mazzini

Title: Senior Researcher at Research Centre Rez

Acknowledgments

I would like to express my gratitude to my supervisors Prof. Francesc Reventos of the Polytechnic University of Catalonia and Dr. Ing. Guido Mazzini of the Research Centre Rez for all the help provided and for monitoring the progression of my work.

I wish to thank Ing. Miroslav Hrehor for allowing me to perform my internship at the Research Centre Rez and do my master thesis. Also I wish to thank Ing. Milos Kyncl for providing and assisting with the TRACE model and to Ing. Bruno Miglierini and Ing. Vit Kopecek for technical help.

I would like to also thank the U.S. NRC for helping me with several technical issues with the coupling procedure.

Last but not least I would like to thank my dear wife Nikola and my family for providing me strength to finish my thesis.

Contents

1	Introduction	16
2	State of the Art	19
2.1	The Code of Federal Regulations - Energy	19
2.2	NUREG-0800	21
2.2.1	Areas of review	22
2.2.2	Acceptance criteria	23
2.2.3	Review procedures	23
2.2.4	Evaluation findings	23
2.2.5	Implementation	24
3	VVER 1000 Description	25
3.1	General Introduction	25
3.2	Primary Circuit	26
3.3	Core	27
3.4	Fuel Assembly	28
3.5	Control rods	29
3.6	Technical Parameters	31

4	Computational Codes	34
4.1	SCALE	34
4.2	SERPENT 2	35
4.3	PARCS	36
4.3.1	Flux calculation method in the hexagonal geometry	38
4.4	TRACE	40
4.4.1	Code Characteristics	42
5	Model Description	44
5.1	SCALE	44
5.2	SERPENT 2	46
5.3	PARCS	53
5.3.1	Control card, CNTL	53
5.3.2	Parameter card, PARAM	54
5.3.3	Cross-sections, XSEC	54
5.3.4	Geometry, GEOMHEX	54
5.3.5	Thermal-hydraulics, TH	57
5.3.6	Transient definitions, TRAN	57
5.4	TRACE	57
6	Coupling procedure	61
6.1	MATLAB Mapping Script	61
7	Event description	64
7.1	Accident causes	64
7.1.1	General sequence of events during RE	65
7.2	Effects of the accident	66

7.2.1	Acceptance criteria	66
8	Results	68
8.1	Calculation Process	68
8.2	SCALE	70
8.3	SERPENT 2	75
8.4	Reference data	78
8.5	Steady state, stand alone, SCALE	79
8.6	Steady state, stand alone, SERPENT	83
8.7	Steady state, coupled	87
8.8	Transient, PARCS/TRACE coupled	89
8.8.1	Sequence description	89
8.8.2	Rod Ejection without SCRAM, SCALE	92
8.8.3	Rod Ejection with SCRAM, SCALE	109
8.8.4	Rod Ejection without SCRAM, SERPENT 2	127
8.8.5	Rod Ejection with SCRAM, SERPENT 2	142
9	Conclusions	160
A	Glossary	165

List of Figures

3-1	VVER 1000 primary circuit [7].	26
3-2	VVER 1000 steam generator [16].	27
3-3	VVER 1000 core layout.	27
3-4	Diagram of VVER 1000 fuel assembly [5].	28
3-5	Drawing of Russian type fuel for VVER 1000 generated by SCALE.	29
4-1	PARCS code logic	37
4-2	Fluxes in a triangle	38
4-3	Fluxes in a full hexagon	39
4-4	Phases of a TRACE calculation	41
5-1	Inputs of F130/F200 (left) and inputs of FF36G9/FF40G9 (right)	45
5-2	Input of F30G9 (left) and input of F40G6 (right)	45
5-3	Axial input of A130 in SERPENT 2	47
5-4	Radial input of A130 in SERPENT 2	47
5-5	Axial input of A200 in SERPENT 2	48
5-6	Radial input of A200 in SERPENT 2	48
5-7	Axial input of A30E9 in SERPENT 2	49
5-8	Radial input of A30E9 in SERPENT 2	49

5-9	Axial input of A40E6 in SERPENT 2	50
5-10	Radial input of A40E6 in SERPENT 2	50
5-11	Axial input of P36E9 in SERPENT 2	51
5-12	Radial input of P36E9 in SERPENT 2	51
5-13	Axial input of P40E9 in SERPENT 2	52
5-14	Radial input of P40E9 in SERPENT 2	52
5-15	Core layout	55
5-16	Bank layout	56
5-17	TRACE RPV model nodalization	59
8-1	Calculation Process	69
8-2	Calculation Process	70
8-3	Thermal flux plot of FA F130 from SCALE	72
8-4	Thermal flux plot of FA F200 from SCALE	72
8-5	Thermal flux plot of FA F30G9 from SCALE	73
8-6	Thermal flux plot of FA F40G6 from SCALE	73
8-7	Thermal flux plot of FA FF36G9 from SCALE	74
8-8	Thermal flux plot of FA FF40G9 from SCALE	74
8-9	Thermal flux plot of FA F130 from SERPENT	75
8-10	Thermal flux plot of FA F200 from SERPENT	76
8-11	Thermal flux plot of FA F30G9 from SERPENT	76
8-12	Thermal flux plot of FA F40G6 from SERPENT	76
8-13	Thermal flux plot of FA FF36G9 from SERPENT	77
8-14	Thermal flux plot of FA FF40G9 from SERPENT	77
8-15	Thermal flux plot of the core from SERPENT	77
8-16	Reference state bank configuration. Blue (1-6) Red (7-10)	78

8-17	Normalized radial power profile for SA PARCS	79
8-18	Normalized axial power profile for SA PARCS	80
8-19	Radial flux profile for SA PARCS, fast group	81
8-20	Radial flux profile for SA PARCS, thermal group	81
8-21	Axial flux profile	82
8-22	Flux profile central cross section	82
8-23	Normalized radial power profile for SA PARCS	84
8-24	Normalized axial power profile for SA PARCS	84
8-25	Radial flux profile for SA PARCS, fast group	85
8-26	Radial flux profile for SA PARCS, thermal group	85
8-27	Axial flux profile	86
8-28	Flux profile central cross section	86
8-29	Steady State, Coupled pressure	88
8-30	Ejected bank position	90
8-31	Core power	95
8-32	Normalized power at ejection point	95
8-33	Maximum energy deposited in fuel pin	97
8-34	Averaged fast flux	97
8-35	Averaged fast flux after 100 s	98
8-36	Averaged thermal flux	98
8-37	Averaged thermal flux after 100 s	99
8-38	Axial flux profile	99
8-39	Axial flux profile after 100 s	100
8-40	Flux profile central cross section	100
8-41	Flux profile central cross section after 100 s	101
8-42	Flux profile cross section at ejection point	101

8-43 Flux profile cross section at ejection point after 100 s	102
8-44 Averaged radial normalized power profile	102
8-45 Averaged radial normalized power profile after 100 s	103
8-46 Axial normalized power	103
8-47 Axial normalized power after 100 s	104
8-48 Reactivity	104
8-49 Coolant temperature at ejection point	105
8-50 Fuel temperature at ejection point	105
8-51 Maximal hot rod temperature	106
8-52 Averaged liquid density	106
8-53 Coolant density at ejection point	107
8-54 Averaged liquid temperature	107
8-55 Mass flow through the break	108
8-56 System Pressure	108
8-57 Core power	111
8-58 Normalized power at ejection point	111
8-59 Maximum energy deposited in fuel pin	112
8-60 Averaged fast flux	112
8-61 Averaged fast flux after SCRAM	113
8-62 Averaged fast flux after SCRAM after 100 s	113
8-63 Averaged thermal flux	114
8-64 Averaged thermal flux after SCRAM	114
8-65 Averaged thermal flux after SCRAM after 100 s	114
8-66 Axial flux profile	115
8-67 Axial flux profile after SCRAM	115
8-68 Axial flux profile after SCRAM after 100 s	116

8-69 Flux profile central cross section	116
8-70 Flux profile central cross section after SCRAM	117
8-71 Flux profile central cross section after SCRAM after 100 s	117
8-72 Flux profile cross section at ejection point	118
8-73 Flux profile cross section at ejection point after SCRAM	118
8-74 Flux profile cross section at ejection point after SCRAM after 100 s	119
8-75 Averaged radial normalized power profile	119
8-76 Averaged radial normalized power profile after SCRAM	120
8-77 Axial normalized power	120
8-78 Axial normalized power after SCRAM	121
8-79 Axial normalized power after SCRAM after 100 s	121
8-80 Reactivity	122
8-81 Coolant temperature at ejection point	122
8-82 Fuel temperature at ejection point	123
8-83 Maximal hot rod temperature	123
8-84 Averaged liquid density	124
8-85 Coolant density at ejection point	124
8-86 Averaged liquid temperature	125
8-87 Mass flow through the break	125
8-88 System Pressure	126
8-89 Core power	129
8-90 Normalized power at ejection point	129
8-91 Maximum energy deposited in fuel pin	130
8-92 Averaged fast flux	130
8-93 Averaged fast flux after 100 s	131
8-94 Averaged thermal flux	131

8-95	Averaged thermal flux after 100 s	131
8-96	Axial flux profile	132
8-97	Axial flux profile after 100 s	132
8-98	Flux profile central cross section	133
8-99	Flux profile central cross section after 100 s	133
8-100	Flux profile cross section at ejection point	134
8-101	Flux profile cross section at ejection point after 100 s	134
8-102	Averaged radial normalized power profile	135
8-103	Averaged radial normalized power profile after 100 s	135
8-104	Axial normalized power	136
8-105	Axial normalized power after 100 s	136
8-106	Reactivity	137
8-107	Coolant temperature at ejection point	137
8-108	Fuel temperature at ejection point	138
8-109	Maximal hot rod temperature	138
8-110	Averaged liquid density	139
8-111	Coolant density at ejection point	139
8-112	Averaged liquid temperature	140
8-113	Mass flow through the break	140
8-114	System Pressure	141
8-115	Core power	144
8-116	Normalized power at ejection point	144
8-117	Maximum energy deposited in fuel pin	145
8-118	Averaged fast flux	145
8-119	Averaged fast flux after SCRAM	146
8-120	Averaged fast flux after SCRAM after 100 s	146

8-121	Averaged thermal flux	147
8-122	Averaged thermal flux after SCRAM	147
8-123	Averaged thermal flux after SCRAM after 100 s	147
8-124	Axial flux profile	148
8-125	Axial flux profile after SCRAM	148
8-126	Axial flux profile after SCRAM after 100 s	149
8-127	Flux profile central cross section	149
8-128	Flux profile central cross section after SCRAM	150
8-129	Flux profile central cross section after SCRAM after 100 s	150
8-130	Flux profile cross section at ejection point	151
8-131	Flux profile cross section at ejection point after SCRAM	151
8-132	Flux profile cross section at ejection point after SCRAM after 100 s	152
8-133	Averaged radial normalized power profile	152
8-134	Averaged radial normalized power profile after SCRAM	153
8-135	Axial normalized power	153
8-136	Axial normalized power after SCRAM	154
8-137	Axial normalized power after SCRAM after 100 s	154
8-138	Reactivity	155
8-139	Coolant temperature at ejection point	155
8-140	Fuel temperature at ejection point	156
8-141	Maximal hot rod temperature	156
8-142	Averaged liquid density	157
8-143	Coolant density at ejection point	157
8-144	Averaged liquid temperature	158
8-145	Mass flow through the break	158
8-146	System Pressure	159

List of Tables

3.1	VVER 1000 technical specifications 1/2	32
3.2	VVER 1000 technical specifications 2/2	33
5.1	Fuel enrichment description	46
5.2	SCALE Branch structure	46
5.3	Colour description for core layout	55
5.4	Bank layout group description	56
5.5	TRACE axial distribution	59
8.1	SCALE Steady State coupled results	87
8.2	SERPENT Steady State coupled results	88
8.3	Chronological sequence of the events	94
8.4	Chronological sequence of the events	110
8.5	Chronological sequence of the events	128
8.6	Chronological sequence of the events	143

Nomenclature

ADF	Assembly Discontinuity Factors
ATWS	Anticipated Transient Without SCRAM
BDBA	Beyond Design Basis Accident
BWR	Boiling Water Reactor
C	Coupled
CAMP	Code Application Maintenance Program
CFR	Code of Federal Regulations
CR	Control Rod
CVR	Research Centre Rez
DBA	Design Basis Accident
Dm	Moderator Density
ECCS	Emergency Core Cooling System
FA	Fuel Assembly
HZP	Hot Zero Power
LOCA	Loss Of Coolant Accident
NPP	Nuclear Power Plant
PWR	Pressurized Water Reactor
RE	Rod Ejection
RIA	Reactivity Initiated Accident
RPV	Reactor Pressure Vessel
SA	Stand Alone
SCRAM	Safety Control Rod Axe Man
SR	SCRAM Rod
SS	Steady State
SUJB	State office for nuclear safety (SONS)
Tf	Fuel Temperature
Tm	Moderator Temperature
Tr	Transient
VVER	Water-Water Energetic Reactor

Chapter 1

Introduction

The technology progress allows the industry to push the accuracy of calculations to the new level. Alongside with the progress, there is an approach to simplicity. The current trend is to couple already existing codes to enable simultaneous complex scenarios and sub-sequential analysis. The thermo-hydraulic system code TRACE is the next generation code being a successor to RELAP, both of which however have the capability of coupling with the neutronics code PARCS. Many countries, the Czech Republic included, have applied the procedures into their own legislation based on the US Code of Federal Regulations (CFR) 10 - Energy. A part of the licensing process is a duty of the licensee to submit analyses proving safety of the designed systems. The guide containing the requirements is called the standard review plan (SRP) or NUREG-800. The description of this document is explained further below. Chapter 15 of the NUREG-0800 contains not only the guideline on how to perform a safety analysis, but also which analyses need to be done. This work focuses on the chapter 15.4.8, spectrum of rod ejection accidents for pressurized water reactors (PWR). The rod ejection accident is classified a Reactivity Initiated Accident (RIA),

however the goal is not to perform complete safety analysis, but only the thermo-hydraulic and neutronic part. Therefore the material analysis is not included within this thesis.

After the Fukushima accident, the regulatory bodies of many countries having nuclear power reactors were required to perform stress tests in order to evaluate robustness of existing NPPs against extreme external hazards, such as extreme seismic events, climatic conditions and behaviour of the plant in conditions of loss of UHS, SBO and severe accidents. As a part of this effort, several Design Based Analysis (DBA) are combined with a long term Station Blackout (SBO). As a follow up of the stress tests in the Czech Republic there was a research project financed by the Ministry of Interior (MoI) called "Fukushima project" (Prevention, preparedness and mitigation of severe accidents of Czech nuclear power plants in connection with new findings of the stress tests after the Fukushima accident - VG20132015105) an objective of which was to analyse in addition to stress tests additional accident scenarios, in particular combinations of SBO with failures of other technological systems, such as LOCA accidents or loss of SG feed water system.

In parallel of this effort a rod ejection analysis under SBO conditions (ECCS disabled) was performed, although it was clear that such event would not differentiate by its character too much from the small break loss of coolant accident scenario under SBO, as the rod ejection transient lasts only a few seconds.

The PARCS/TRACE coupling for full VVER 1000 reactor has never been done before in the Czech Republic with the cross sections generated by either SERPENT 2 or SCALE/TRITON. Therefore a methodology had to be developed, which proved to be a challenge on its own regarding the lack of documentation for coupling models with hexagonal geometries. Because this is the first time the neutronic and TH models using PARCS and TRACE are coupled for VVER 1000 in the Czech Republic,

the results are still rough and more sensitivity studies have to be done in order to prepare these models for validation. Most of the geometrical, material and structural data are taken from a reference VVER 1000. The TRACE model, which was only adjusted by the author and created and owned by the Research Centre Rez as well as the SERPENT 2 model. These models contain privileged information and therefore are not a part of this thesis. The author created the SCALE and PARCS models as well as the coupling methodology.

It is important to note, that results in this thesis are not final and much longer process of model developing will be required in order to submit the coupled model for validation. Main objective of this thesis is to demonstrate in a practical example of three-dimensional accident scenario of VVER 1000 reactor an acquisition of PARCS code for 3D reactor kinetics and its coupling with system thermo-hydraulic code TRACE.

This work contains the state of the art status, code descriptions, model and sequence description. The second part presents the results and comments on the success of the analyses.

Chapter 2

State of the Art

2.1 The Code of Federal Regulations - Energy

The Code of Federal Regulations is the codification of the general and permanent rules published in the Federal Register of the USA. The Energy title is composed of four volumes (1-50, 51-199, 200-499, 500-end). Parts 1-199 are concerning the Nuclear Regulatory Commission and the rest are managed by the Department of Energy and Department of Defence.

A particularly interesting part to the licensing processes is part 50 – Domestic licensing of production and utilization facilities and part 52 - Early site permits; standard design certifications; and combined licenses for nuclear power plants. Since the beginning of the commercial nuclear power usage under the Atomic Act of 1954, the so called Two-Step process was implemented which involves a issuance of a construction permit and followed by the issuance of an operating license. This process is currently described in the 10 CFR 50 document. A new approach for licensing of nuclear reactor was adopted in 10 CFR 52. The 10 CFR 50 document has several

appendixes (A to S).

The Two-Step licensing under the 10 CFR 50 is following. The regulator staff performs a safety review of the proposed design in accordance with the Standard Review Plan (SRP) and prepares the Safety Evaluation Report (SER), the Advisory Committee on Reactor Safeguards (ACRS) meets with the applicant and the regulator staff with the outcomes of its review of SER. After that the regulator conducts an environmental review of the application and prepares an environmental impact statement (EIS). Later the decision itself is given by the Atomic Safety Licensing Board. After the licensee gets the construction permit and before the construction is finished, the construction-permit holder files an application for an operating license. If the power plant has been constructed according to the approved design and that there is a reasonable assurance that the plant can be operated without endangering the public health and safety, the operating license is granted. Also a public meeting may be conducted, however it is not required.

The 10 CFR 52 is used to obtain an early resolution of safety and environmental issues and simplifies the Two-Step process. The main idea is that anyone that applies for the construction permit under 10 CFR 50 (or combined license under 52) can apply to issue an Early Site Permit under 52. Also the 10 CFR 52 authorizes the regulator to issue combined construction permits and operating license (combined licenses).

In the Czech Republic, since the end of 1970 basic design requirements have followed philosophy of U.S. regulations (10.CFR.50 Appendix A). Consequently, to the extent possible, Safety Assessment Reports for the NPP Temelín units are developed in accordance with U.S. NRC Regulatory Guide 1.70 and reviewed by the SUJB in accordance with standard review plan specified in U.S. NRC NUREG 800. [1]

2.2 NUREG-0800

NUREG-0800 is a document issued by the U.S. Nuclear Regulatory Commission (USNRC) in order to provide guidance to USNRC staff to perform safety reviews of the following areas:

- Construction permit
- Operating license
- Applications under 10 CFR Part 50
- Early site permit
- Design certification
- Combined license
- Standard design approval
- Manufacturing license
- Applications under 10 CFR Part 52

The main purpose of NUREG-0800 is to standardize the structure and to assure quality and uniformity of staff safety reviews. Because this document is made public, many countries adopt the procedure implemented by the USNRC and therefore the licensing processes in different countries (which take the US standards, such as Spain) are uniform and it is easier for foreign contractor to operate in other countries. Another example of a country following the structure of NUREG-0800 (although having its own legislation) is the Czech Republic. The most important chapter of the NUREG 0800 for this work is chapter 15 - Transient and Accident Analyses. In accordance with chapter 15 of SRP and Regulatory Guide (RG) 1.70 the initializing events are categorized into following categories.

- Increase in heat removal from the primary system
- Decrease in heat removal by the secondary system

- Decrease in reactor coolant system (RCS) flow rate
- Reactivity and power distribution anomalies
- Increase in reactor coolant inventory
- Decrease in reactor coolant inventory
- Anticipated transients without scram (ATWSs)

The rod ejection scenario is a Reactivity Initiated Accident (RIA) connected with a decrease in reactor coolant inventory (SBLOCA). The complete description of the transient is provided later in the document. The most used codes (suggested by U.S. NRC in NUREG-0800) to use to calculate neutron behavior are PARCS or TWINKLE. Both are multidimensional spatial neutronic codes, however TWINKLE is being replaced with PARCS, because it is possible to be coupled with a system code called TRACE.

The general structure of the SRP is following:

1. Areas of Review
2. Acceptance Criteria
3. Review Procedures
4. Evaluation Findings
5. Implementation

2.2.1 Areas of review

This section generally gives the scope of the review. It contains a description of the systems, components, analyses, data or anything to be reviewed by the staff. It also discusses the information needed in order to complete the review.

2.2.2 Acceptance criteria

The acceptance criteria includes the regulator requirements including specific regulations, orders and industry codes and standards. However the SRP is not a substitute for the regulators regulations and compliance with it is not required. Also this section contains the technical bases for applicability of the requirements to the subject areas of review or relationship of regulatory guidance to the associated requirement. The list of the acceptance criteria for VVER 1000320 is described later in the thesis.

2.2.3 Review procedures

In the Review procedures subsection describes how the review is accomplished. These procedures are adjusted according to the acceptance criteria in place for the specific scenario. The step by step guideline is included to assure a reasonable assurance that the requirements have been met.

2.2.4 Evaluation findings

The type of conclusions which is needed is described in this section and for each SRP section, the staff conclusion is incorporated into a published Safety Evaluation Report (SER). There are five aspects of review in Safety Evaluation Report. First it identifies the changes, that the licensee made to the application. Second it deals with the matters addressed by provided additional information. Third, the matters for which additional information is expected to be forthcoming. Fourth, the matters remaining to be unresolved and finally the fifth, it identifies the deviations from the SRP in design and operational programs and the bases for the acceptability of such deviations.

2.2.5 Implementation

This section provides guidance to applicants and licensees regarding the regulators plans for using the SRP section. [2] [14]

Chapter 3

VVER 1000 Description

3.1 General Introduction

VVER technology is the most used in the East European countries (Czech Republic, Slovakia, Romania, Turkey, Russia). It is a Russian design light water reactor and the acronym translated to English would be WWER as in Water (cooled) Water (moderated) Energy Reactor. In the Czech Republic there are two types of VVER reactors, VVER 1000 (NPP Temelin) and VVER 440 (NPP Dukovany). This design competes with the traditional western PWR and differs in several key aspects. What concerns the active core most important one is the core lattice, which is triangular compared to PWR's square. This however is not the only difference and more detailed description follows in later sections. This analysis concerns the VVER 1000 type v-320 and therefore it will be the should focus in this description noting, that there are large differences even within the VVER family.

3.2 Primary Circuit

VVER 1000 primary circuit components are in general same as in traditional PWR. There is the pressure vessel (RPV), pressurizer, steam generators (SG) and reactor coolant pumps (RCP). The main difference however is the steam generator, which unlike in PWR is horizontal. This design brings several advantages and disadvantages if compared to the vertical SG, however this comparison is not the focus of this work. In the Figure 3-1 on page 26 the primary circuit of VVER 1000 is shown. As can be seen, this is a four loop system, with horizontal steam generators. The general diagram of VVER 1000 SG is shown in the Figure 3-2 on page 27. The specific dimensions and thermo-hydraulic data are contained in tables 3.1 to 3.2.

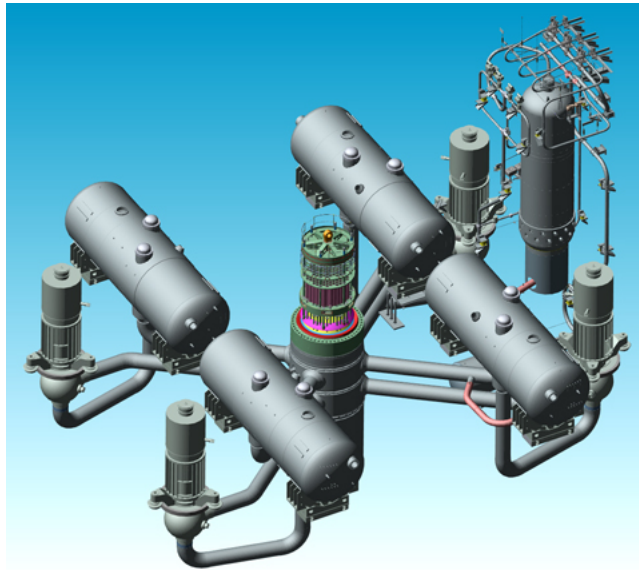


Figure 3-1: VVER 1000 primary circuit [7].

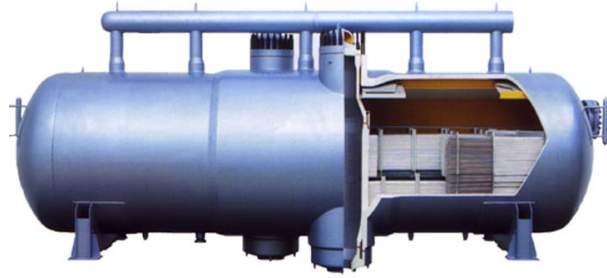


Figure 3-2: VVER 1000 steam generator [16].

3.3 Core

The active core of VVER 1000 reactor is composed of 163 fuel assemblies of hexagonal shape, which are distributed uniformly with step 236 mm between the centres of the fuel assemblies. Location of fuel assembly in the core is defined by the need to secure the prescribed requirements for performance, while complying with safety requirements and efforts to achieve the lowest fast neutron fluence in the reactor vessel.

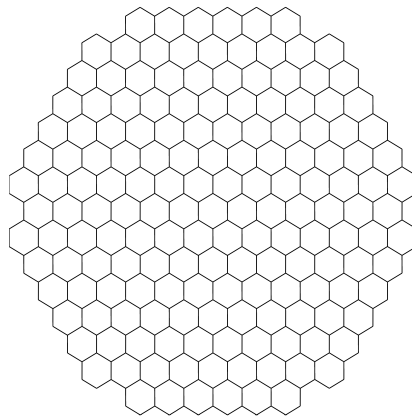


Figure 3-3: VVER 1000 core layout.

Systems affecting the reactivity of the reactor core include two independent sys-

tems, based on different principle effects - fluid system with boron control and mechanical system control and reactor protection employing absorptive rods grouped into a cluster (absorption volume) that can be positioned over the entire height of the fuel assembly.

3.4 Fuel Assembly

The fuel assembly of VVER 1000 has a hexagonal geometry, the main components are shown on Figure 3-4 with the technical specifications are shown in table 3.1. The Russian fuel used also in this analysis uses a central hole filled with helium design as shown on Figure 3-5. The Figure shows a central hole (light blue), the fuel pellet (red), the gap between fuel and cladding filled with helium (light blue), cladding (green) and water (blue). More detailed information are contained in chapter of Model Description, section SCALE/SERPENT2.

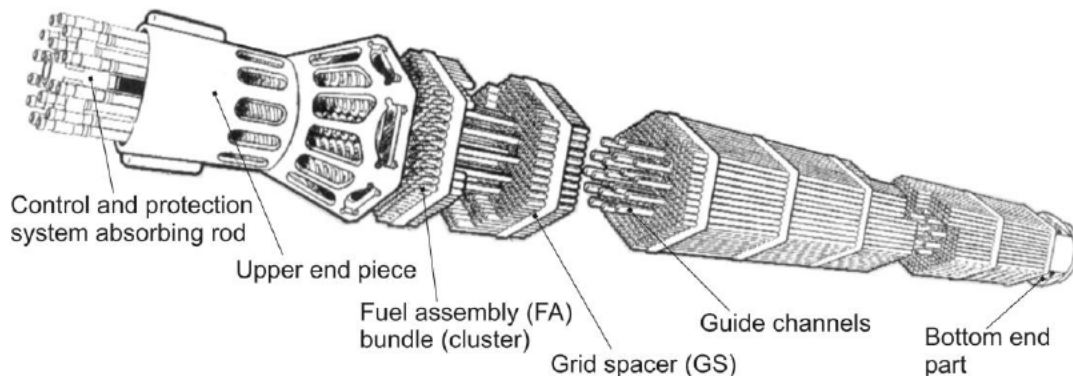


Figure 3-4: Diagram of VVER 1000 fuel assembly [5].

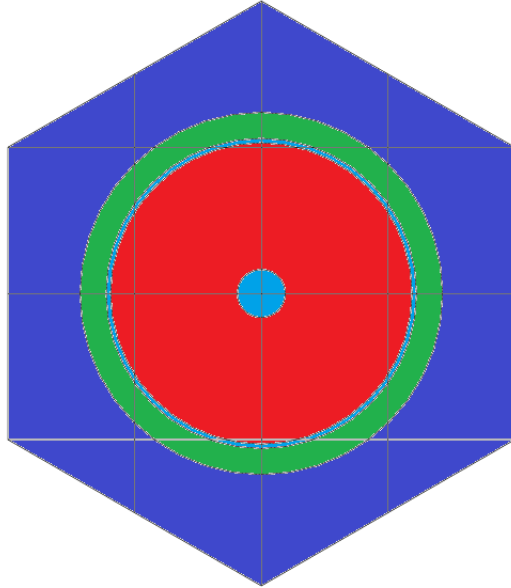


Figure 3-5: Drawing of Russian type fuel for VVER 1000 generated by SCALE.

3.5 Control rods

Mechanical reactor protection system consists of 61 physically and geometrically identical absorption banks. Absorber clusters are divided into 10 groups, each containing 6 absorptive pins except the 9th group of them containing 7, with absorbent beam positioned above the central position in the zone.

First to sixth group of absorption banks is designated for the purpose of protection of the reactor and seventh to tenth groups are used as control, but also cooperate in protecting the reactor. In order to reach the critical condition of the reactor, the rods are withdrawn sequentially in the order of increasing group numbers of 7, 8, 9 and 10. while inserting the groups into the zone is carried out in reverse order. Absorbing clusters of each group are transferred at the same time. Location of absorptive bundle determines the distance of the lower-end section of the absorbent absorptive bundle

from the bottom of the core or the lower limit of the fuel column. The positions of the control rod banks are shown in the model description of PARCS.

In the lower part of the absorption pin (lower 300 mm) the pin consist of dysprosium titanium oxide (Dy_2TiO_5 with 6 g/cm^3 density. Dysprosium isotopic composition is natural. In the upper part of the absorption pin is boron carbide (B_4C with 1.8 g/cm^3 . Again the isotropic composition of boron is natural. [14]

3.6 Technical Parameters

The general technical parameters are in the tables below. These data are public information provided by the Czech NPP owner CEZ and they correspond to NPP Temelin using the VVER 1000 reactors. [6]

Table 3.1: VVER 1000 technical specifications 1/2

Reactor Type	
Heterogeneous, pressurized water power reactor VVER 1000	1000 typ V 320
Nominal heat output	3000 MWt
Reactor Parameters	
Pressure vessel height	10,9 m
Inner diameter of RPV	4,1 m
Outer diameter of RPV	4,5 m
Total wall thickness of RPV	200 mm
The thickness of the lining of austenitic steel	7 mm
Top block height	8,2 m
Total height of top block	19,1 m
Total weight	cca 800 t
Active Zone	
Number of fuel assemblies	163
Number of pins per FA	312
Number of control rod banks	61
Number of absorption elements per cluster	18
Height of active zone	3,53 m
Diameter of active zone	3,16 m
Fuel enrichment for fresh core.	1,3 - 3,8 % U 235
Weight of FA	766 kg
Weight of fuel per FA	563 kg
Total weight of fuel in the core	92 t
Maximum burnup	60 MWd/kg

Table 3.2: VVER 1000 technical specifications 2/2

Reactor Colling System	
Number of loops	4
Working pressure	15,7 MPa
Cold leg coolant temperature	290 C
Hot leg coolant temperature	320 C
Primary flow rate through the core	84 600 m ³ /h
Inner diameter of main coolant pipe	850 mm
Outer diameter of main coolant pipe	995 mm
Steam Generator	
Heterogeneous, pressurized water power reactor VVER 1000	1000 typ V 320
Number per one block	4
Inletoutlet temperature on primary side	320/290 C
Inletoutlet temperature on secondary side	220/278,5 C
Pressure	6,3 MPa
Amount of steam generated	1 470 t/h
Volume of primary/secondary side	21/66 m ³
Diameter of SG	4,1 m
Length of SG	14,8 m
Weight of SG	cca 416 t
Main Circulation Pump	
Number per one block	4
Pump power	5,1 MW
Operational performance	21 200 m ³ /h
Number of rotations per minute	1 000 ot/min
Weight of MCP	156 t

Chapter 4

Computational Codes

4.1 SCALE

The SCALE code package is a comprehensive modelling and simulation suite for nuclear safety analysis and design. SCALE provides a comprehensive, verified and validated, user-friendly tool set for criticality safety, reactor physics, radiation shielding, radioactive source term characterization, and sensitivity and uncertainty analysis. SCALE provides a “plug-and-play” framework with several computational modules including three deterministic and three Monte Carlo radiation transport solvers that are selected based on the desired solution strategy. SCALE includes current nuclear data libraries and problem-dependent processing tools for continuous-energy and multigroup neutronics calculations, multigroup coupled neutron-gamma calculations, as well as activation and decay calculations. SCALE has unique capabilities for automated variance reduction for shielding calculations as well as sensitivity and uncertainty analysis. SCALE’s graphical user interfaces assist with accurate system modelling and convenient access to desired results. In particular the TRITON Mod-

ule is used for the generation of cross-sections useful for PARCS code. It is a control module in computation code SCALE 6.1.2. It uses several computational sequences like CENTRM, NEWT, BONAMI, etc., that are depending on user's requirements. TRITON performs 2-D calculations for square and hexagonal geometry of the fuel assembly. Its main computational features are cross-section calculation and isotopic compositions of the fuel assembly. In the CENTRM-based discrete ordinates (SN) option, the Bondarenko self-shielding method is used to determine the problem-dependent multigroup cross-sections in the unresolved resonance energy range. The unresolved resonance calculation is performed by the BONAMI functional module. For the resolved resonance energy range, the CENTRM functional module is used to determine the 1D pointwise (105 energy groups) flux solution using the SN method.

4.2 SERPENT 2

SERPENT 2 is a Monte Carlo reactor physics burnup calculation code developed by the VTT Technical Research Centre of Finland. SERPENT 2 is a successor to SERPENT 1 and still is in testing period. SERPENT is a 3D, continuous energy Monte Carlo physics burnup calculation code specifically designed for lattice physics applications. It uses implemented calculation routines in order to generate homogenized multi group constants for deterministic calculations. Usually the output contains infinite and effective multiplication factors, homogenized cross sections, scattering matrices, diffusion coefficients, assembly discontinuity factors, point-kinetic parameters, effective delayed neutron fractions and precursor group decay constants. The output is fairly similar to SCALE. As mentioned before, SERPENT can calculate burnup and through a transfer code GenPMAXS all cross-sections can be implemented in PARCS including the burnup information in PMAXS files. This code is

written in ANSI-C language and runs only in linux and a parallel calculation mode is available. [10]

4.3 PARCS

This section contains a brief overlook on the state of the art of the PARCS and TRACE codes. More detailed description is contained in further chapter.

PARCS (Purdue Reactor Core Simulator) is a three-dimensional (3D) reactor core simulator which solves the steady-state and time-dependent, multi-group neutron diffusion and low order transport equations in orthogonal and non-orthogonal geometries. PARCS can be coupled directly to the thermal-hydraulics system code TRACE which provides the temperature and flow field information to PARCS during the transient calculations via the few group cross sections. PARCS is available as a standalone code for performing calculations which do not require coupling to TRACE or RELAP5. PARCS can also be coupled to the RELAP5 systems code. A separate code module, GENPMAXS, is used to process the cross sections generated by lattice physics codes such as TRITON (SCALE 6.1.2), HELIOS, or SERPENT into the PMAXS format that can be read by PARCS.

The most recent version of the PARCS code is 3.2 (November 2015). Although PARCS is a very good tool for square geometry core lattice, there are still limitations concerning hexagonal geometry. By the fall the Code Application Maintenance Program (CAMP) of 2015 it is not possible to calculate pin power of hexagonal assemblies. It is not possible to use the Symbolic Nuclear Analysis Package (SNAP) for automatic mapping of TRACE heat structures and thermal hydraulic components onto PARCS. Also presented at the CAMP by Dr. Guido Mazzini and by the author there is a problem using gadolinium as a burnable absorber in the core in TRACE.

There several additional issues concerning the coupling procedure, mainly due to a lack of proper guiding material provided by the code authors. In numerous cases impact and importance of several parameters can only be found by performing a sensitivity analysis on them, which requires significant amounts of time and therefore it is difficult to build a near-perfect model.

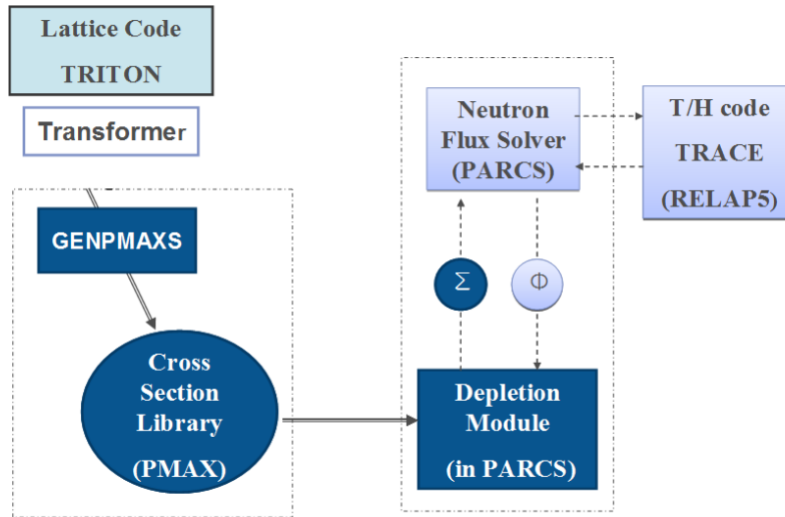


Figure 4-1: PARCS code logic

The major calculation features in PARCS which include the ability to perform eigenvalue calculations, transient (kinetics) calculations, and xenon transient calculations, decay heat calculations, pin power calculations and adjoint calculations have been extended to include not just Light Water Reactors, but also the Pressurized Heavy Water and High Temperature Gas Reactors.

The major application of the PARCS code is to be coupled with a system code TRACE in order to provide more complex, multi-dimensional multi-group power input. As can be seen from the calculation scheme shown in figure 4-1 on page 37, the main input for PARCS are the cross-sections calculated from previously mentioned

codes. In case of a stand alone calculation, the output of PARCS for hexagonal geometry is planar and axial both normalized power profiles and flux distributions. There is a basic thermo-hydraulic component embedded inside PARCS in order to be able to calculate coolant temperature, fuel temperature and coolant density. PARCS is also able to calculate k_{eff} , boron concentration or rod position with respect to the remaining two. For example in order to remain critical, either k_{eff} , ppm or the rod position is changing either in time, when calculating a steady state.

Another major possibility, which PARCS provides, is to calculate transients at specific burnup step of the cycle and to estimate burnup of the assemblies after a set period of time (for example for the stretch-out calculations).

4.3.1 Flux calculation method in the hexagonal geometry

This work deals with the hexagonal geometry and because a hexagon is combined of six triangles, the diffusion problem can be simplified into one triangle.

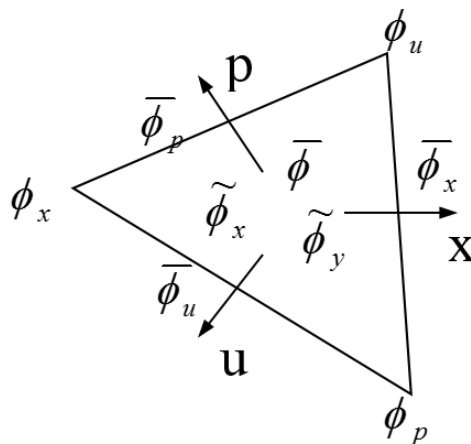


Figure 4-2: Fluxes in a triangle

In the figure 4-2 on page 38 there is a nodal flux $\bar{\phi} = \frac{1}{V} \iint \phi(x, y) dy dx$, flux in the

apexes of the triangle $\phi_i = \phi(r_i)$ and the surface average fluxes at the three surfaces $\bar{\phi}_x = \frac{1}{h} \int \phi(x, y) dy$. The moments are following:

- $\widetilde{\phi}_x = \frac{2\sqrt{3}}{3h} \frac{1}{V} \iint x \phi(x, y) dy dx$
- $\widetilde{\phi}_y = \frac{2}{h} \frac{1}{V} \iint y \phi(x, y) dy dx$

The whole hexagon with \mathbf{j} being incoming partial current it is shown on figure 4-3 on page 39.

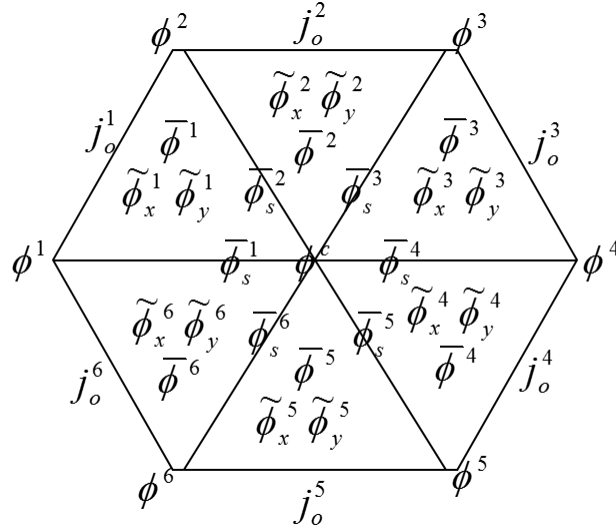


Figure 4-3: Fluxes in a full hexagon

The code is solving a system of equations of:

- 6 Nodal Balance Equations for 6 Node Average Flux
- 12 WRM Equations for 12 Moments
- 6 Net Current Continuity Conditions for 6 Inner Surface Flux
- 6 Incoming Current Conditions for 6 Outgoing Currents
- 1 Net Leakage Balance Equation for 1 Center Flux

$$\begin{pmatrix} C_{aa} & 0 & 0 & C_{as} & C_{aj} & C_{ap} \\ 0 & C_{xx} & 0 & C_{xs} & C_{xj} & C_{xp} \\ 0 & 0 & C_{xx} & C_{ys} & 0 & C_{yp} \\ C_{sa} & C_{aa} & C_{xx} & C_{ss} & 0 & C_{sp} \\ C_{ja} & C_{jx} & 0 & 0 & C_{jj} & C_{jp} \\ 0 & C_{px} & 0 & 0 & C_{pj} & C_{pp} \end{pmatrix} \begin{pmatrix} \phi \\ \widetilde{\phi}_x \\ \widetilde{\phi}_y \\ \phi_s \\ j_0 \\ \phi_s \end{pmatrix} = \begin{pmatrix} q + S_{ji} \\ \widetilde{q}_x + \widetilde{S}_{xji} \\ \widetilde{q}_y \\ \mathbf{0} \\ S_{(j_0)(ji)} \\ S_{pji} \end{pmatrix} \quad (4.1)$$

[13] [15] [12] [4]

4.4 TRACE

The TRACRELAP Advanced Computational Engine (TRACE - formerly called TRAC-M) is the latest in a series of advanced, best-estimate reactor systems codes developed under U.S. Nuclear Regulatory Commission for analysing transient and steady-state neutronic-thermal-hydraulic behaviour in light water reactors. It is the product of a long term effort to combine the capabilities of the NRC's four main systems codes (TRAC-P, TRAC-B, RELAP5 and RAMONA) into one modernized computational tool. It is able to analyse large/small break Loss of Coolant Accidents (LOCAs) and other system transients in both pressurized water reactors (PWRs) and boiling water reactors (BWRs). The version used in this analyses is TRACE v5 patch 4 released in 2014.

For the user point of view, there are three major steps in performing a calculation in TRACE and those are: input processing, initialization and results. During the input processing, TRACE checks the user model and checks for errors. If the model passes the processing, it is initialized and again checks for possible boundary error as well as the model will be prepared for calculation. Once the calculation is finished,

there are several output files, among which there is the actual output, a restart file and a binary file containing all data to be read by apt plot. This process is shown in the Figure 4-4 on page 41.

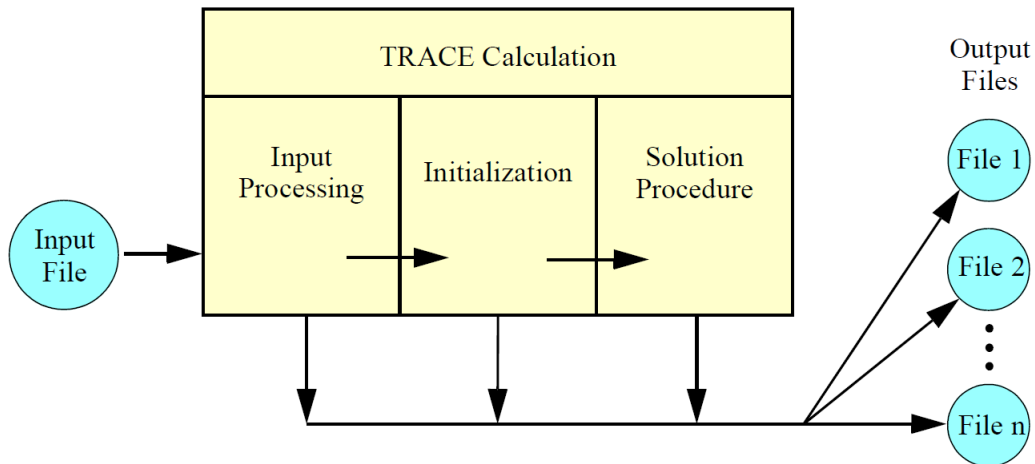


Figure 4-4: Phases of a TRACE calculation

TRACE operates with a six field equation model for two-phase flow:

- Conservation of mass, liquid phase
- Conservation of mass, vapor phase
- Conservation of momentum, liquid phase
- Conservation of momentum, vapor phase
- Conservation of energy, liquid phase
- Conservation of energy, vapor phase

Additional equations are solved for non-condensable gases (tracked with the vapor phase) and dissolved boron (tracked with the liquid phase) when they are present in the fluid.

TRACE was designed in order to be able to perform best-estimate analyses of a several accidents and transients. Among those are the loss of coolant accidents

(LOCAs), the operational transient analyses and other accident scenarios in pressurized water reactors (PWRs) and boiling water reactors (BWRs). It is however also possible to model phenomena occurring in the experimental facilities designed to simulate transients in reactor systems. These models contain multidimensional two-phase flow, non-equilibrium thermo-dynamics, generalized heat transfer, reflood, level tracking and reactor kinetics. The in-built reactor kinetics solver is only based on the point kinetics solution, however it is possible to couple TRACE code with PARCS in order to implement 3D multidimensional and multigroup neutron kinetics.

4.4.1 Code Characteristics

Multi-Dimensional Fluid Dynamics

Inside the components, where 3D phenomena takes place, TRACE can simulate a 3D flow in either Cartesian coordinates (x,y,z) and/or in the cylindrical geometry (r, θ, z) . Among these 3D components we can find a reactor vessel or reactor water storage tank. Flows within pipes are usually modeled one dimensional. By using a combination of both 3D and 1D, TRACE is able to calculate accurately with reasonable computation speed.

Non-homogeneous, Non-equilibrium Modeling

The gas-liquid flow is evaluated through usage of a full two-fluid hydrodynamic model, which allows an explicit simulation of all the important phenomena, such as counter-current flow. Also a stratified-flow regime has been added to the 1D hydrodynamics. Seventh field equation (mass balance) describes a non-condensable gas field and the eighth field equation follows dissolved solute in the liquid field.

Flow-Regime-Dependent Constitutive Equation Package

The transfer of mass, momentum and energy between the steam-liquid phases and the interaction of these phases with heat from modelled structures is described by the thermal-hydraulic equations. These interactions are dependent on the flow topology, therefore a flow-regime-dependent constitutive-equation package was included inside the code.

Comprehensive Heat Transfer Capability

A detailed heat transfer analysis is available in TRACE for the vessel and the loop components with a 2D (r,z) treatment of conduction heat transfer within metal structures. The simulation of the heat transfer characteristics of quench fronts is possible due to the implementation of a heat conduction with dynamic fine-mesh rezoning during a reflood. The flow regime dependent heat transfer coefficients are used to calculate the heat transfer from the fuel rods and the other structures. These coefficients are obtained from a generalized boiling curve based on a combination of local and historical effects. Also the inner and/or outer surface convection heat transfer and a tabular or point kinetics (stand alone) or 3D kinetics (coupled with PARCS) can be modelled.

Limitations of TRACE

However TRACE does not accurately calculate the flow of energy across junctions that have large pressure differences between adjacent volumes. For choked flow junctions from reactor to containments modeled with TRACE components (i.e., not with one of the various containment analysis codes), TRACE will under predict the containment pressurization due to the internal energy formulation. [3]

Chapter 5

Model Description

5.1 SCALE

The model of fuel assembly is created by TRITON in SCALE 6.1.2 and the geometrical and material parameters from a VVER 1000 type NPP. There are six types of fuel assemblies with different enrichment as shown in the Table 5.1 on page 46. In the first step it is necessary to define several parameters of the fuel, such as density, temperature and enrichment as well as cladding, which consist of 99% Zr and 1% Nb. Moderator is comprised from main an additional materials. The main material is water (H₂O) with density of 0,73 g/cm³, temperature 575 K and the additional material is boron with 1065 ppm. Inside the fuel pellets there are the central holes filled with helium. The geometrical definition and parameters of the fuel assemblies and fuel pellets are defined as following. Simulation of active length of fuel assembly as infinite because calculation code TRITON computes only 2D (radial) geometry. The inputs are shown in Figure 5-1 and Figure 5-2 on page 45. Fuel assembly consists of nine nodes and each node has power level that depends on the active length

power distribution. The analyses in SCALE are performed with average power and temperature distribution, also the calculation are done at time 0, practically after refuelling without the effect of xenon and samarium. The calculations are based on ENDF/B-VII.0 in 238 groups. The plots below are a visualization of defined geometry, where different colours represent different materials.

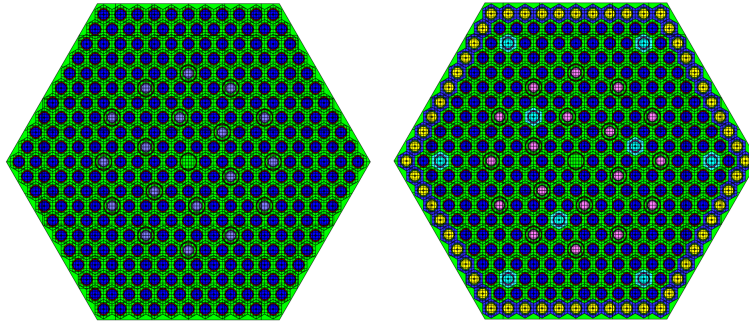


Figure 5-1: Inputs of F130/F200 (left) and inputs of FF36G9/FF40G9 (right)

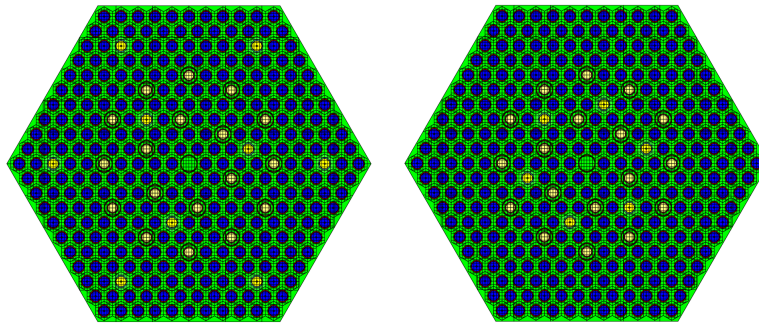


Figure 5-2: Input of F30G9 (left) and input of F40G6 (right)

There are five branches considered plus a reference one. The branch information is in the table 5.2 on page 46. These branches are used for calculation of the differential cross sections.

Table 5.1: Fuel enrichment description

	Fuel 1 %	Fuel 2 %	Fuel Gd %	Gd %	Gd pins
F200	2.0	-	-	-	-
F130	1.3	-	-	-	-
F40G6	4.0	-	3.3	5	6
F30G9	3.0	-	2.4	5	9
FF36G9	3.6	3.3	3.3	5	9
FF40G9	4.0	3.6	3.3	5	9

Table 5.2: SCALE Branch structure

	Tf (K)	Tm (K)	Dm (g/cm3)	CR	Sb (ppm)
Reference Branch	980	575	0.73	Out	1065
Branch 1	980	575	0.73	In	1065
Branch 2	980	575	0.73	Out	565
Branch 3	980	575	0.83	Out	1065
Branch 4	980	675	0.73	Out	1065
Branch 5	1080	575	0.73	Out	1065

5.2 SERPENT 2

Model of fuel assembly was created by SERPENT 2. For all codes a similar approach was applied in order to respect a common procedure. All the geometrical and material parameters that are similar yet not the same with real fuel assembly from the NPP Temelin. There are six types of fuel assemblies with different enrichment as shown in the Table 5.1 and these are the same as used with SCALE/TRITON. The input files contain one of the most important part which deals with parameters of fuel, such as density, temperature, and enrichment. Geometrical parameters of fuel assembly and fuel pellets are defined with surfaces and cells in geometrical block of input file. Inside the fuel pellets there is considered a central hole filled with helium. In general, the input is as close to the one of SCALE/TRITON as possible. The main difference between SERPENT 2 and SCALE is that SERPENT 2 uses 3D geometry,

where SCALE/TRITON only uses 2D, which is why the input also includes the axial mode. Both radial and axial representation is shown on figures 5-3 to 5-14 on pages 47 to 52. In the plots below, similarly to SCALE/TRITON input description, different colours mean different materials.

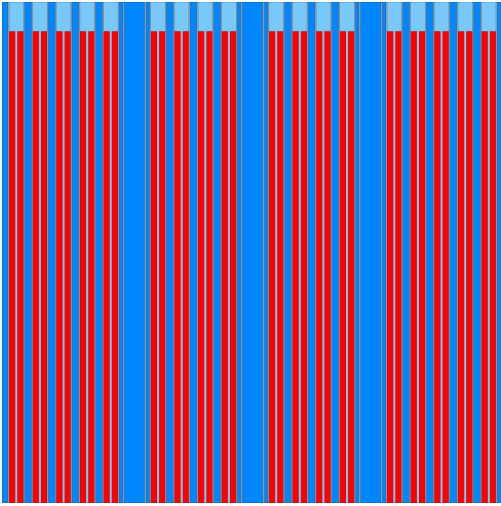


Figure 5-3: Axial input of A130 in SERPENT 2

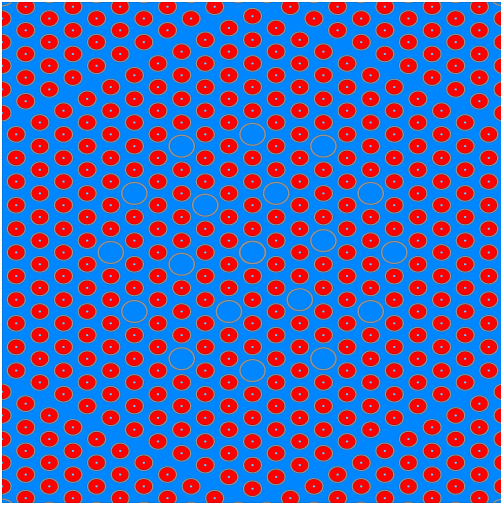


Figure 5-4: Radial input of A130 in SERPENT 2

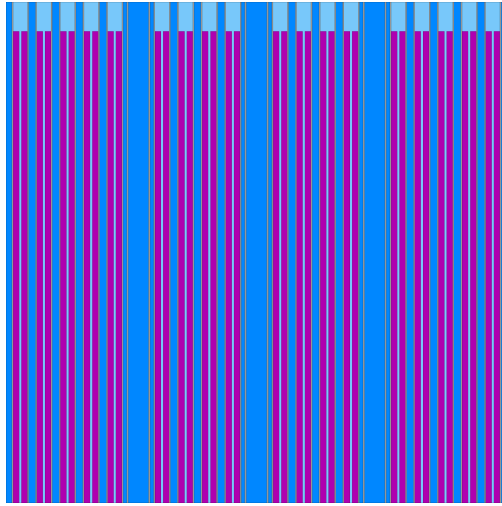


Figure 5-5: Axial input of A200 in SERPENT 2

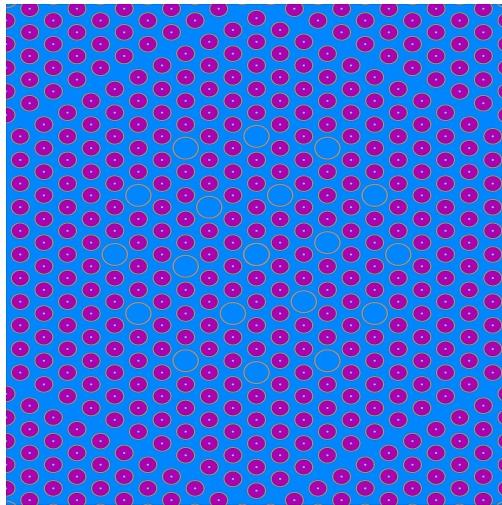


Figure 5-6: Radial input of A200 in SERPENT 2

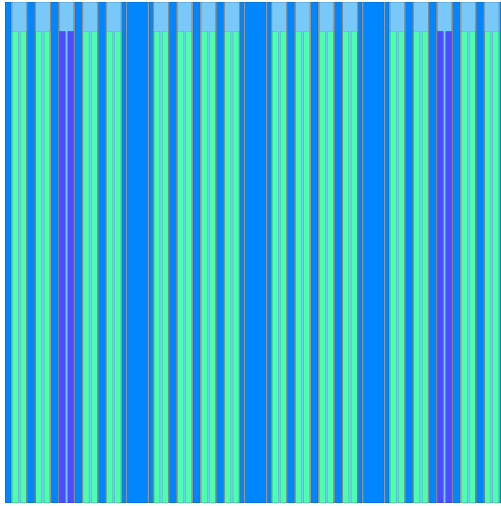


Figure 5-7: Axial input of A30E9 in SERPENT 2

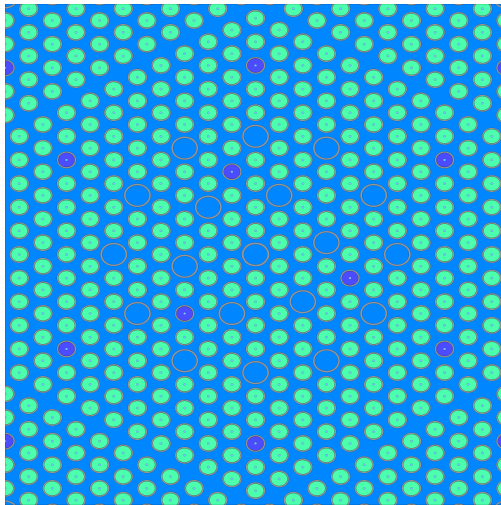


Figure 5-8: Radial input of A30E9 in SERPENT 2

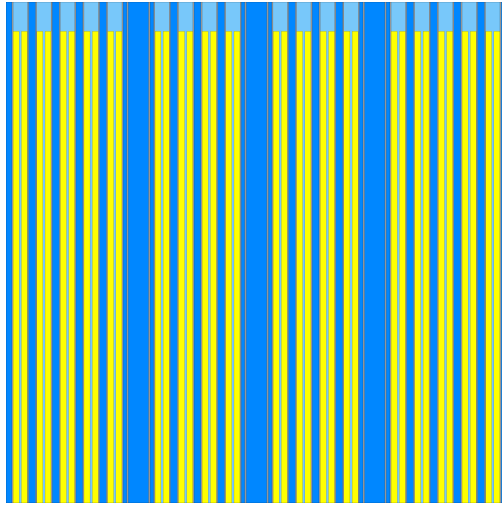


Figure 5-9: Axial input of A40E6 in SERPENT 2

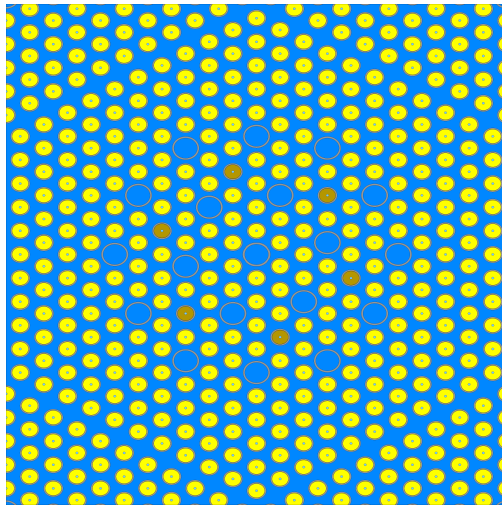


Figure 5-10: Radial input of A40E6 in SERPENT 2

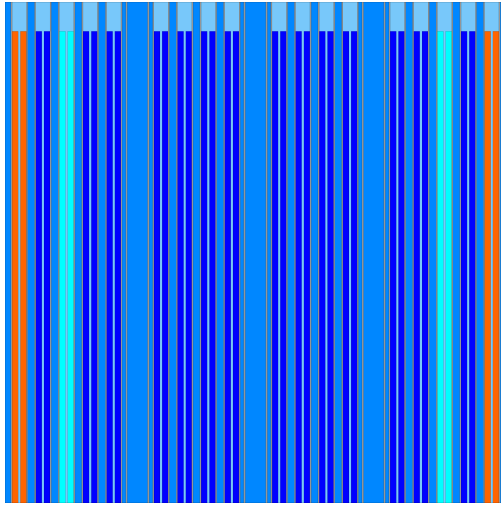


Figure 5-11: Axial input of P36E9 in SERPENT 2

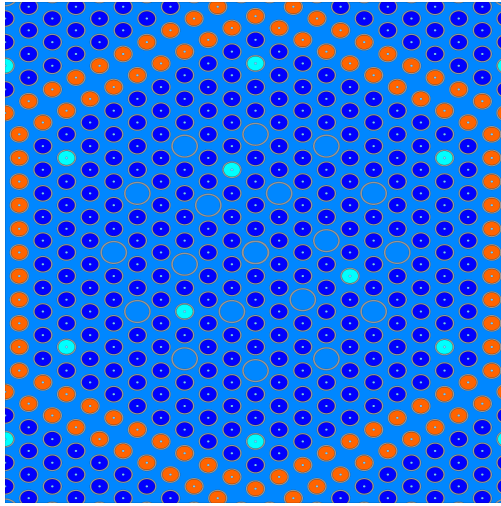


Figure 5-12: Radial input of P36E9 in SERPENT 2

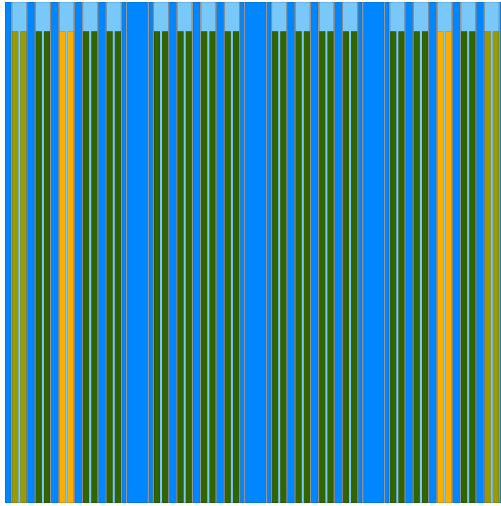


Figure 5-13: Axial input of P40E9 in SERPENT 2

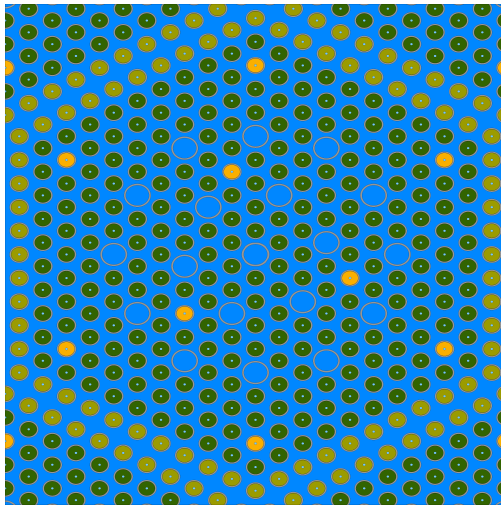


Figure 5-14: Radial input of P40E9 in SERPENT 2

5.3 PARCS

The neutronic model of VVER 1000 in the PARCS code is fairly simple and short, compared to system codes or MC codes, such as SERPENT 2 or MCNP. Version 3.2 is used in this thesis, which is also the most recent one. PARCS is composed of several cards such as CNTL (control), XSEC (cross-sections) and so on.

PARCS code is only concerned about neutronic definitions, most importantly the macroscopic cross sections, radial and axial fuel assembly maps, meshing and others. This section contains the card-by-card description of the input, therefore also a description of the model.

5.3.1 Control card, CNTL

In the CNTL card, the main parameters are defined, such as reactor type (PWR), core power (0-100%), bank positions (0 - 352, inserted - fully out) and the initial boron concentration (ppm). Also there are several binary options such as print definitions. Very important parameter is the criticality search option. The eigenvalue calculation in PARCS is performed using the Wielandt eigenvalue shift method to accelerate convergence. User can either set search for keff or ppm or rod. When the model is set to search ppm, it maintains keff = 1 and adjust the boron concentration. In case of keff search, the boron concentration is fixed and the keff is the variable. There is also the third option, to search CR position.

In this model the CR position is set to three different positions. For the all-rods-in scenario, the SCRAM rods are all out (352 cm) and all control rods are fully inserted (0 cm). For the All-out scenario, both control rods and SCRAM rods are fully withdrawn (352 cm).

5.3.2 Parameter card, PARAM

In the PARAM card, most of the parameters are kept default. The only important parameter specified is the nodal kernel used, in this case the triangular polynomial expansion nodal (TPEN) method. This method first decouples the 3-D defined geometry into 2-D axial and radial that are coupled through transverse-leakages. More details are in the PARCS theory chapter.

5.3.3 Cross-sections, XSEC

The XSEC (cross-section) card is one of the most important ones. The macroscopic cross sections for each fuel assembly and control banks are defined here. Each definition consists of the base macroscopic XSs (two energy groups; transport, absorption, nu-fission, kappa-fission and down-scattering). Also there are differential cross-sections, which are the macro XS per unit (ppm, first and second differential of moderator density, fuel temperature) change for all components in two groups. In addition in this part of PARCS input there are definitions and information about the nuclides families in an assembly as well as delayed neutron definitions (e.g. lambda and beta). Same applies to control rods. In this block there are either the cross-sections generated by SCALE/TRITON, or by SERPENT 2. The differences in results are described in the analysis.

5.3.4 Geometry, GEOMHEX

The geometry card defines the radial and axial configuration as well as control rod banks positions. Core has to have same dimensions and meshing as in the TRACE model, in order to couple. Therefore there are 14 axial nodes and 8 radial rings as

shown in 5-15 on page 55 and 5.5 on page 59. The description of Figure 55 is shown in Table 5.3 on page 55.

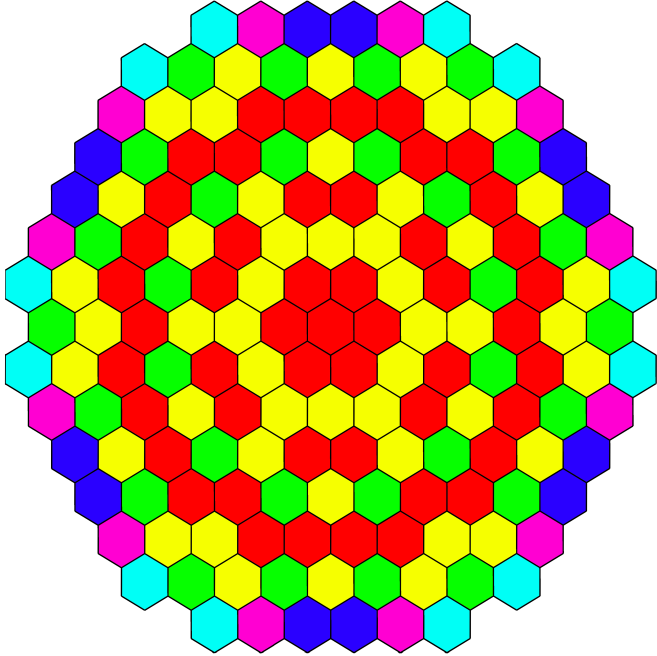


Figure 5-15: Core layout

Table 5.3: Colour description for core layout

Colour	FA type
Red	F130
Yellow	F200
Green	F30G9
Azur	F40G6
Blue	FF36G9
Purple	FF40G9

The general configuration of control and SCRAM banks is shown in Figure 5-16 on page 56 and described in the Table 5.4 on page 56

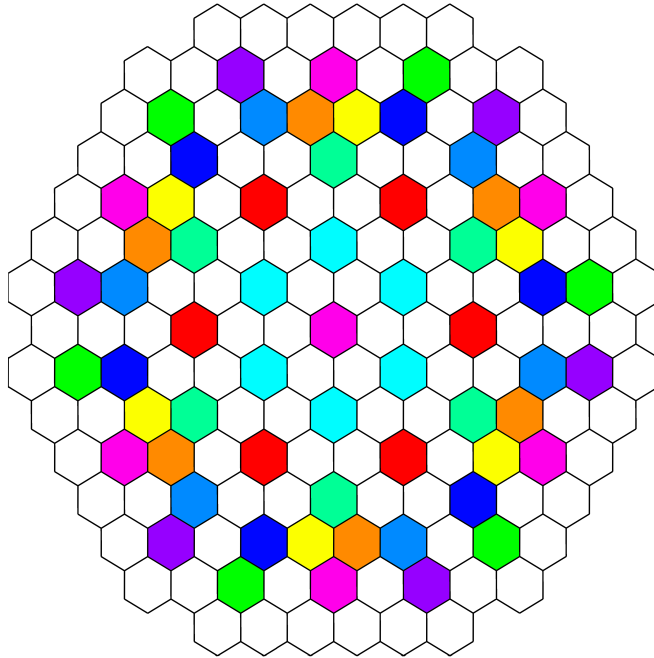


Figure 5-16: Bank layout

Table 5.4: Bank layout group description

Group Number	Color
Group 1	Orange
Group 2	Yellow
Group 3	Purple
Group 4	Green
Group 5	Light Green
Group 6	Cyan
Group 7	Blue
Group 8	Dark Blue
Group 9	Magenta
Group 10	Red

This model however does not include reflector, due to the complexity of implementation. Whole TRACE model would have to be changed in order to include one

additional ring containing the reflector.

5.3.5 Thermal-hydraulics, TH

The thermo-hydraulic card includes basic TH parameters, which are overwritten by TRACE. They are however important for PARCS stand-alone calculation. The parameters defined in this card are for example: number of pins in FA, assembly power and pitch, pin dimensions and flow conditions. The thermal-hydraulic part of PARCS is fairly basic (since it is meant to be coupled with TH code) and for example it is unable to consider two-phase flow. However for the purposes of neutronic analyses

5.3.6 Transient definitions, TRAN

The TRAN block is the control point of the transient simulation. It contains the length of the simulation as well as time step changes. It is possible to simulate several transients such as in our case the rod ejection, but also changes in boron concentration or SCRAM.

5.4 TRACE

The VVER 1000 model developed by CVR was originally prepared for Relap5Mod3.3 code and subsequently converted for TRACE V5.0 code. It represents the primary and secondary systems, as well as the safety components of the plant. The model of the primary circuit consists first of the vessel component representing the reactor pressure vessel (RPV) as illustrated in Figure 5-17 on page 59. Radially, three zones nodalization scheme is adopted with two inner zones representing the lower plenum, the core, and the upper plenum. Third (outer) zone models the downcomer. Axially,

37 zones are modelled with 14 of them representing the active core. Further, the model of the primary circuit consists of models of each individual primary system loop subdivided into hot leg pipes, horizontal steam generators hot and cold collectors and heat exchange tube bundles, loop seal pipes, reactor coolant pumps, and cold legs. To complete the primary circuit model the pressurizer, pressurizer surge and spray lines are modelled. The pressurizer power operated relive valve and safety valves are simulated. TRACE V5.0 pipe and valve components are used to model the secondary system steam lines up to the turbine. Steam dump valves and steam generator safety valves are simulated individually. Feedwater system model consists of the pipes and valves located in the containment. The plant model further contains the control components and trips to simulate actions of safety grade portions of I&C. The basic idea of this model development was to develop a tool for the licensing audit calculations of DBA events included in Chapter 15 of the SAR. As such, the model was systematically validated against the number of plant start up tests including the loss of flow (RCP trips), loss of feedwater, etc. The model is considered suitable to simulate the initial phases of SBO transient including the loss of forced circulation in the primary system, loss of steam generator secondary side coolant inventory, loss of natural circulation in the primary system, loss of coolant via pressurizer PORV and resulting in core heat-up.

With this, and considering that Best-estimate codes are more accurate than severe accident codes in phases before core degradation started, the TRACE V5.0 model is a reference model for initial phases of the transients simulated. [8]

The transient model is a reduced version of the steady state input, in order to reduce the computational costs. Also it includes the Small Break Loss Of Coolant Accident (SBLOCA), (trip number 1005) which occurs at the point of ejection when the upper part of the control mechanism breaks and is ejected from the pressure vessel. This

trip is set manually and the setpoint is time.

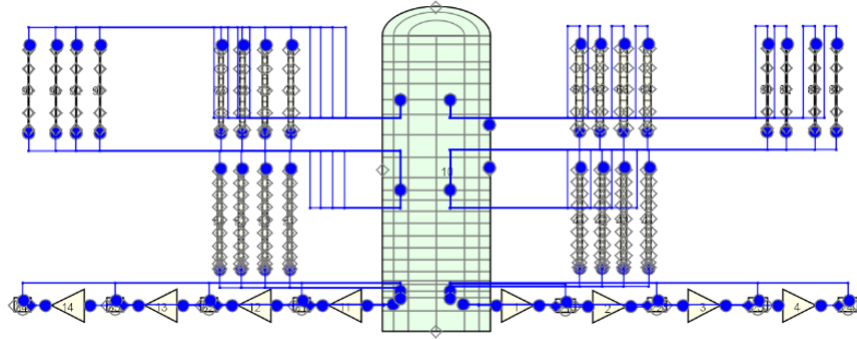


Figure 5-17: TRACE RPV model nodalization

The axial core control volume distribution is shown in the Table 5.5 on page 59. This table does not include all pressure vessel nodes, but only the active core, since the entire nodalization is not essential for the purposes of this work.

Table 5.5: TRACE axial distribution

Axial level	Mesh size
Axial level 14	46.3
Axial level 13	25.5
Axial level 12	25.5
Axial level 11	25.5
Axial level 10	25.5
Axial level 9	25.5
Axial level 8	25.5
Axial level 7	25.5
Axial level 6	25.5
Axial level 5	25.5
Axial level 4	25.5
Axial level 3	37.73
Axial level 2	13.27
Axial level 1	29.55

The time steps are crucial part of the model, especially when coupling. The most

important parameter is that the time step in TRACE should be about three orders greater than the timestep set in PARCS, but small enough to allow the calculation to perform. From experience however, TRACE terminates due to high time step, yet after rigorous sensitivity analysis the problem is not solved simply by reducing the time step even further. This particular problem will be one of a subjects of further study after this work.

Chapter 6

Coupling procedure

Coupling procedure differs greatly with the lattice of the reactor. For square pitch all the user needs are PARCS and TRACE inputs and graphical interface called SNAP in order to use the auto mapping feature. This auto mapping procedure generates a "map" file to be run with the coupled calculation. This automatic process is not however available for this case. Therefore in case of hexagonal pitch this procedure has to be done manually. This means manually assigning each neutronic control volume (mesh) to the one of TRACE's hydraulic and heat structure meshes. To do this by hand would require a substantial amount of time and this is why to achieve mapping a secondary script done in MATLAB is used.

6.1 MATLAB Mapping Script

The general structure of the script has four main sections. The general constants such as number of radial rows or axial planes, number of assemblies, number of planes and the vessel ID defined in the TRACE model. In the second section there

are the radial definitions of both PARCS and TRACE. First there is PARCS radial numbering (given by stand alone PARCS output) and then the PARCS radial weight map (0.0 - 1.0) where on azimuthal boundaries the assembly weight is 0.5 and doubled (two assemblies by 0.5 instead of one by 1.0) and the central node is divided into 6 by 1/6. This map is shown below as a ASCII code. The TRACE radial TH map and a Heat Structure (HS) map are defined according to a logic set in TRACE.

```

[ 1.0 1.0 1.0 1.0 1.0 1.0 ];
[ 1.0 0.5 0.5 1.0 1.0 1.0 1.0 1.0 0.5 0.5 1.0 ];
[ 1.0 1.0 0.5 0.5 1.0 1.0 1.0 1.0 0.5 0.5 1.0 1.0 ];
[ 1.0 1.0 1.0 0.5 0.5 1.0 1.0 1.0 0.5 0.5 1.0 1.0 1.0 ];
[ 1.0 1.0 1.0 1.0 0.5 0.5 1.0 1.0 0.5 0.5 1.0 1.0 1.0 1.0 ];
[ 1.0 1.0 1.0 1.0 1.0 0.5 0.5 0.5 0.5 0.5 0.5 1.0 1.0 1.0 1.0 1.0 ];
[ 1.0 1.0 1.0 1.0 1.0 0.5 0.5 0.5 0.5 0.5 0.5 0.5 1.0 1.0 1.0 1.0 ];
[ 0.5 0.5 0.5 0.5 0.5 0.5 1/6 1/6 1/6 0.5 0.5 0.5 0.5 0.5 0.5];
[ 0.5 0.5 0.5 0.5 0.5 0.5 1/6 1/6 1/6 0.5 0.5 0.5 0.5 0.5 0.5];
[ 1.0 1.0 1.0 1.0 1.0 0.5 0.5 0.5 0.5 0.5 0.5 0.5 1.0 1.0 1.0 1.0 ];
[ 1.0 1.0 1.0 1.0 1.0 0.5 0.5 0.5 0.5 0.5 0.5 1.0 1.0 1.0 1.0 1.0 ];
[ 1.0 1.0 1.0 1.0 0.5 0.5 1.0 1.0 0.5 0.5 1.0 1.0 1.0 1.0 ];
[ 1.0 1.0 1.0 0.5 0.5 1.0 1.0 1.0 0.5 0.5 1.0 1.0 1.0 ];
[ 1.0 1.0 0.5 0.5 1.0 1.0 1.0 1.0 0.5 0.5 1.0 1.0 ];
[ 1.0 0.5 0.5 1.0 1.0 1.0 1.0 1.0 0.5 0.5 1.0 ];
[ 1.0 1.0 1.0 1.0 1.0 1.0 ];

```

The third section of the mapping script concerns the axial meshing and mapping. It is important to note, that the number of axial levels has to be same as in the geometry definition in both PARCS and TRACE as well as the node numbering. Usually the vessel component in TRACE has 1 to n nodes where the core (k) itself occupies only n-k nodes and the numbering has to respect the numbering in TRACE for the core. The mapping file includes a table in the following columns; vessel ID, TRACE radial ID, TRACE axial ID, PARCS radial and multiplication of radial and axial weights.

After the mapping file is generated it is included with the PARCS and TRACE inputs in order for the codes to recognize the geometry.

Chapter 7

Event description

According to NUREG 0800, the standard review plan, chapter 15 on Transient and Accident analyses, the rod ejection scenario is a Design Basis Accident (DBA), ANSI category IV. This accident is defined as a mechanical failure of the pressure housing of the control rod bank which leads to an ejection of the RCCA and of its motor component. This results in a rapid introduction of positive reactivity alongside with the uneven power distribution in the reactor core.

7.1 Accident causes

Control rod ejection is defined as a rapid withdrawal of the control bank from the core (about 8000 km/h see [11]) to an uppermost position. This event can occur due to a failure of the control rod driving mechanism cover along the whole perimeter with the hydrostopper failure. Therefore the failure is either hardware or software induced.

7.1.1 General sequence of events during RE

Almost instant release of the control rod bank has the following effects on the system. A large amount of positive reactivity is introduced by poison removal resulting in an increase of the neutron flux and heat resulting in a short time increase of power production. Very shortly after the ejection the control rod bank breaks, following with SBLOCA.

There are however negative feedbacks that can limit the power growth in the RE scenario. The most important one is the Doppler effect (**Glossary**). The fuel temperature coefficient of reactivity (Doppler) is defined as the change in reactivity with the effective fuel temperature change by one degree while holding a constant moderator temperature and is primarily a measure of Doppler extension of resonant absorption peaks of U-238 and Pu-240. Doppler extension with other isotopes such as U-236, Np-237 and so on are contemplated as well, but their contributions to the Doppler effect is small. Increasing the fuel temperature increases the effective resonance absorption cross sections and causes a corresponding decrease in reactivity.

The power rise is connected to a fast fuel temperature rise, and the Doppler effect, as the broadening of U-238 resonances in the epithermal region, takes place and actuates as an almost immediate negative reactivity source. Another negative feedback is an increase of the moderator temperature over all core resulting in a change of moderator properties. When the moderator (in this case light water) temperature increases, the density of the moderator decreases and therefore the moderation is lower resulting in less fissions. However when the SCRAM occurs, the moderator temperature decreases and the opposite effect takes place, increase in density and therefore better moderation.

In case the some parameters such as the rate of the neutron flux growth or the

neutron flux level or the over temperature and over power delta temperature signal (OTDT) reach the emergency set points, the reactor safety systems are initiated such as SCRAM or the emergency feedwater into all SGs. Following are examples of such set points:

- Minimum DNBR < 1.35
- Power level $> 104 \%$

7.2 Effects of the accident

When the control rod cluster is ejected, a large amount of positive reactivity is introduced to the system possibly resulting in a fuel damage or fuel melt. The worst case is the rod ejection at zero power, because the Doppler Effect feedback is most limited. The fuel and moderator temperatures are at their lowest, so also the moderator density and moderating potential is highest. Second important parameter is the position of the ejected control rod. In the steady state condition under certain core layout, the rod should be ejected from the region of the highest neutron flux to reach maximum reactivity peak. With this implementation this scenario is considered as an envelope and the most conservative.

7.2.1 Acceptance criteria

The acceptance criteria are taken from the safety report of an existing VVER 1000 in the Czech Republic. The most important one is the maximum enthalpy given to the fuel. The second is the fuel and subsequently the cladding temperatures. According to the safety report [14], the fuel melting in the hot pellet should not exceed 10 %. The list of the acceptance criteria is below.

- In order to prevent fuel damage and to meet the relevant requirements of General Design Criteria (GDC) 28 [USNRC], the reactivity excursions should not result in radially averaged fuel rod enthalpy greater than 280 cal/gm at any axial location in any fuel rod for fresh fuel. For the end of campaign the limit is 235 cal/gm. Limit given by the Czech regulator SUJB is however 200 cal/g.
- The maximum cladding temperature does not exceed 1649 C.
- Fuel melting in the hot pellet will not exceed 10 %.
- The number of damaged fuel elements cannot exceed 10% of their total number in the nuclear core.

Chapter 8

Results

8.1 Calculation Process

The coupling procedure for reactors with hexagonal lattice is much more difficult, when compared to the square one. The sequence of calculation is shown in 8-1 on page 69. In this work there are two sets of cross sections generated by the SCALE and SERPENT 2 codes. Later on the results will show the differences between the two and possible ways of improvement. Once the cross sections are implemented with the PARCS code, geometry definitions of PARCS and TRACE codes have to be the same. After ensuring that the geometry is same in either code, it is possible to begin the coupling process, which begins with mapping of the geometry definitions. This procedure is shown in Figure 8-2 on page 70. In order to couple PARCS and TRACE there are four files needed. The PARCS and TRACE inputs (in the diagram they are shown as *NAME.inp*) and TRACE Stand Alone (SA) restart file are generated by the Stand Alone (SA) TRACE and of course the mapping file. With these files it is possible to run Steady State (SS) Coupled (C) calculation. This calculation

outputs several files including the restart files of both PARCS and TRACE, which are necessary for transient (Tr) calculation. The SS, C restart files are then used for the Tr, C calculation along with the transient inputs of PARCS and TRACE.

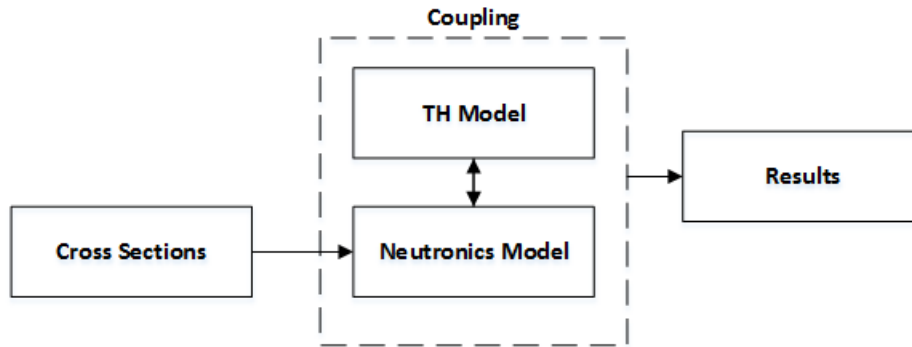


Figure 8-1: Calculation Process

The output of the transient coupled calculation consist of all the thermo-hydraulic available information from TRACE. PARCS provides variables such as reactivity and its components as a function of time, fuel temperature, coolant density and other core-related parameters and all data is available for specified axial and radial location in the Core.

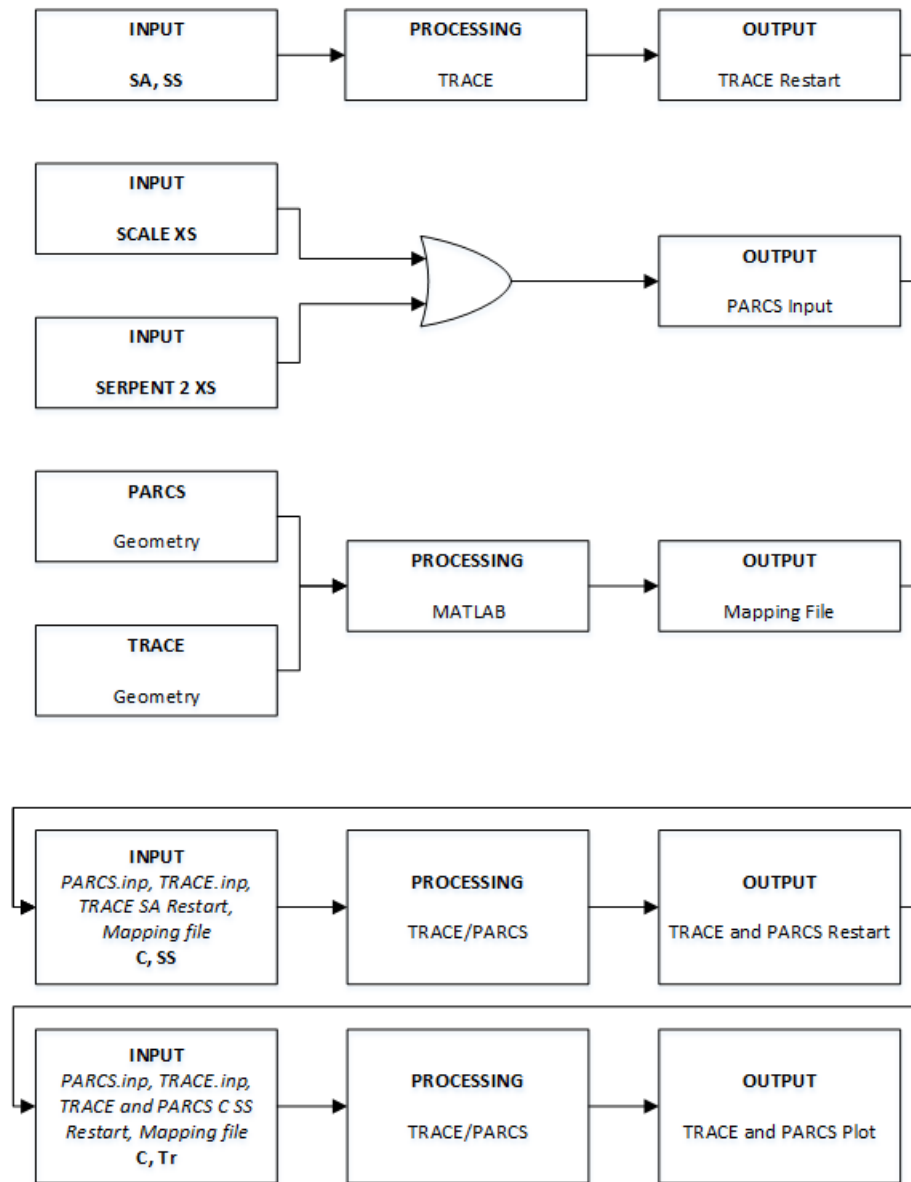


Figure 8-2: Calculation Process

8.2 SCALE

The output of SCALE contains large amount of information ranging from macroscopic cross sections for each specified branch to mass inventories of the specified

fuel assemblies. The most important output for this work are the macroscopic homogenized cross sections for all six fuel assemblies. As specified in the input, there are several branches calculated. PARCS requires differential cross sections in order to run a transient calculation. These cross sections are in regards to boron concentration, control rod position, fuel and moderator temperature and density of coolant. Therefore there are five different sets of homogenized cross sections for the same geometry, only with different reference conditions. To have a differential XS set for, for example, boron concentration, one must subtract the cross sections for the reference case from the XS set with different initial boron concentration (1065 being reference, 1064 is the branched one). This is done for all five parameters. In general, the easier methodology is to create binary "PMAXS" files, which contain all necessary information and these are generated using GenPMAXS code, however there were several difficulties making these and in the end it was faster to do so by hand. However, in the future the implementation of PMAXS cross sections will be done. The outputs are provided with this work.

SCALE also outputs the flux plots (blue to red scale means low to high) shown in figures from number 8-3 to 8-8 on pages 72 to 74.

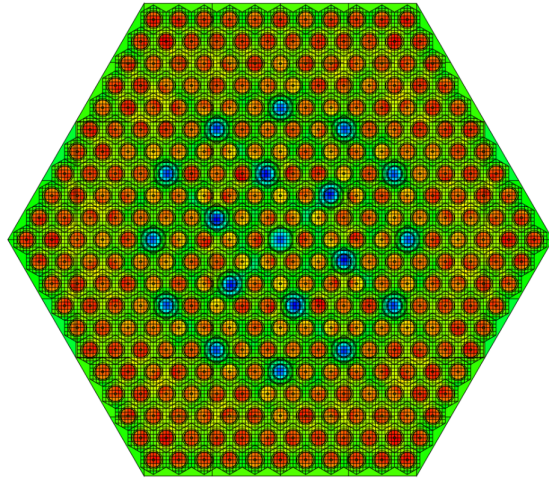


Figure 8-3: Thermal flux plot of FA F130 from SCALE

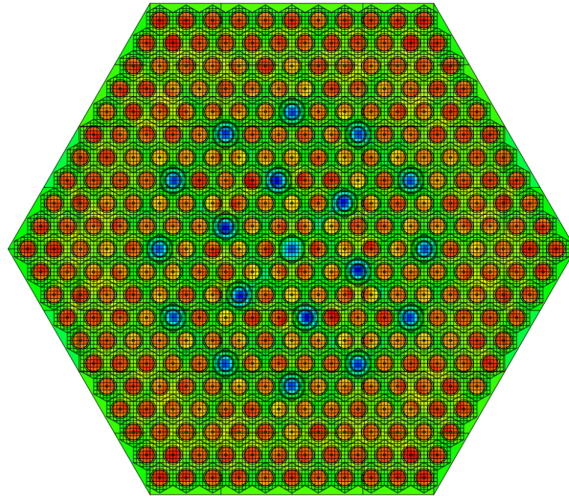


Figure 8-4: Thermal flux plot of FA F200 from SCALE

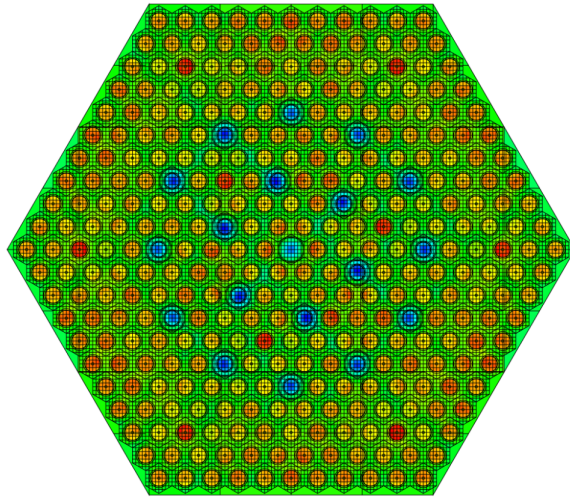


Figure 8-5: Thermal flux plot of FA F30G9 from SCALE

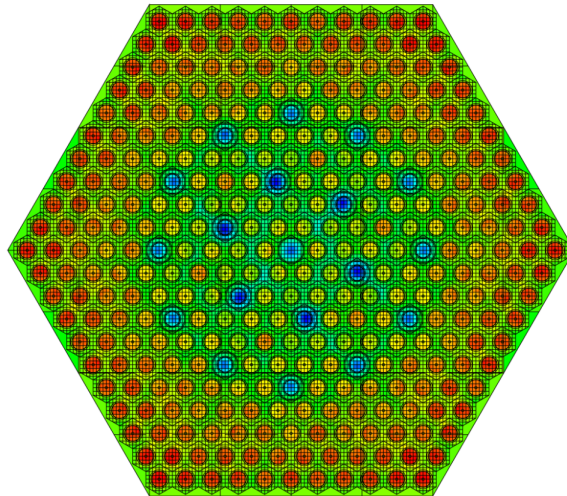


Figure 8-6: Thermal flux plot of FA F40G6 from SCALE

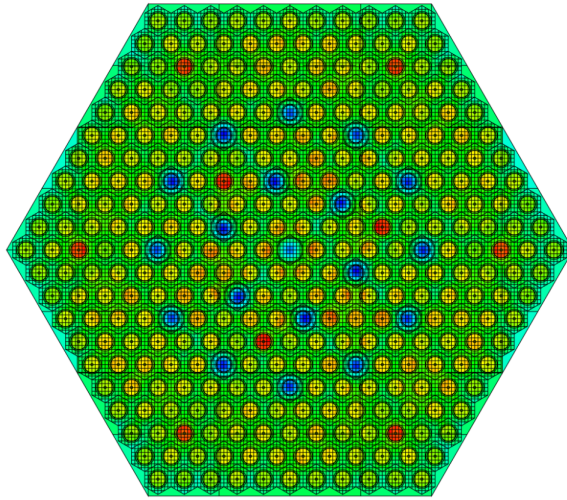


Figure 8-7: Thermal flux plot of FA FF36G9 from SCALE

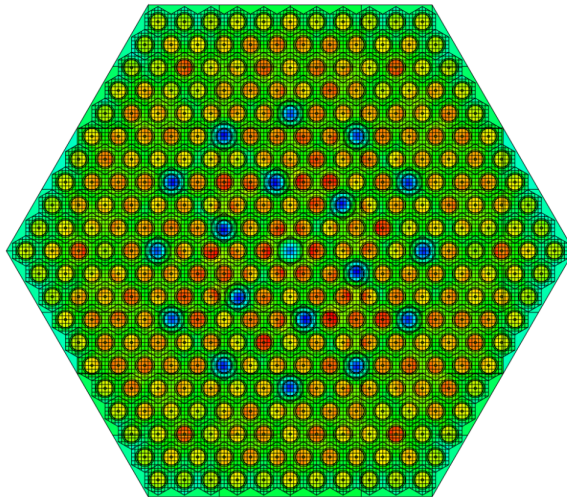


Figure 8-8: Thermal flux plot of FA FF40G9 from SCALE

8.3 SERPENT 2

The output structure of SERPENT 2 is fairly similar to SCALE, however it is not possible to create branches within one calculation, therefore in order to generate differential cross sections as mentioned above, five different calculations had to be performed, resulting in higher CPU time. Unlike SCALE, which has 238 energy groups, SERPENT 2 has continuous energy spectrum similarly to MCNP. This model was benchmarked with MCNP code with only tens of pcm of difference in the k-effective calculation.

Similarly as in the SCALE output section, there are flux plots shown in figures from number 8-9 to 8-14 on pages 75 to 77.

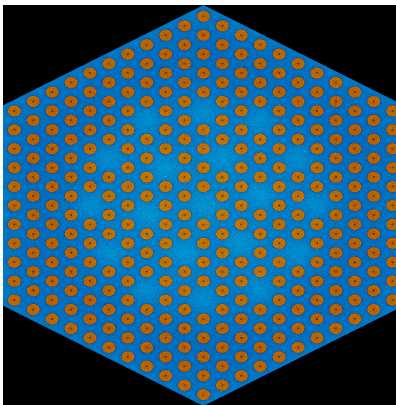


Figure 8-9: Thermal flux plot of FA F130 from SERPENT

In the figure number 8-15 on page 77 there is a flux plot of the whole core, which however is only an illustration, since it is not being used in the coupled calculation.

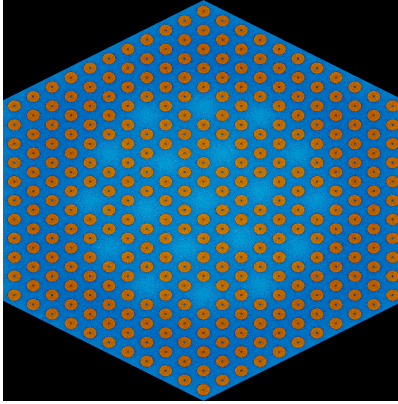


Figure 8-10: Thermal flux plot of FA F200 from SERPENT

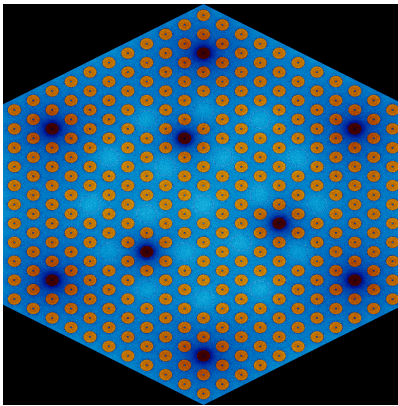


Figure 8-11: Thermal flux plot of FA F30G9 from SERPENT

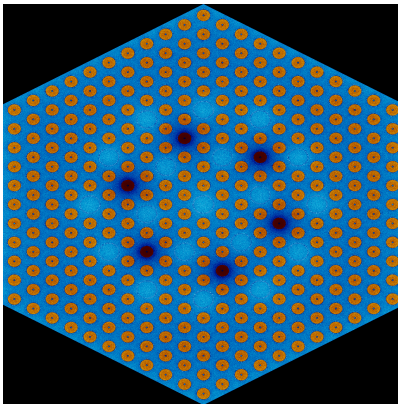


Figure 8-12: Thermal flux plot of FA F40G6 from SERPENT

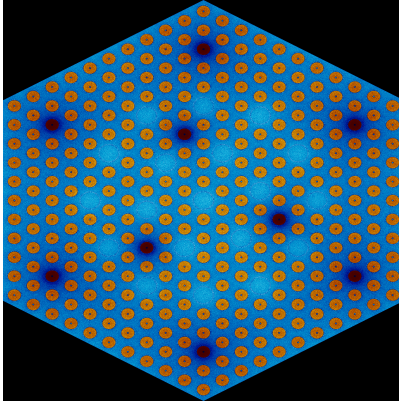


Figure 8-13: Thermal flux plot of FA FF36G9 from SERPENT

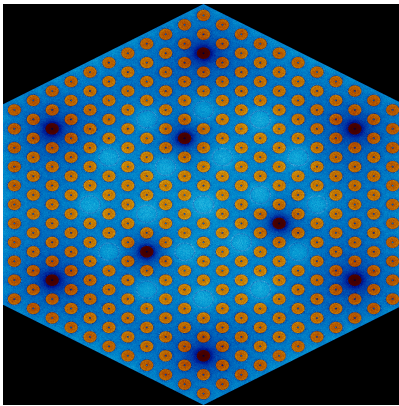


Figure 8-14: Thermal flux plot of FA FF40G9 from SERPENT

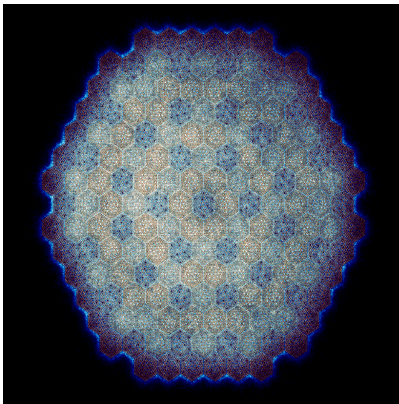


Figure 8-15: Thermal flux plot of the core from SERPENT

8.4 Reference data

While performing similar analyses, an enveloping scenario is chosen, impact of which is most severe and therefore similar scenarios with lower impact or resulting damage can be skipped. In the case of rod ejection the following criteria are regarded as most damaging. To minimize the Doppler effect, the thermal power is set to zero (or in the case of PARCS almost zero like 0.000001% of power) to reach the Hot Zero Power (HZP) mode and all the control rods (groups 7 to 10, see the model description section) are inserted. This is because when they are inserted, the ejection involves a greater positive reactivity insertion. The cross sections are calculated for fresh fuel with 0 burnup. The TRACE model is set for Station Black-Out (SBO) scenario, therefore ECCS system is not operational and no operator action is done. In the figure 8-16 on page 78 is shown the reference bank configuration.

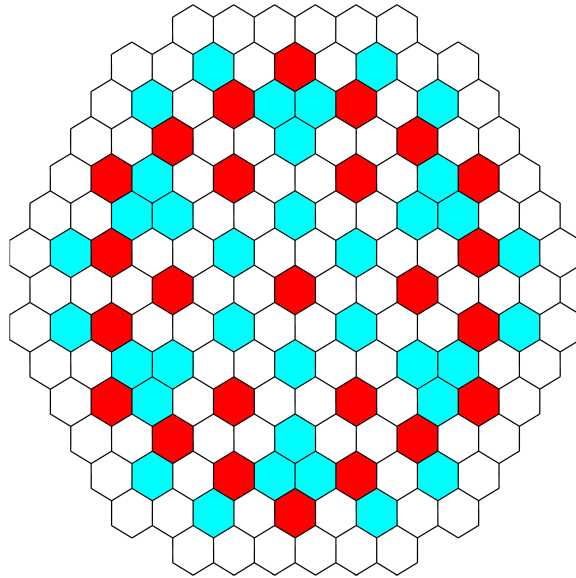


Figure 8-16: Reference state bank configuration. Blue (1-6) Red (7-10)

8.5 Steady state, stand alone, SCALE

The stand alone steady state calculation serves as a verification point of the neutronic model. In this stage the general flux shape, k-effective and normalized power are the key parameters that are analysed. Through the stand alone calculation, the position of control rod ejection is chosen. As it is possible to see in figure 8-17 on page 79, the general power shape is reasonable and when compared with internal documentation of CVR on an existing VVER 1000, both the shape and values are reasonably comparable. The original VVER 1000 normalized power map cannot be shared within this work, because it is a private property.

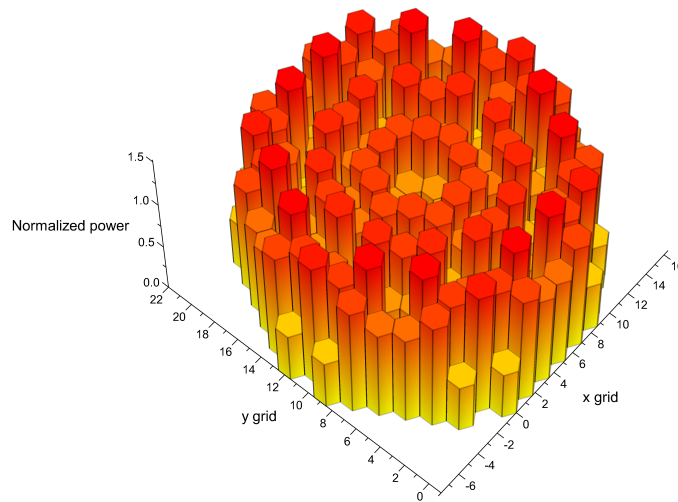


Figure 8-17: Normalized radial power profile for SA PARCS

Both radial and axial normalized power profiles are realistic considering that the reflector is only set by albedo, without actually placing it with the PARCS model. In the correspondence with the normalized power profiles there are the radial and axial

Axial Power Distribution

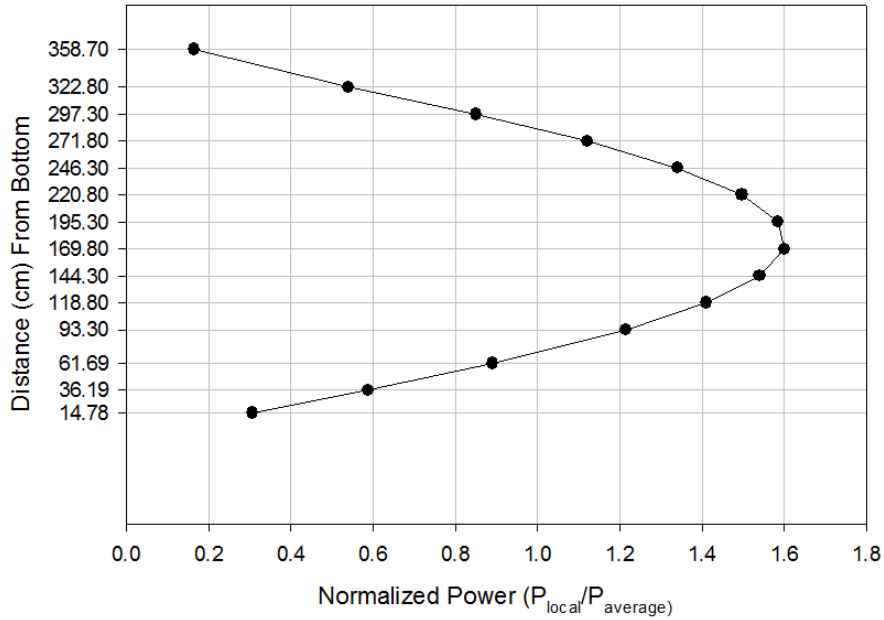


Figure 8-18: Normalized axial power profile for SA PARCS

flux map. In the following plots, there are shown fluxes of both high and thermal energies. There are several reasons why the high energy neutrons have higher flux. First, in general there are many more neutrons in the high energy group, then in thermal. Second, thermal neutrons are more likely to be absorbed by either the fuel or by control rods. Lastly, the reason why this difference is not so large is that fast neutrons have higher probability for leakage. The second point is best seen in figure number 8-22 on page 82, where in radial points 4, 7 and 10 are inserted control rods and thermal flux is significantly lower, then fast flux.

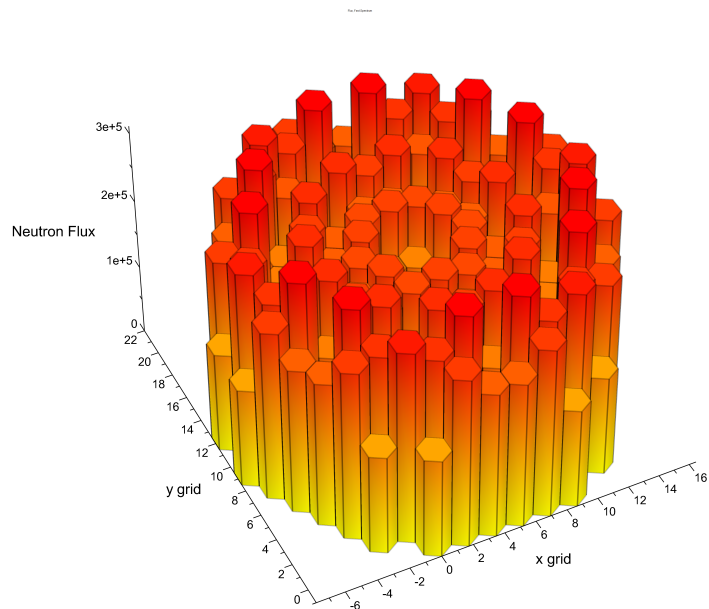


Figure 8-19: Radial flux profile for SA PARCS, fast group

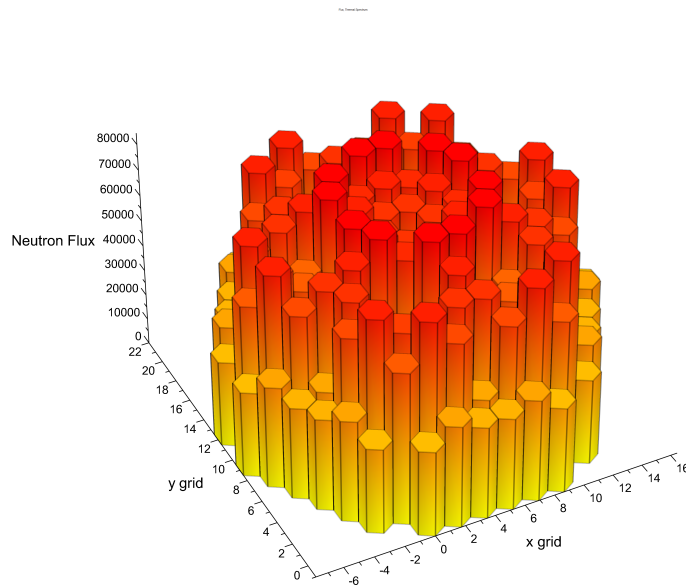


Figure 8-20: Radial flux profile for SA PARCS, thermal group

Axial Flux Distribution

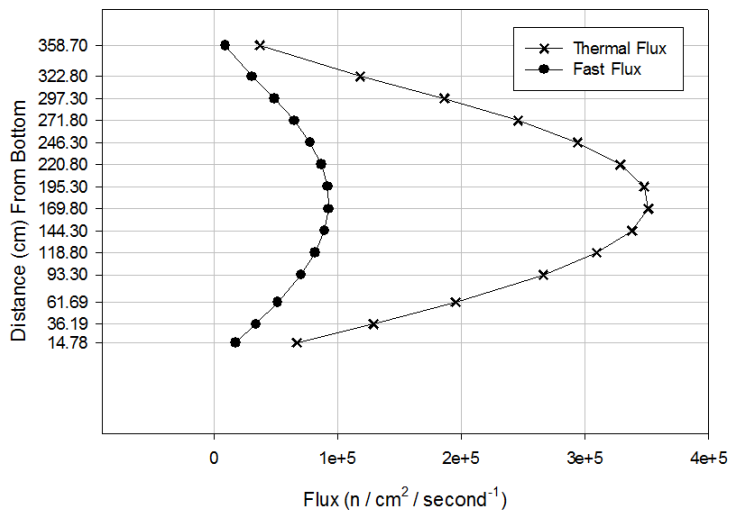


Figure 8-21: Axial flux profile

Central Flux Cross Section

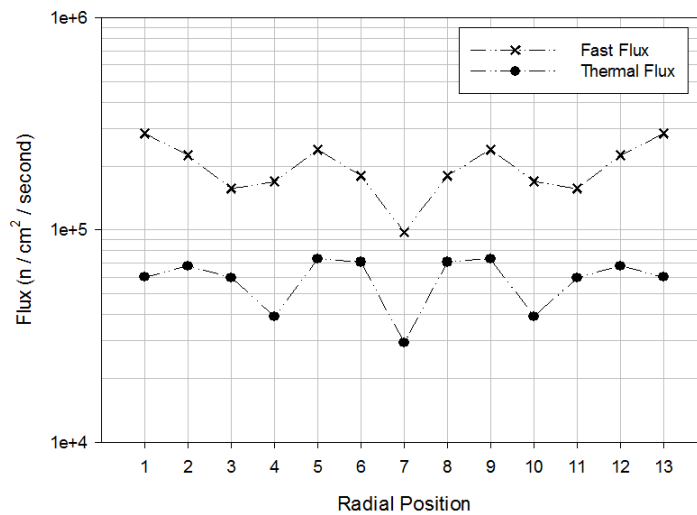


Figure 8-22: Flux profile central cross section

8.6 Steady state, stand alone, SERPENT

The general characteristics explained in the stand alone, steady state SCALE section apply also here. There are noticeable differences between using the two sets of cross sections. Firstly by comparing the normalized power profile it is possible to see a slightly different profile shape. Using SERPENT 2 cross sections, there is a distinctive difference between inner and outer rings. This may be due to a difference in the cross sections causing higher power and therefore the albedo definition may have to be re-evaluated. This also corresponds to the difference in peaking normalized power, where with SERPENT 2 cross sections the peaking power factor is 1.6 while using SCALE calculated cross sections the factor is 1.52. Similarly there is a flux difference between the two. SERPENT 2 model gives for fast and thermal flux values of $3.1\text{E}+5$ and $8.4\text{E}+4$ respectively, while the SCALE model gives $8.6\text{E}+5$ for fast flux and $2.1\text{E}+5$ for thermal flux. All values are in expressed in neutrons per cm^2 per second. The SERPENT 2 cross sections give slightly higher flux and hence the power, than would be expected. It is important to note, that these values as well as the graphs correspond to averaged values for all height of the core, and more precise values for different axial levels is available in the output. Nevertheless using the averaged values is enough to see the general trend of the differences. The high flux peaks at the edge on figures 8-25 and 8-26 on page 85 can be also explained by the albedo definition. However more research and sensitivity analysis have to be performed in the future regarding this issue.

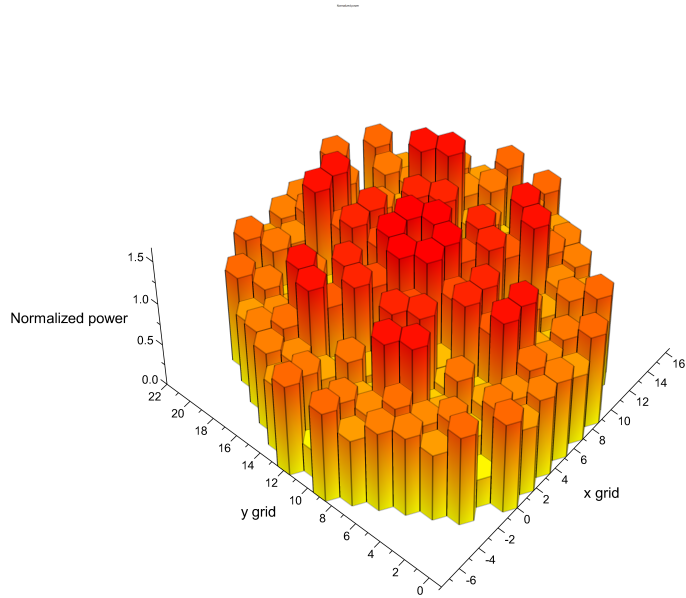


Figure 8-23: Normalized radial power profile for SA PARCS

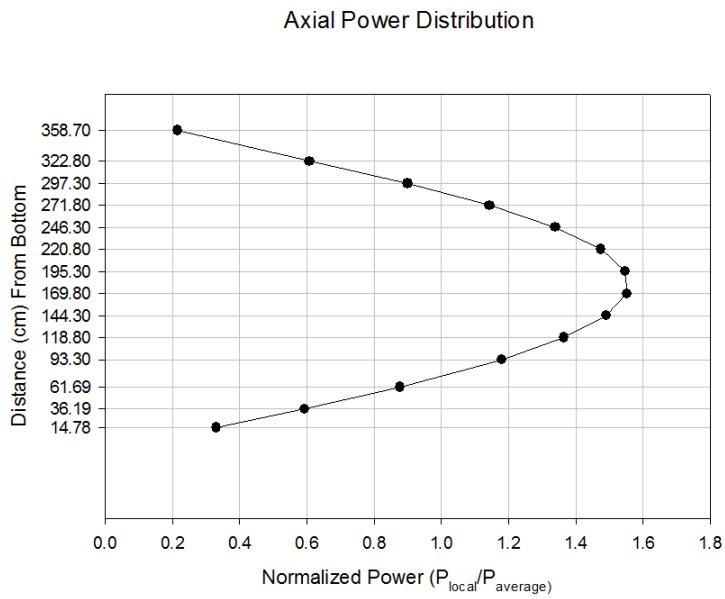


Figure 8-24: Normalized axial power profile for SA PARCS

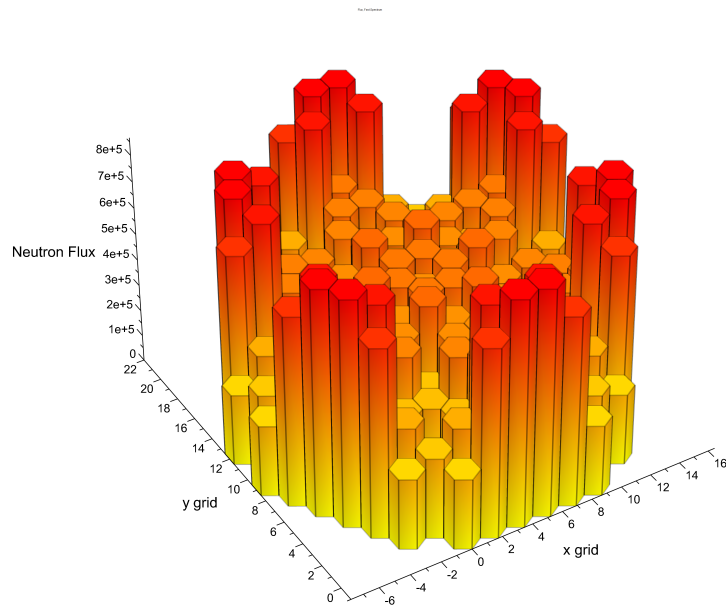


Figure 8-25: Radial flux profile for SA PARCS, fast group

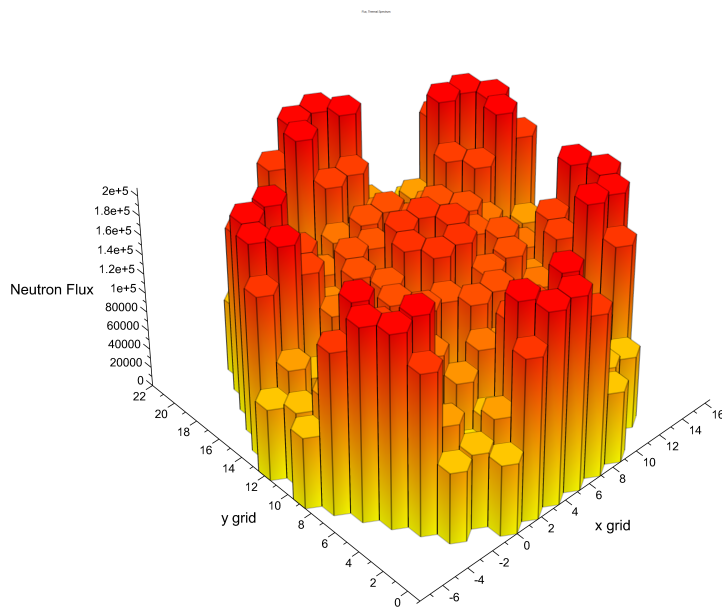


Figure 8-26: Radial flux profile for SA PARCS, thermal group

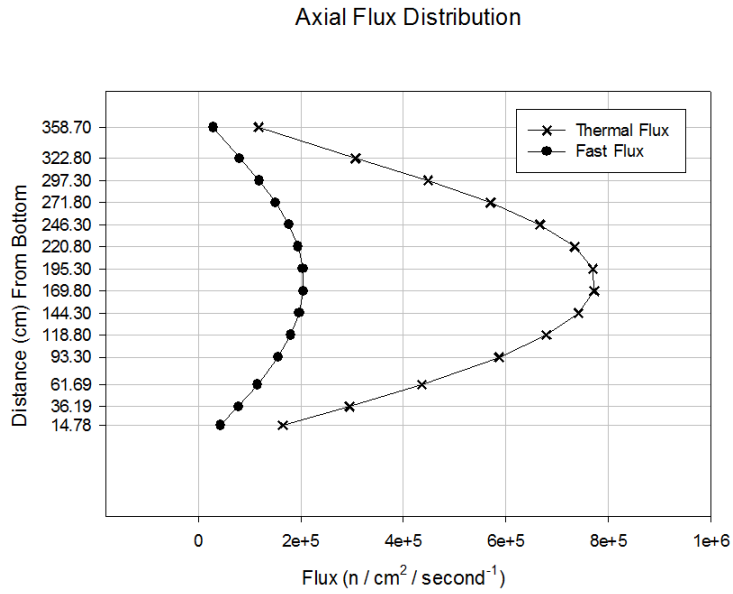


Figure 8-27: Axial flux profile

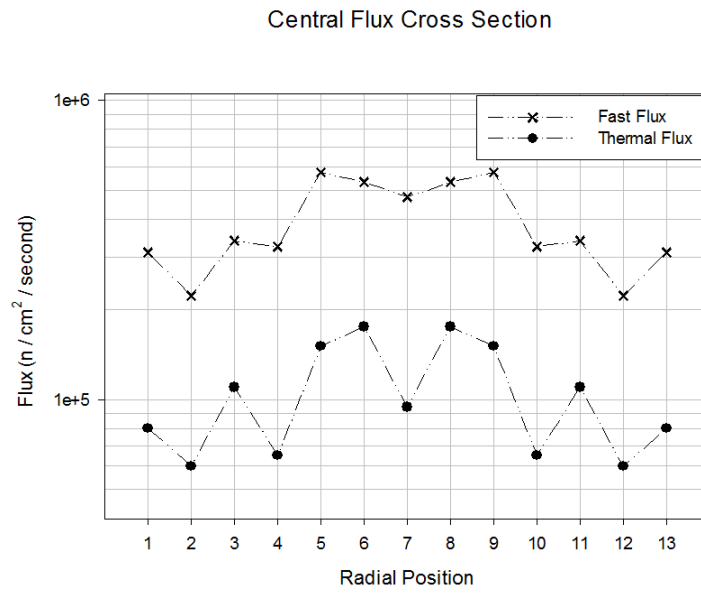


Figure 8-28: Flux profile central cross section

8.7 Steady state, coupled

The steady state coupled calculation serves as a restart point for the transient. The goal of this step is to achieve stabilized state at which later the transient calculation can begin. In this case both versions (SCALE and SERPENT 2) are run for 1000 seconds. This length was agreed upon after consultation with CVR TRACE expert Mr. Kyncl, who suggested that the minimum would be 300 seconds. The results of the steady state do not differ greatly from one another. There is no direct neutronic output, only a restart file to be inserted into the transient calculation. When it is possible to read localised values, the region chosen is in the middle of the core (highest flux) and in the first ring.

SCALE

Results of the Steady State Calculation using SCALE cross sections are shown in table 8.1 on page 87.

Table 8.1: SCALE Steady State coupled results

Parameter	Value	Unit
Maximum average rod temperature	546.55	K
Core saturation temperature	619.82	K
Core temperature	546.77	K
Liquid density	776.17	kg/m ³
Liquid mass flow	19200	kg/s
Total reactor power	3.00E+06	W

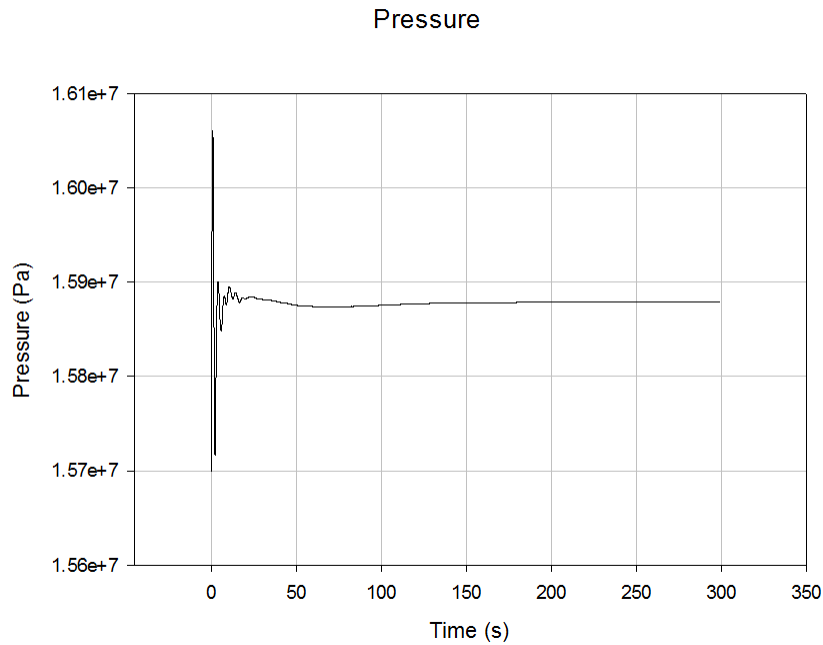


Figure 8-29: Steady State, Coupled pressure

SERPENT 2

Results of the Steady State Calculation using SERPENT 2 cross sections are shown in table 8.2 on page 88. Pressure in the Steady State Coupled SERPENT 2 calculation is identical to Steady State Coupled SCALE shown in figure 8-29 on page 88.

Table 8.2: SERPENT Steady State coupled results

Parameter	Value	Unit
Maximum average rod temperature	544.71	K
Core saturation temperature	619.82	K
Core temperature	546.77	K
Liquid density	779.19	kg/m ³
Liquid mass flow	19200	kg/s
Total reactor power	3.00E+06	W

8.8 Transient, PARCS/TRACE coupled

8.8.1 Sequence description

According to the steady state PARCS results, the position of the control rod bank to be ejected has to be in the highest flux region. However because the highest point is in the position of a SCRAM bank, the closest position is used instead. Figure 8-30 on page 90 shows in red the SCRAM bank positions and control rod bank to be ejected in yellow.

The following scenarios will be calculated and analysed. First, the rod ejection at zero power without SCRAM and second, also at zero power but in this case, SCRAM occurs one second after the ejection. The zero power scenario was chosen as the enveloping one, because the Doppler feedback from fuel is at its lowest when at zero power. During normal operation, all banks (SCRAM and control) are fully withdrawn and the reactivity excess is managed only by adjusting boron concentration in the coolant. Therefore this scenario is most probably when at hot zero power, before the start up of the reactor.

The total calculation time is set to 500 seconds, however for the ATWS TRACE terminates the calculation after approximately 150 second, due to time-step error. However, since transient itself is rather fast (only a few seconds), termination in 150 seconds is sufficient.

During the first few seconds of the simulation, there are small oscillations in several properties such as reactivity, fuel and moderator/coolant temperature. The total reactivity stabilizes at about 0.2 \$, which is most likely due to the absence of boron in coolant. This absence is not yet fully understood, since there is non-zero boron concentration set and found in both stand alone steady state and coupled steady

state calculations. Therefore in order to have the initial boron concentration zero, more work and more information about these codes is needed.

The initial oscillations last for about 10 seconds, for the purposes of clearer plots, the first 13 seconds will be skipped.

The system stabilizes at around 9 seconds, which is why the rod ejection is set to occur at 15 seconds and the detailed time tables are shown in each scenario.

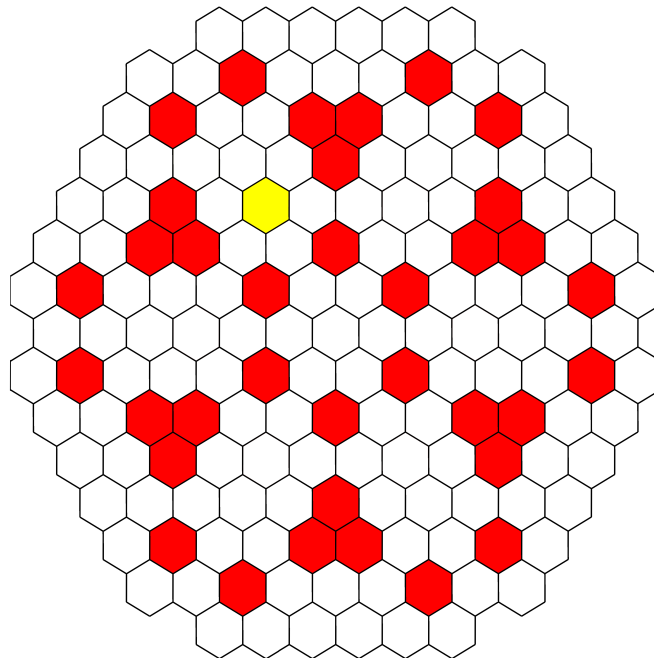


Figure 8-30: Ejected bank position

Because the implemented SCRAM function of PARCS does not function properly, a manual override is used to set SCRAM at 1 second after the rod ejection and the time of insertion is 1 second. Therefore groups 1 to 6 are fully inserted in 0.1 second. At the same time of the ejection a SBLOCA is triggered to simulate opening in the pressure vessel. After consulting excerpts of the Research Centre Rez and using a

safety report of an existing VVER 1000, the size of the break is agreed to be 50 mm in diameter. After the SCRAM there is no operator action until the end of simulation at 500 s.

For the transient calculations and analyses, all plots will be showing data after the rod ejection accident, since the state before is equal to the one in stand alone calculations.

8.8.2 Rod Ejection without SCRAM, SCALE

The oscillations at the beginning of the simulation are being neglected as mentioned before, however there are a few possible explanations for them. Probably the biggest impact has so called null factor, which acts as a balancing reactivity factor. In the case during the transient calculation, if the k-effective differs from 1, this null factor acts to balance reactivities to achieve $k\text{-eff} = 1$. The bigger the difference between k-effective actual and 1, the bigger the null factor. Another possible reason for these oscillations are the cross sections themselves and more tuning may be needed. This major reason is the lack of boron reactivity feedback, which still remains to be a problem. This is suspected to be the reason why the reactivity stabilizes at 0.2 \$ (see figure number 8-48). Lastly the minor source of these oscillations is the instability transition of TRACE from steady state to transient calculation. Because the access to the source code of either PARCS or TRACE is limited, the only way of addressing these uncertainties is through benchmarking with existing results.

The general progression of the transient calculation is shown in the table 8.3, the times chosen are 5 seconds before the rod ejection, which in the table occurs at 0 seconds. Then the data are shown for five, ten and 100 seconds after the rod ejection. The power progression is shown in figure 8-31 and it will serve as a main guide for this analysis. There are in total five power peaks in this simulation, while the first two are the most interesting ones.

When the control bank ejects, there is about 1\$ of positive reactivity inserted to the system, resulting higher neutron flux, this resulting in higher fuel temperature (Figure number 8-50) and also causing a rise of the Doppler temperature. Therefore the Doppler effect introduces negative reactivity to the system, decreasing power. This heat is being transferred to the coolant, resulting in increase of coolant temperature

(Figure number 8-49). When the temperature of the coolant (in this case light water) increases, the density decreases (Figure number 8-53) resulting in lower moderation hence decrease in flux, reactivity and power. This is the general behaviour, that occurs in all the peaks. The first peak is so small, because the localised rise in coolant temperature is stopped when it is cooled down by rest of the coolant in the core. However quickly after the power start rising again and the whole process described above occurs again, however much more slowly. The final oscillations show simple balancing between moderator density and moderator temperature. By comparing the results with the chapter 15 of Final Safety Analysis Report of an existing VVER 1000, which unfortunately cannot be shown, the results are fairly comparable also with the results of [9].

By examining the flux behaviour we can see, that in 100 seconds the flux increases during the transient. This can be seen in figures from number 8-34 to 8-47 on pages from 97 to 104. The flux shape is actually one of the major reasons why to use 3D calculations. By examining the flux plots below, most of the core has fairly low flux, in comparison to the area around the ejection point. By using the standard approach of point kinetics, the results would be averaged over the whole core, therefore lower than the actual highest peak.

In the meantime, when the control bank ejects, the driving mechanism breaks and is ejected from the pressure vessel, resulting in a small break LOCA of a 50 mm diameter. The loss of coolant is represented by the mass flow in the figure number (8-55), however for the duration of the transient, SB LOCA has very little effect as seen from the system pressure in figure 8-56. There are pressure oscillations close after ejection, however it stabilizes at the end of the transient.

Table 8.3: Chronological sequence of the events

Time (s)	Event Category	Parameter	Value or cause	Unit
-5.00	Value	Primary Pressure	1.59E+07	Pa
-5.00	Value	Power	3.12E+00	W
-5.00	Value	Max hot rod temperature	5.58E+02	K
-5.00	Value	Liquid Density	7.60E+02	kg/m3
-5.00	Value	Liquid Temperature	5.56E+02	K
-5.00	Value	Total reactivity	1.40E-01	\$
0.00	Event	Rod Ejection	Initiated event	-
0.00	Event	SB LOCA	Time triggered	-
1.00	Value	Primary Pressure	1.60E+07	Pa
1.00	Value	Power	2.77E+05	W
1.00	Value	Max hot rod temperature	5.56E+02	K
1.00	Value	Liquid Density	7.62E+02	kg/m3
1.00	Value	Liquid Temperature	5.55E+02	K
1.00	Value	Total reactivity	9.83E-01	\$
1.01	Event	SCRAM	NO	-
5.00	Value	Primary Pressure	1.59E+07	Pa
5.00	Value	Power	7.28E+08	W
5.00	Value	Max hot rod temperature	5.80E+02	K
5.00	Value	Liquid Density	7.59E+02	kg/m3
5.00	Value	Liquid Temperature	5.56E+02	K
5.00	Value	Total reactivity	5.05E-01	\$
10.00	Value	Primary Pressure	15854938	Pa
10.00	Value	Power	8.71E+08	W
10.00	Value	Max hot rod temperature	588.02429	K
10.00	Value	Liquid Density	757.98785	kg/m3
10.00	Value	Liquid Temperature	557.02478	K
10.00	Value	Total reactivity	0.33761412	\$
100.00	Value	Primary Pressure	15868823	Pa
100.00	Value	Power	8.78E+08	W
100.00	Value	Max hot rod temperature	596.10187	K
100.00	Value	Liquid Density	745.43872	kg/m3
100.00	Value	Liquid Temperature	563.87952	K
100.00	Value	Total reactivity	0.062670238	\$

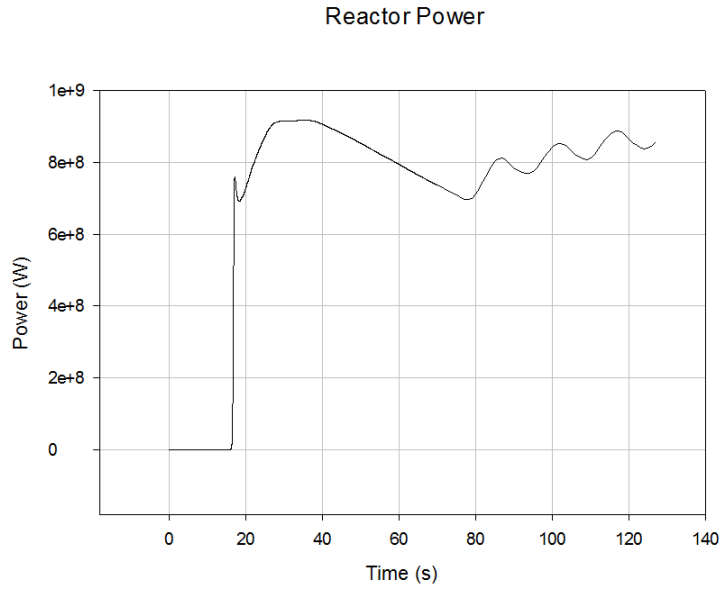


Figure 8-31: Core power

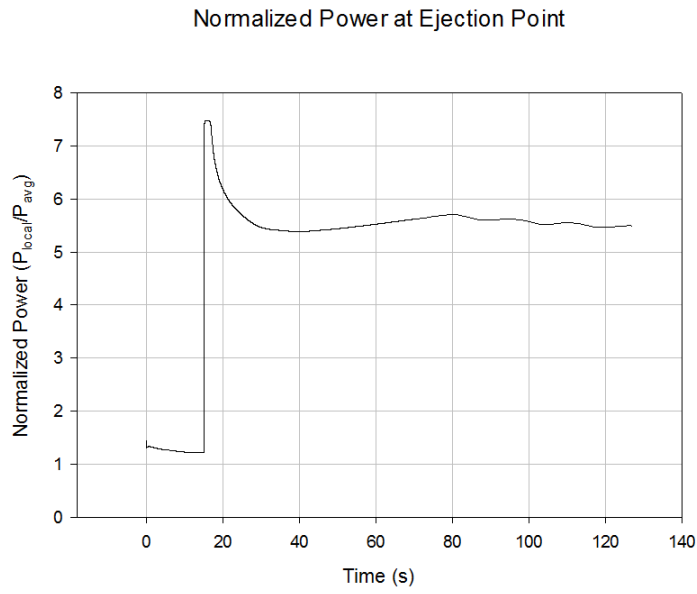


Figure 8-32: Normalized power at ejection point

In order to calculate the main parameter, which is amount of energy per gram (cal/g), it is necessary to integrate over one second the relative power in the ejection point and then multiply by the total power at peak [W] over number of assemblies (Na, 163). Using the hot channel radial peak factor (PF) 1.29 (given through internal communication with VVER 1000 FA specialists) and dividing the total weight of fuel (approximately 470 kg) in one assembly by the number of pins (311). The general calculation is following, having time step t (s), average power (P) [W] and normalized power at ejection point (R_p) [-]. First it is important to calculate power in Watts (W_r) for the ejection point.

$$W_r = P \cdot R_p \cdot \frac{PF}{Na} \quad (8.1)$$

After that by integrating the W_r curve per time and so getting the energy per time [J], it is necessary to convert to calories ($1J = 0.239$ calories) and divide by weight of fuel in one pin in grams. The expected results should be similar to [9] which is 70.5 cal/g. The results are shown in figure 8-33 and it is possible to see, that the maximum value is 75 cal/g and therefore below the limit of 200 cal/g and also that it is reasonably similar to the results of [9], considering the differences in tested reactors.

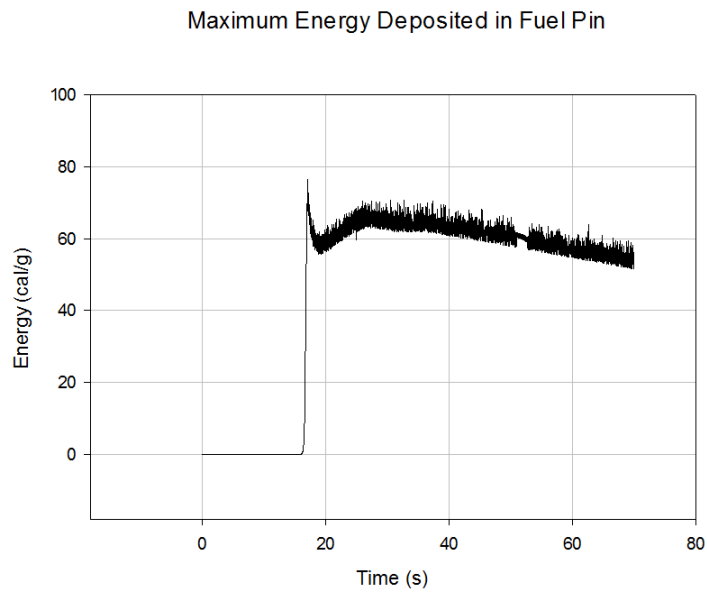


Figure 8-33: Maximum energy deposited in fuel pin

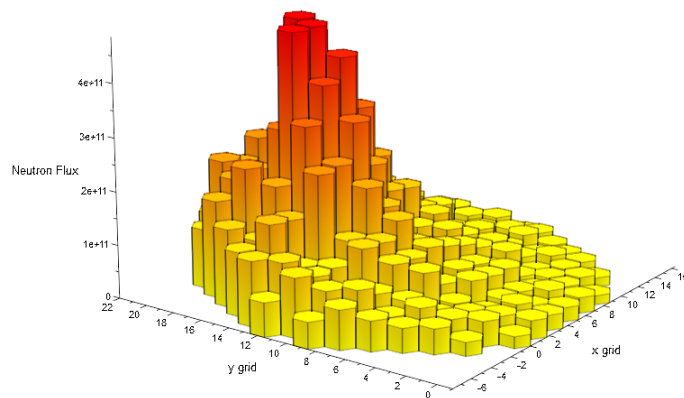


Figure 8-34: Averaged fast flux

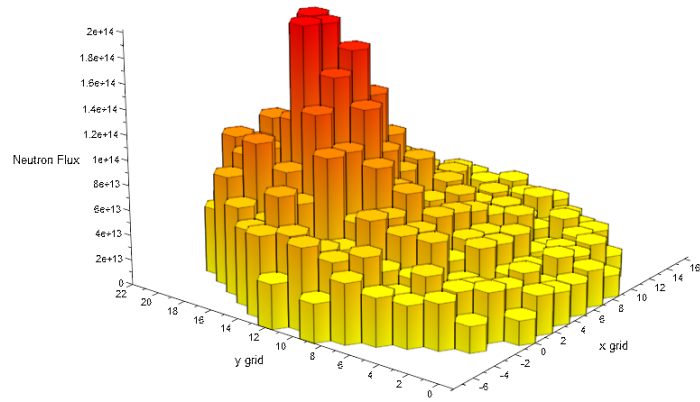


Figure 8-35: Averaged fast flux after 100 s

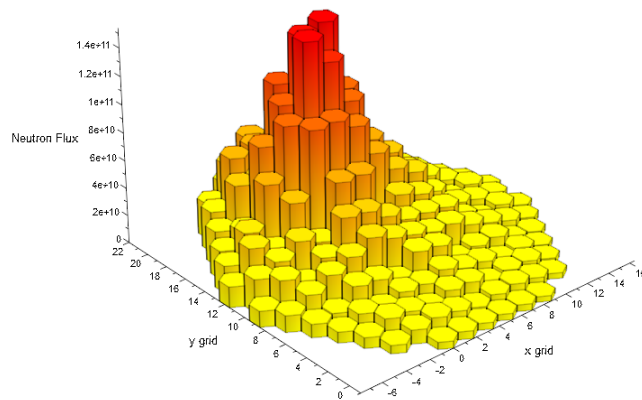


Figure 8-36: Averaged thermal flux

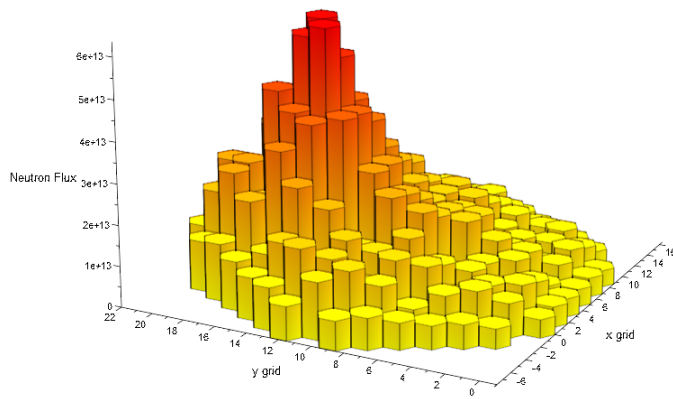


Figure 8-37: Averaged thermal flux after 100 s

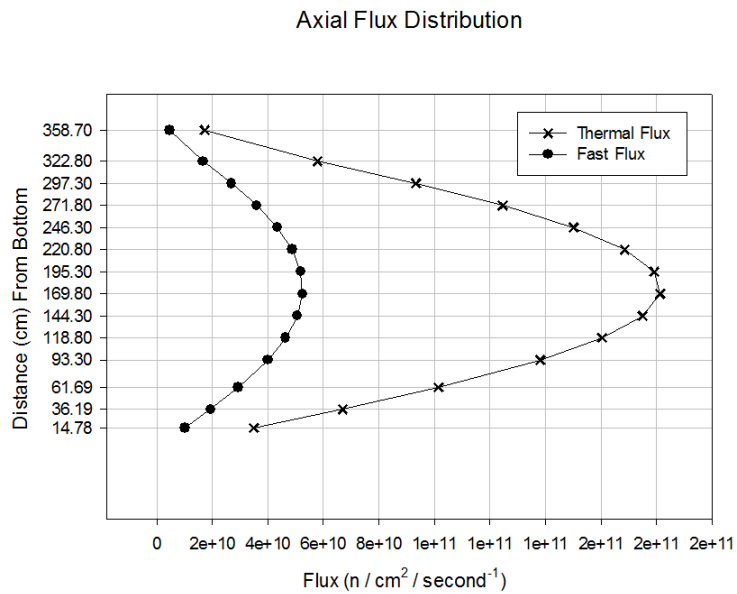


Figure 8-38: Axial flux profile

Axial Flux Distribution

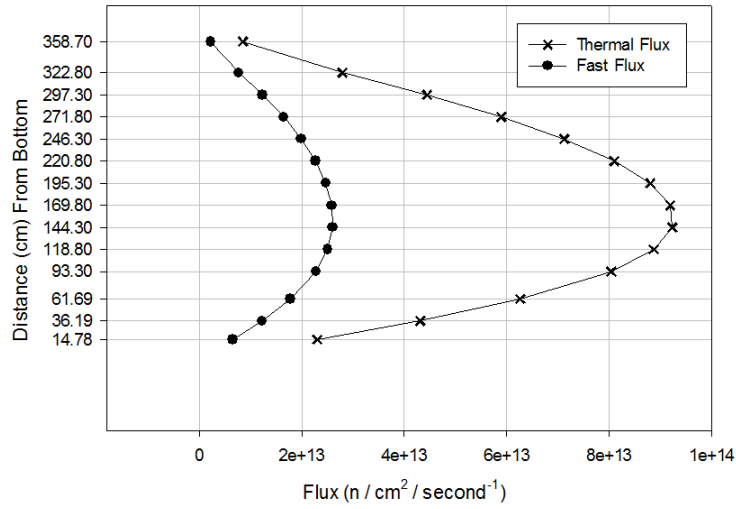


Figure 8-39: Axial flux profile after 100 s

Central Flux Cross Section

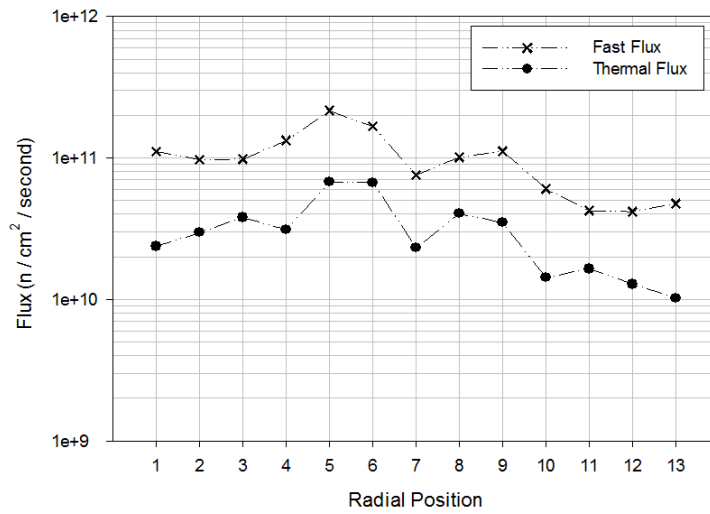


Figure 8-40: Flux profile central cross section

Central Flux Cross Section

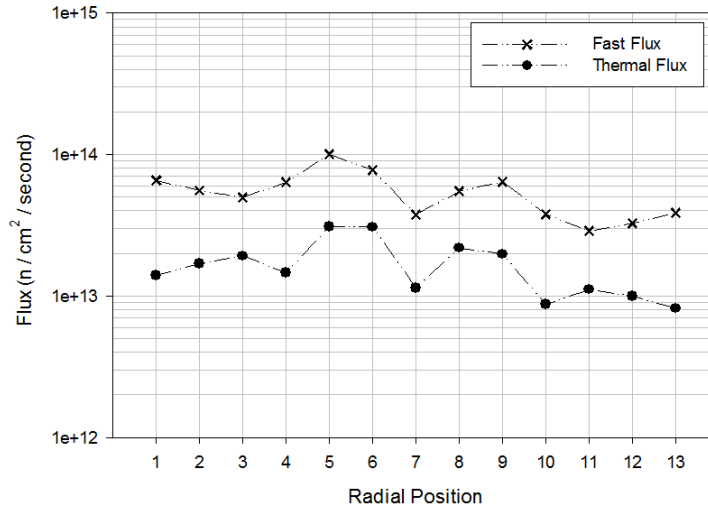


Figure 8-41: Flux profile central cross section after 100 s

Flux Cross Section at Ejection Point

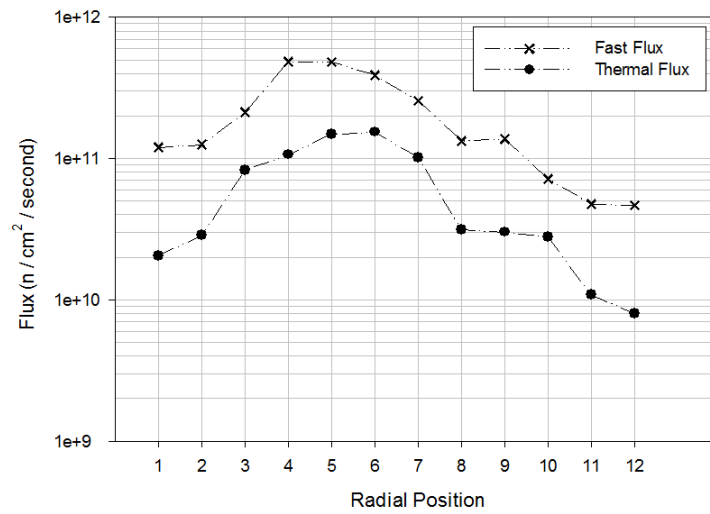


Figure 8-42: Flux profile cross section at ejection point

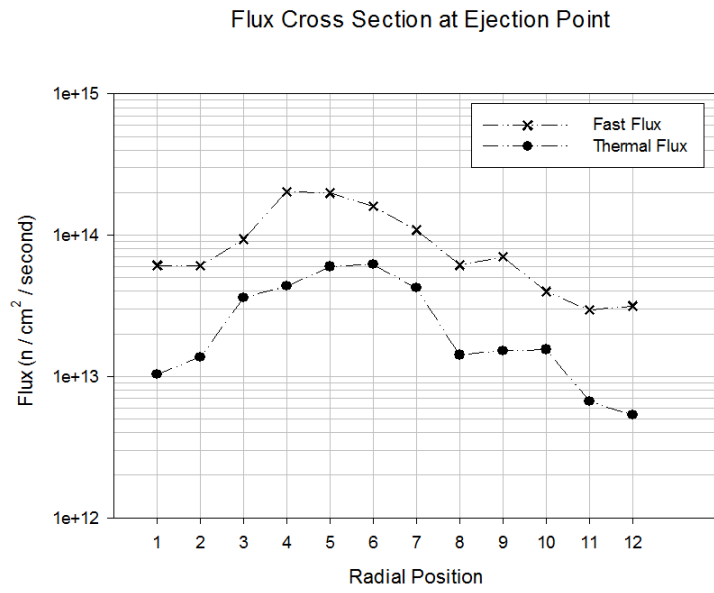


Figure 8-43: Flux profile cross section at ejection point after 100 s

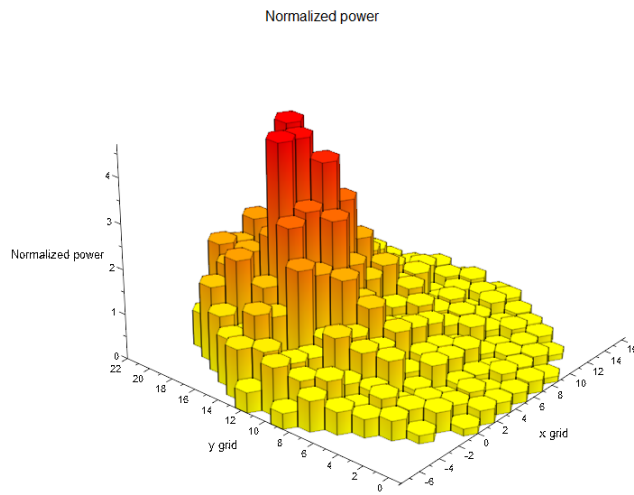


Figure 8-44: Averaged radial normalized power profile

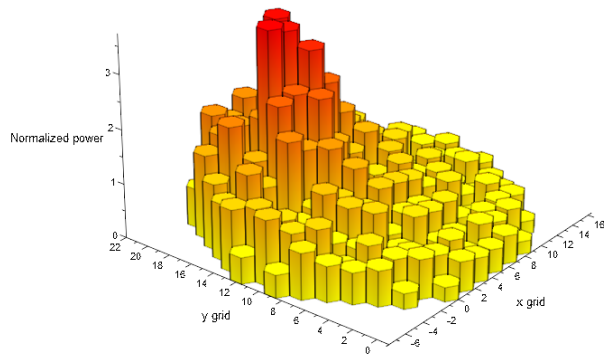


Figure 8-45: Averaged radial normalized power profile after 100 s

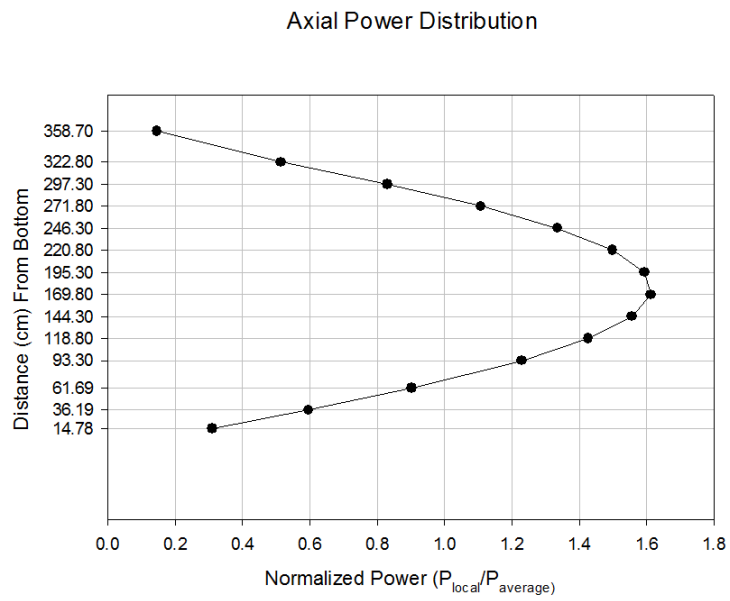


Figure 8-46: Axial normalized power

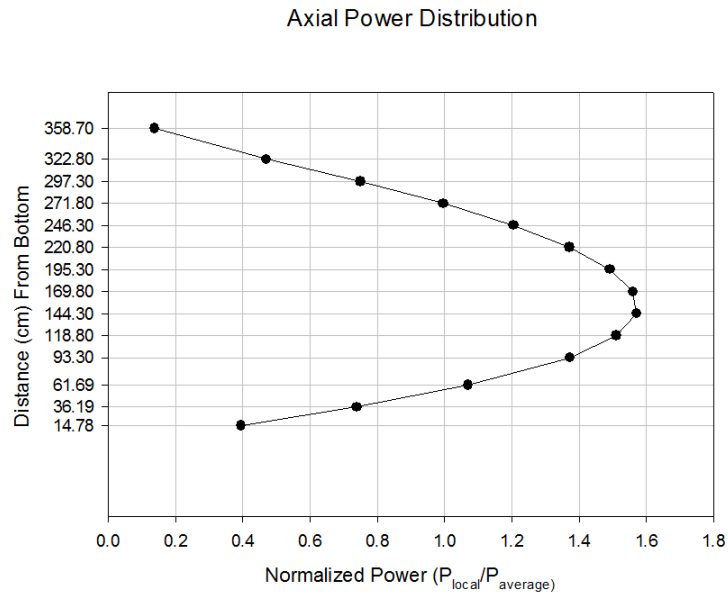


Figure 8-47: Axial normalized power after 100 s

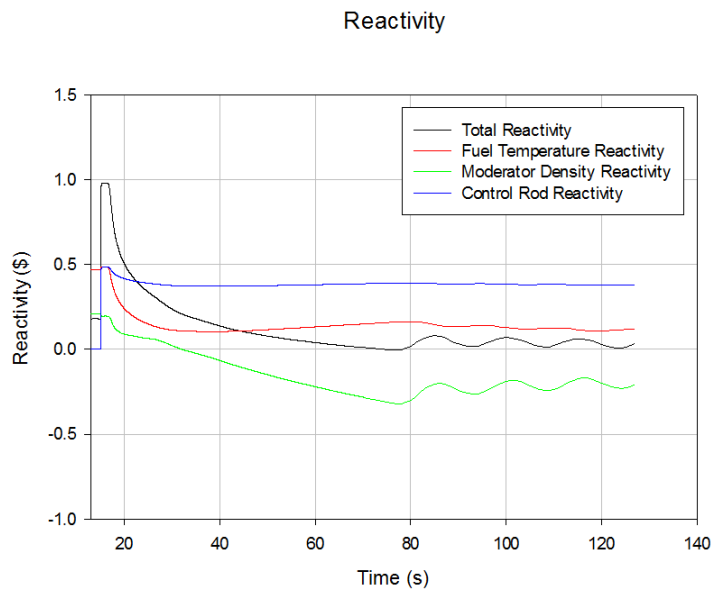


Figure 8-48: Reactivity

Coolant Temperature at Ejection Point

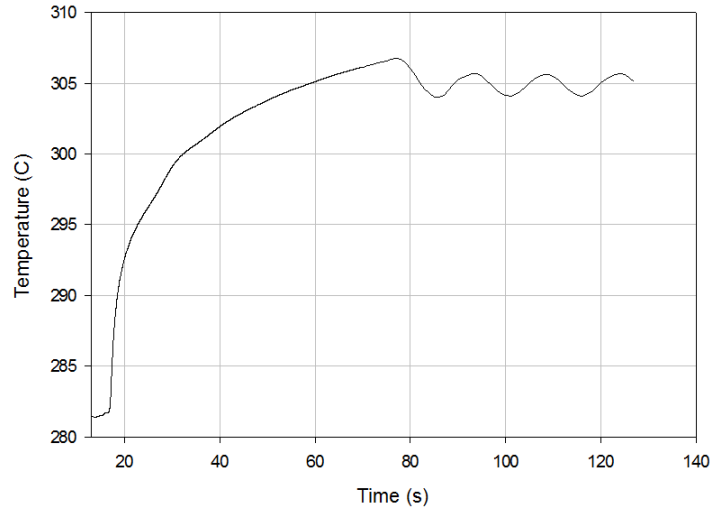


Figure 8-49: Coolant temperature at ejection point

Fuel Temperature at Ejection Point

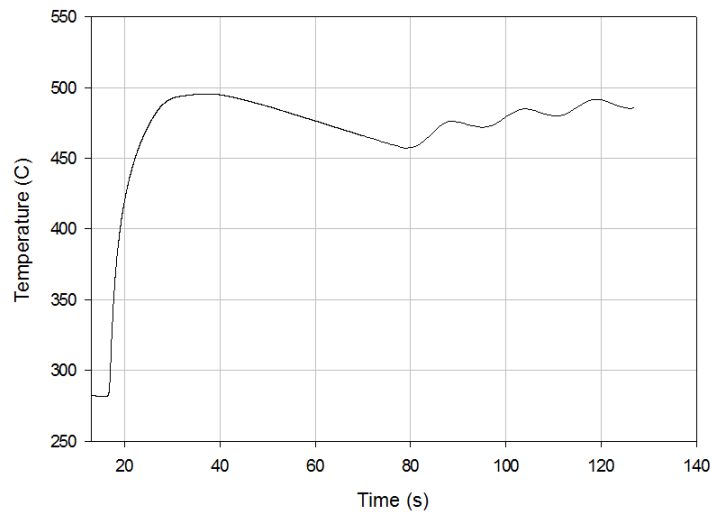


Figure 8-50: Fuel temperature at ejection point

Maximum Hot Rod Temperature

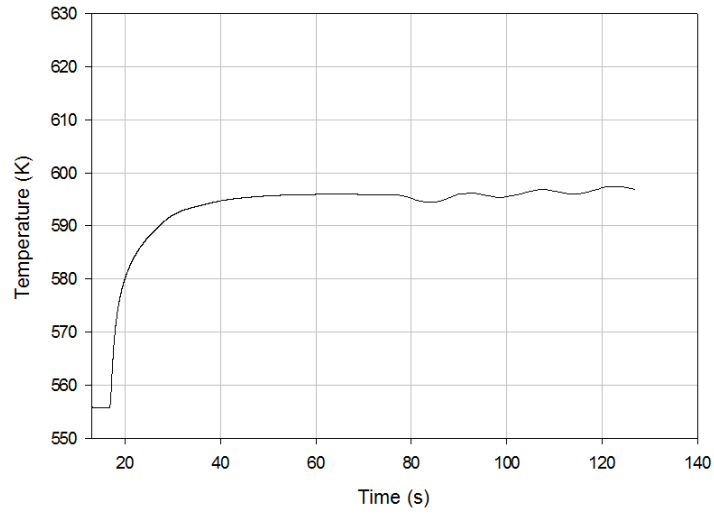


Figure 8-51: Maximal hot rod temperature

Liquid Density

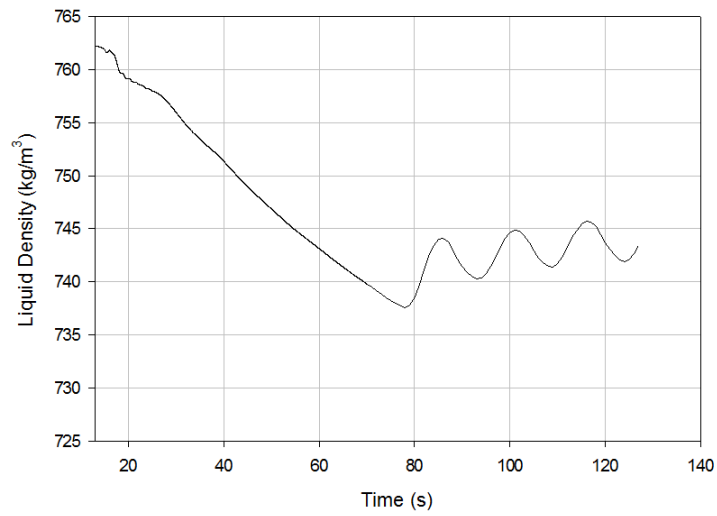


Figure 8-52: Averaged liquid density

Coolant Density at Ejection Point

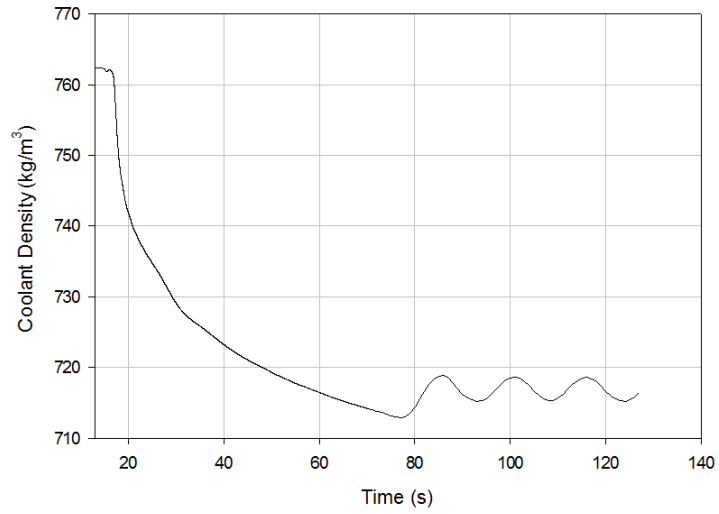


Figure 8-53: Coolant density at ejection point

Liquid Temperature

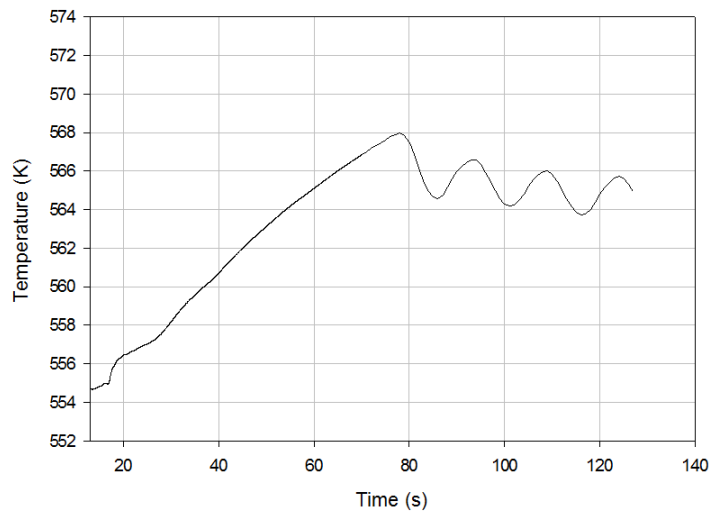


Figure 8-54: Averaged liquid temperature

Liquid Mass Flow Through Break

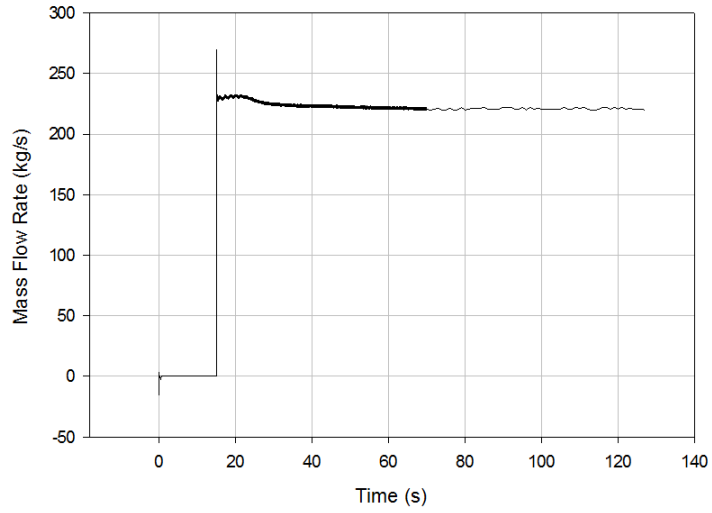


Figure 8-55: Mass flow through the break

Pressure

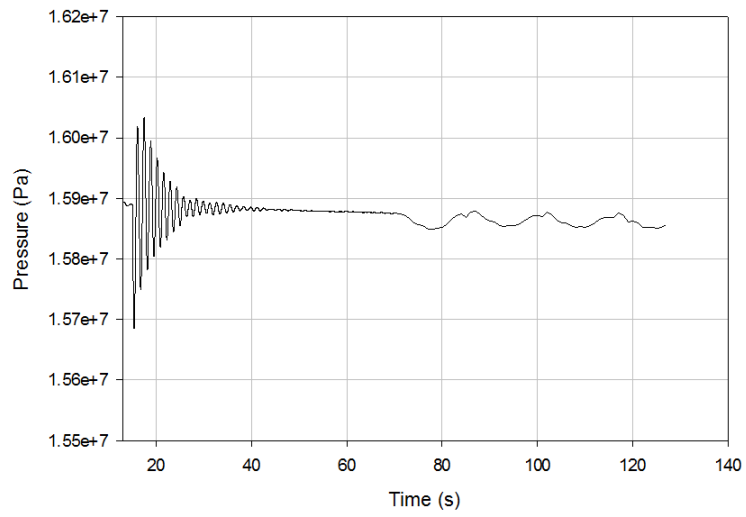


Figure 8-56: System Pressure

8.8.3 Rod Ejection with SCRAM, SCALE

During normal operation, in case the rod ejection accident occurs, all shut-down and control rods are inserted into the reactor, introducing a large amount of negative reactivity (about -7 \$), cutting down power (See figure number 8-57) to zero. The flux however is not immediately effected by SCRAM and only slowly decreases, unlike the power. It is interesting to see the difference in flux between the central cross section of the core and with the cross section at the point of ejection (see figures 8-74 and 8-71 on pages 119 and 117 respectively). There is nicely visible the distinctive difference between the two regions, which is a clear advantage of a 3D calculation, as mentioned above. By examining the axial flux shapes it is noticeable the difference between before and after SCRAM shape, when after the SCRAM the flux peak is pushed downwards as well as the axial normalized power profile.

Because SCRAM occurred only one second after the ejection, the fuel temperature did not rise and after the scram the coolant temperature decreased with an increase of coolant density. Also the separate reactivity components in figure 8-80 on page 122.

Table 8.4: Chronological sequence of the events

Time (s)	Event Category	Parameter	Value or cause	Unit
-5.00	Value	Primary Pressure	1.59E+07	Pa
-5.00	Value	Power	3.12E+00	W
-5.00	Value	Max hot rod temperature	5.58E+02	K
-5.00	Value	Liquid Density	7.60E+02	kg/m3
-5.00	Value	Liquid Temperature	5.56E+02	K
-5.00	Value	Total reactivity	1.40E-01	\$
0.00	Event	Rod Ejection	Initiated event	-
0.00	Event	SB LOCA	Time triggered	-
1.00	Value	Primary Pressure	1.60E+07	Pa
1.00	Value	Power	2.77E+05	W
1.00	Value	Max hot rod temperature	5.56E+02	K
1.00	Value	Liquid Density	7.62E+02	kg/m3
1.00	Value	Liquid Temperature	5.55E+02	K
1.00	Value	Total reactivity	9.83E-01	\$
1.01	Event	SCRAM	YES	-
5.00	Value	Primary Pressure	1.59E+07	Pa
5.00	Value	Power	1.42E+03	W
5.00	Value	Max hot rod temperature	5.55E+02	K
5.00	Value	Liquid Density	7.63E+02	kg/m3
5.00	Value	Liquid Temperature	5.54E+02	K
5.00	Value	Total reactivity	-6.00E+00	\$
10.00	Value	Primary Pressure	1.59E+07	Pa
10.00	Value	Power	5.62E+02	W
10.00	Value	Max hot rod temperature	5.54E+02	K
10.00	Value	Liquid Density	7.64E+02	kg/m3
10.00	Value	Liquid Temperature	5.54E+02	K
10.00	Value	Total reactivity	-5.91E+00	\$
100.00	Value	Primary Pressure	1.59E+07	Pa
100.00	Value	Power	1.33E+01	W
100.00	Value	Max hot rod temperature	5.51E+02	K
100.00	Value	Liquid Density	7.71E+02	kg/m3
100.00	Value	Liquid Temperature	5.49E+02	K
100.00	Value	Total reactivity	-5.62E+00	\$

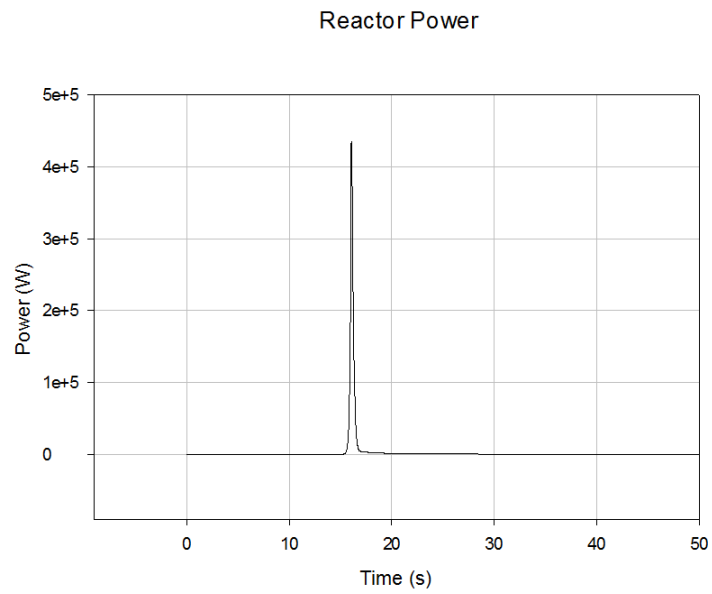


Figure 8-57: Core power

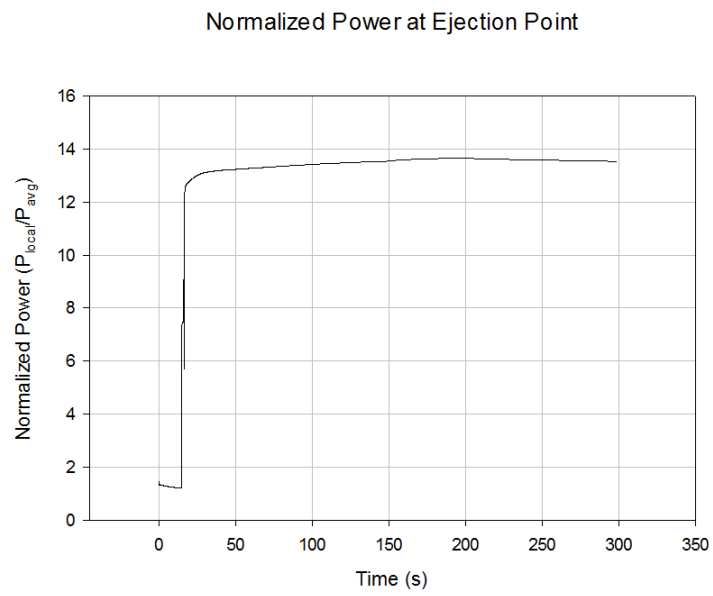


Figure 8-58: Normalized power at ejection point

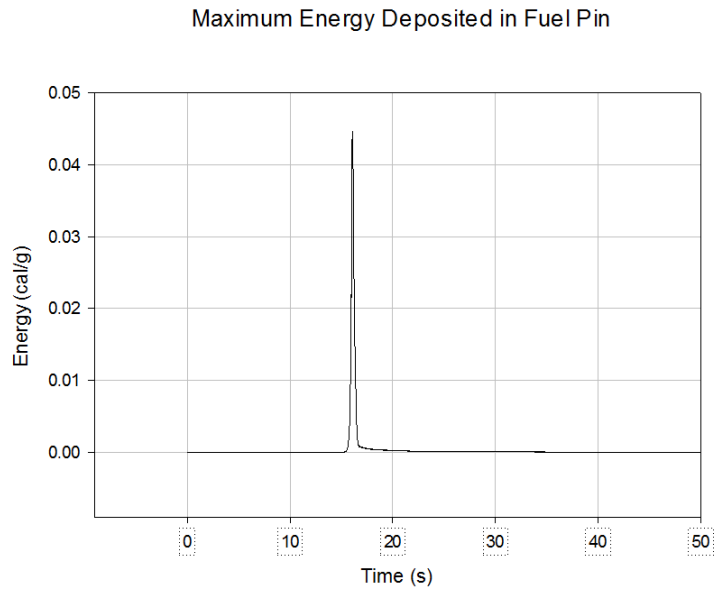


Figure 8-59: Maximum energy deposited in fuel pin

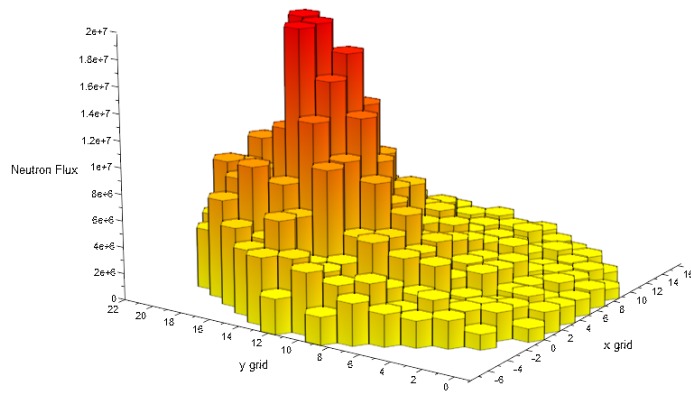


Figure 8-60: Averaged fast flux

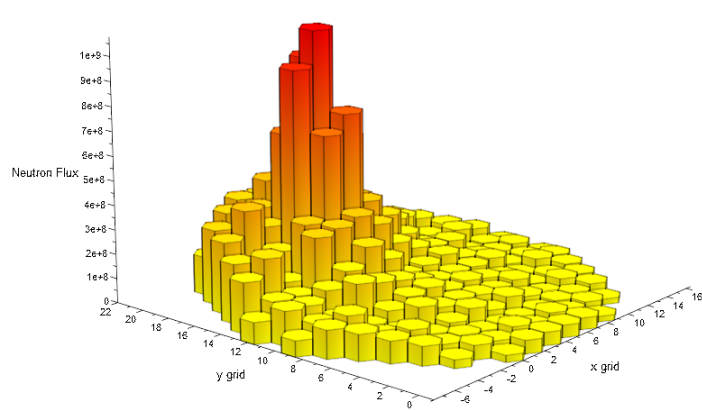


Figure 8-61: Averaged fast flux after SCRAM

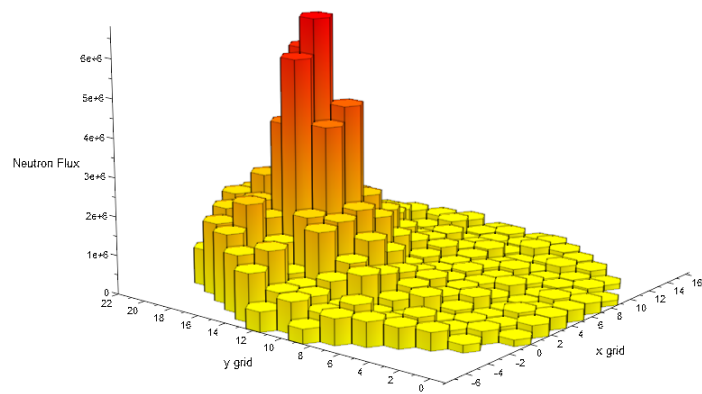


Figure 8-62: Averaged fast flux after SCRAM after 100 s

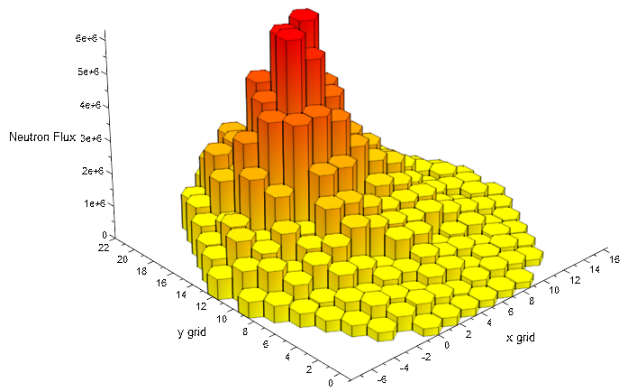


Figure 8-63: Averaged thermal flux

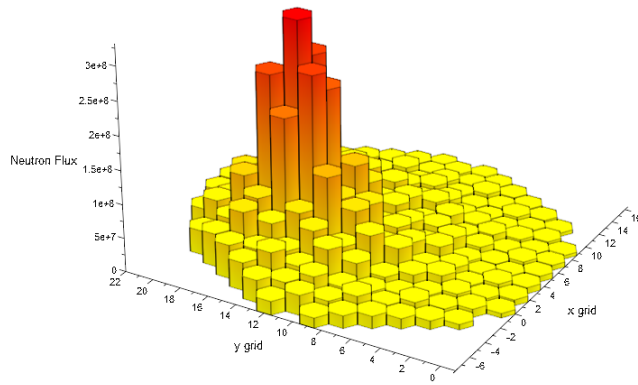


Figure 8-64: Averaged thermal flux after SCRAM

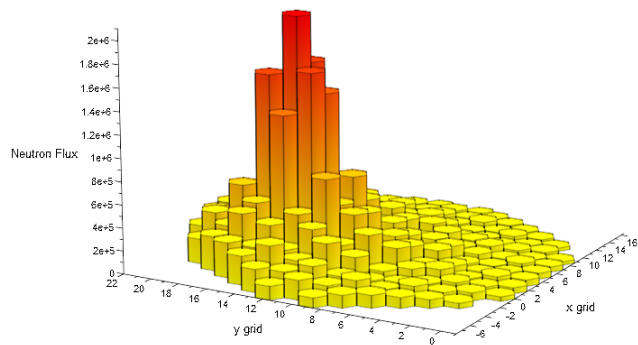


Figure 8-65: Averaged thermal flux after SCRAM after 100 s

Axial Flux Distribution

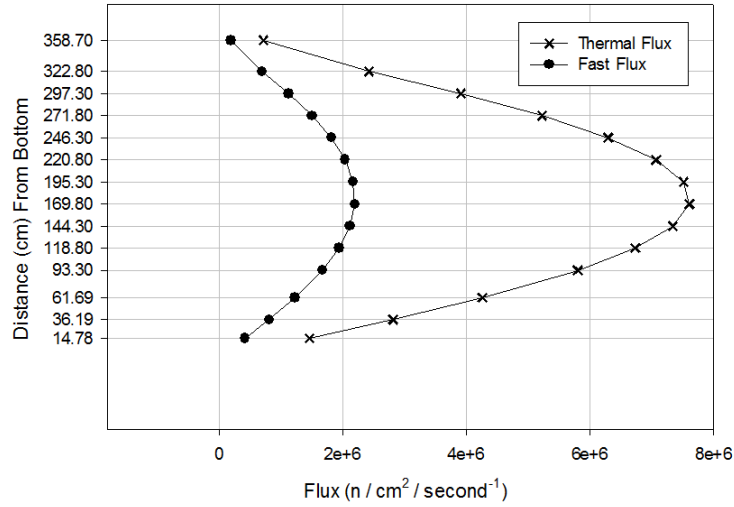


Figure 8-66: Axial flux profile

Axial Flux Distribution

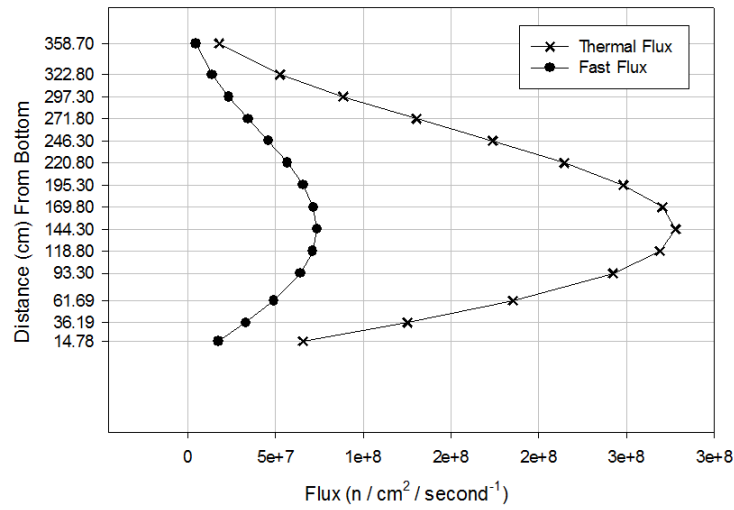


Figure 8-67: Axial flux profile after SCRAM

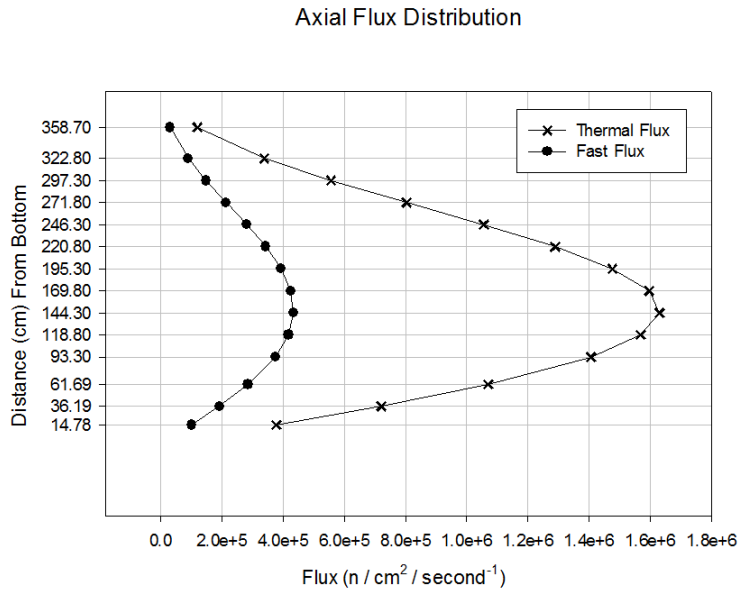


Figure 8-68: Axial flux profile after SCRAM after 100 s

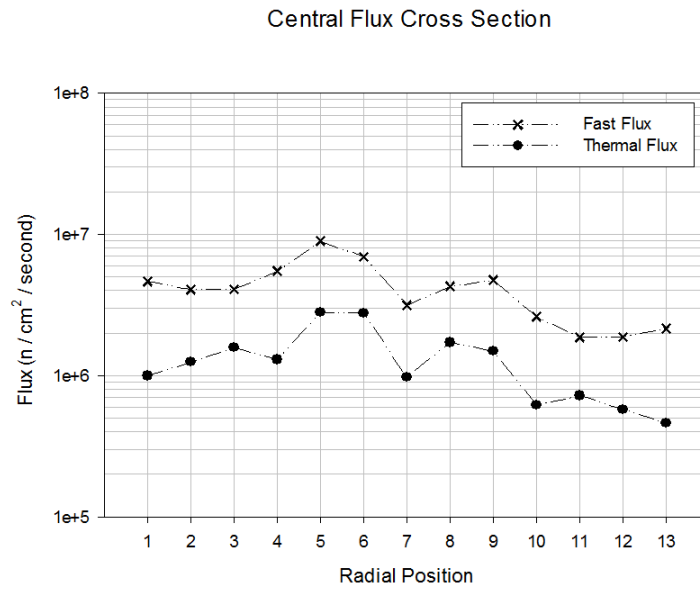


Figure 8-69: Flux profile central cross section

Central Flux Cross Section

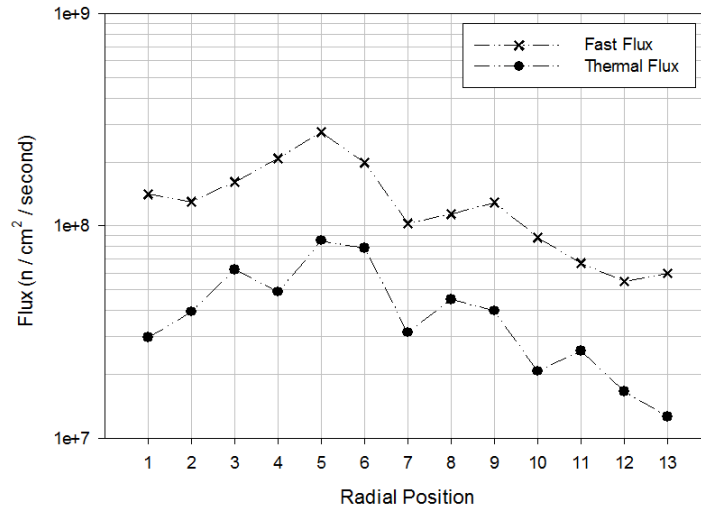


Figure 8-70: Flux profile central cross section after SCRAM

Central Flux Cross Section

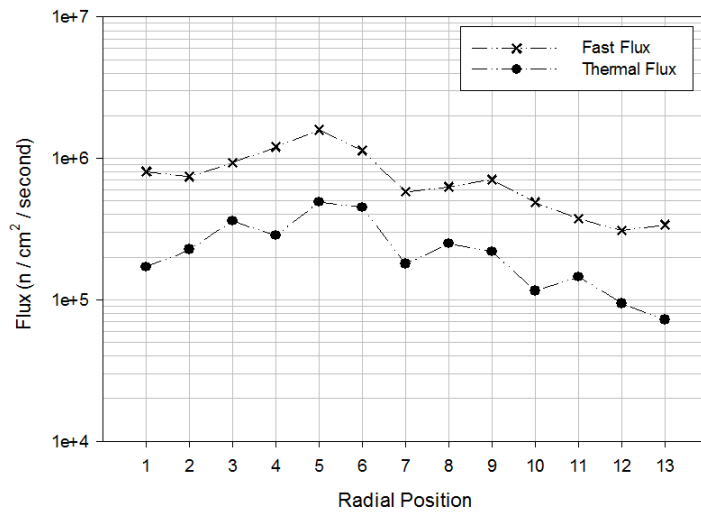


Figure 8-71: Flux profile central cross section after SCRAM after 100 s

Flux Cross Section at Ejection Point

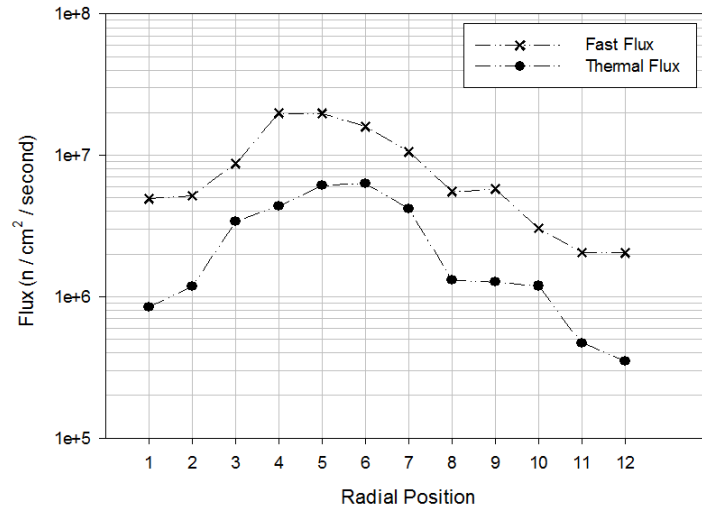


Figure 8-72: Flux profile cross section at ejection point

Flux Cross Section at Ejection Point

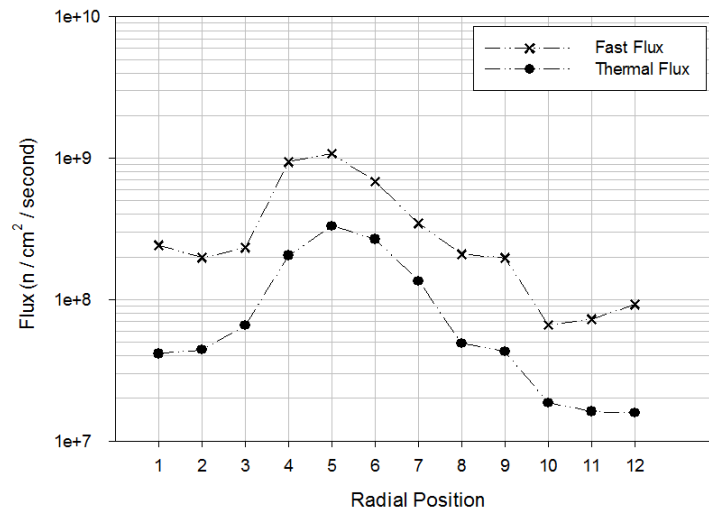


Figure 8-73: Flux profile cross section at ejection point after SCRAM

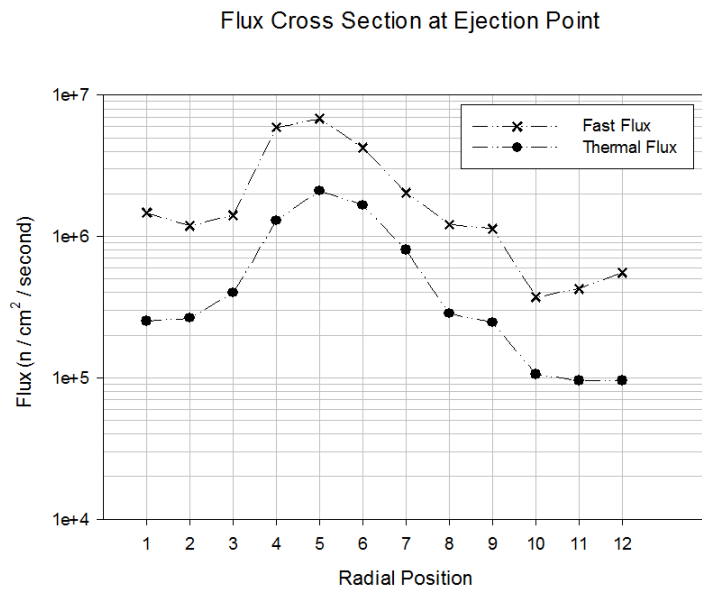


Figure 8-74: Flux profile cross section at ejection point after SCRAM after 100 s

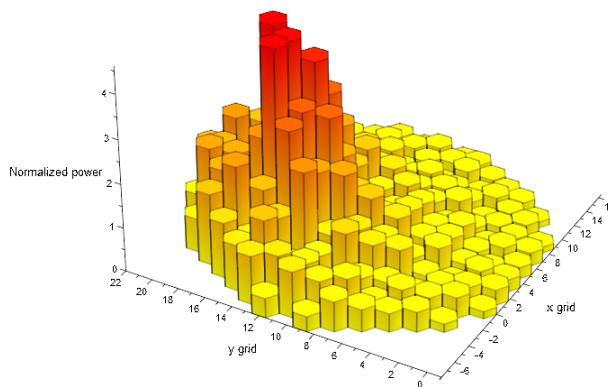


Figure 8-75: Averaged radial normalized power profile

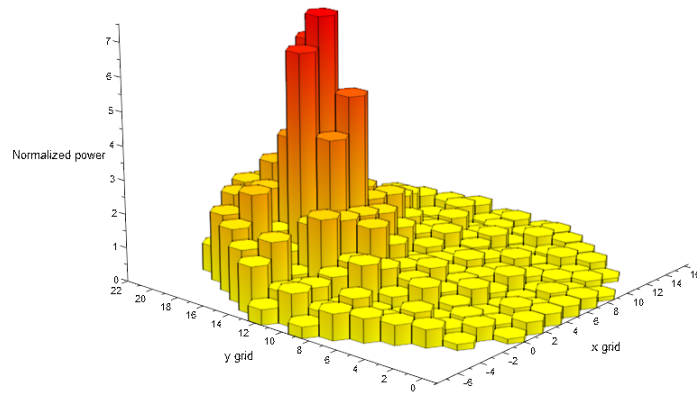


Figure 8-76: Averaged radial normalized power profile after SCRAM

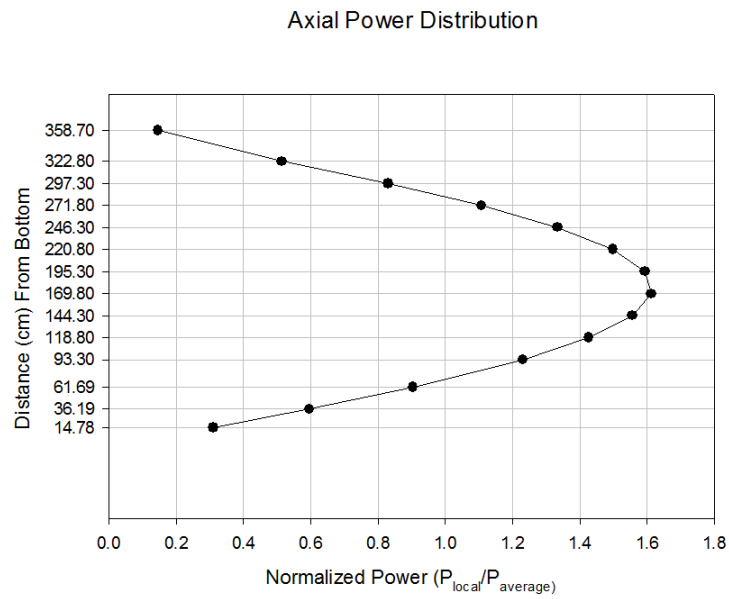


Figure 8-77: Axial normalized power

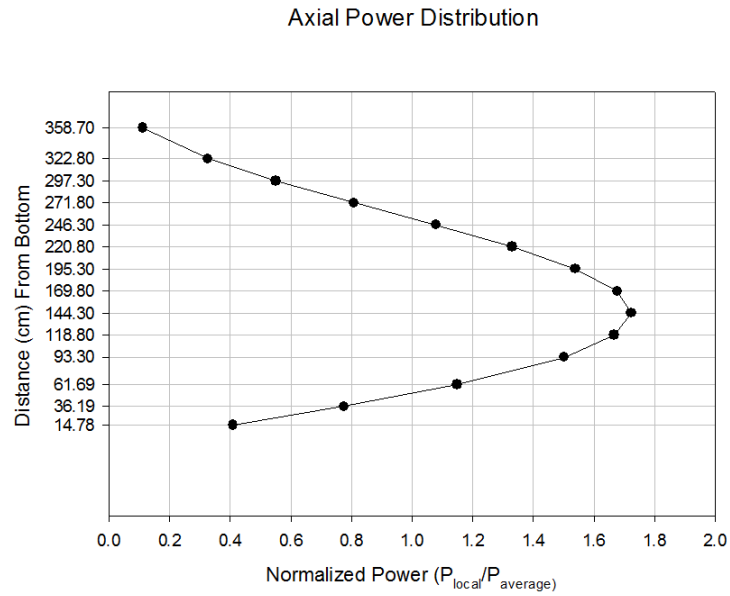


Figure 8-78: Axial normalized power after SCRAM

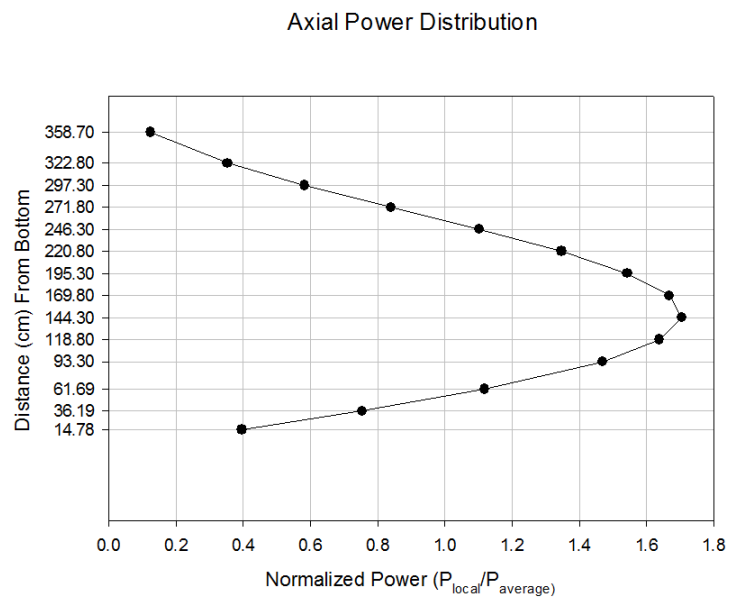


Figure 8-79: Axial normalized power after SCRAM after 100 s

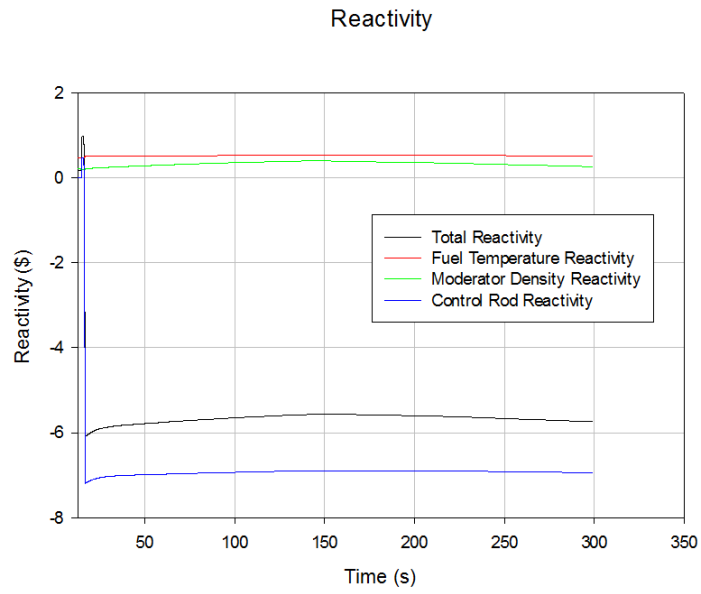


Figure 8-80: Reactivity

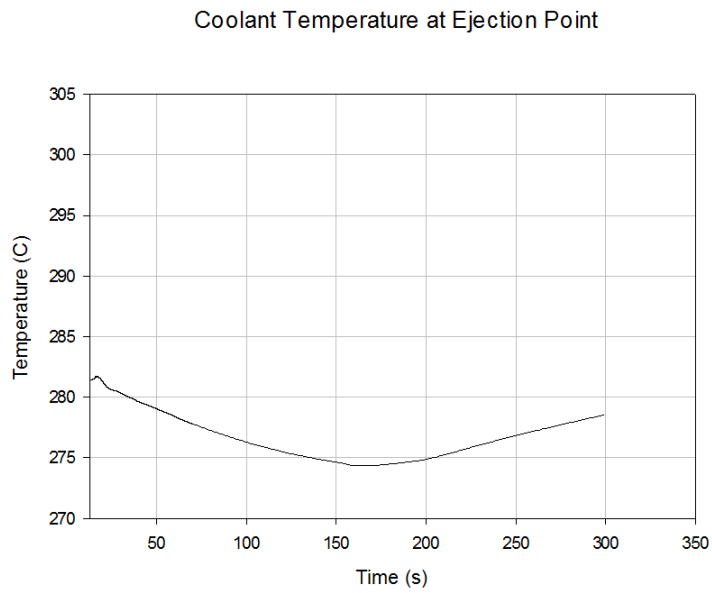


Figure 8-81: Coolant temperature at ejection point

Fuel Temperature at Ejection Point

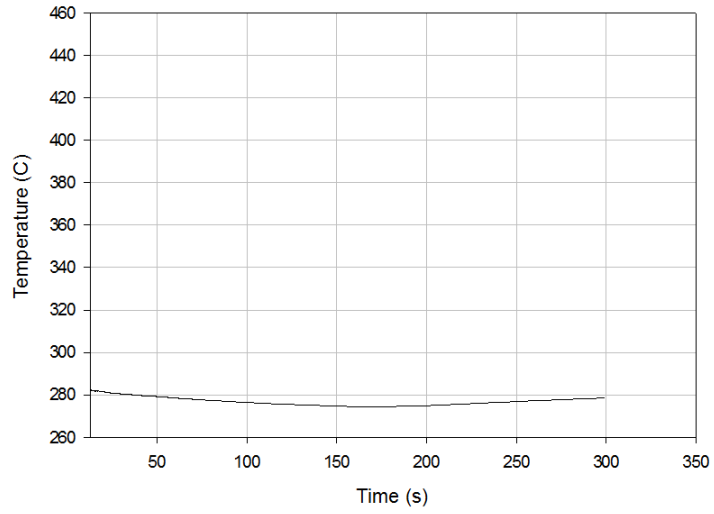


Figure 8-82: Fuel temperature at ejection point

Maximum Hot Rod Temperature

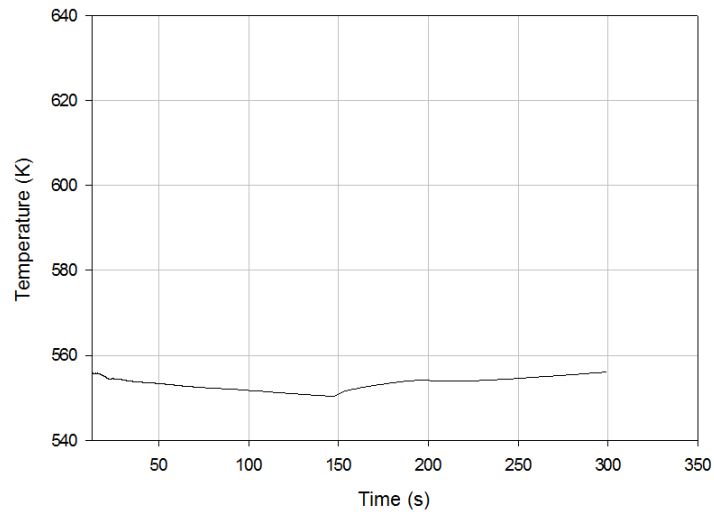


Figure 8-83: Maximal hot rod temperature

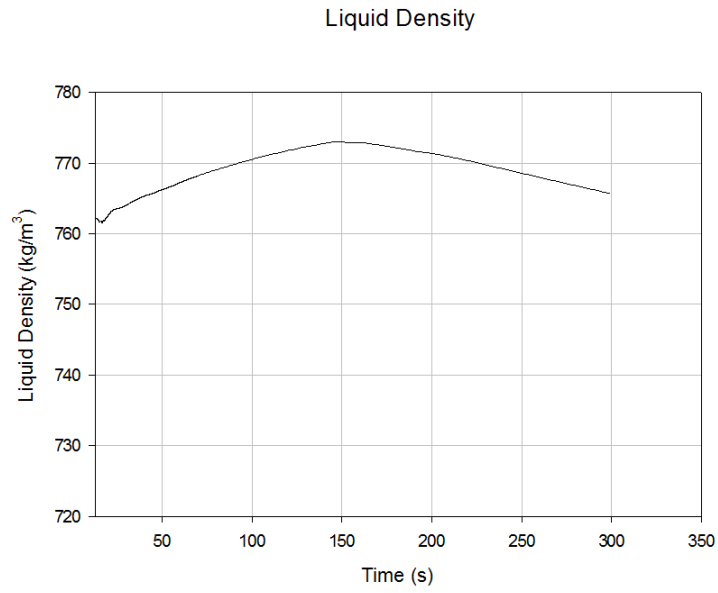


Figure 8-84: Averaged liquid density

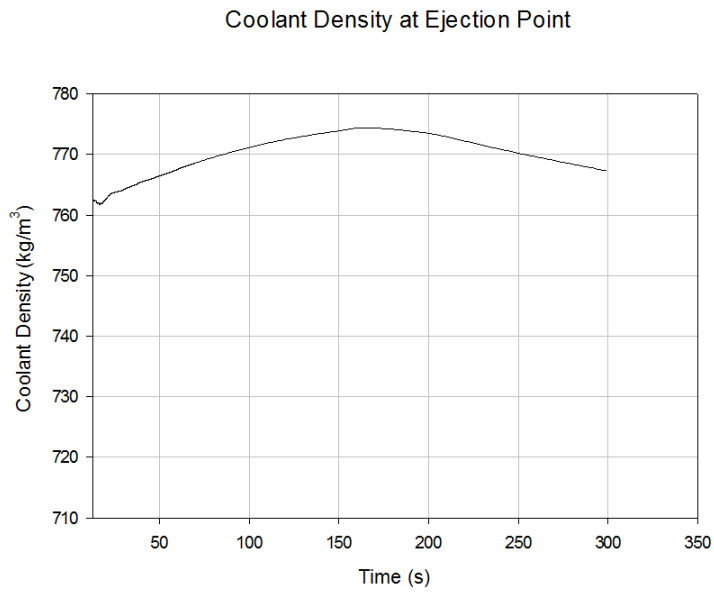


Figure 8-85: Coolant density at ejection point

Liquid Temperature

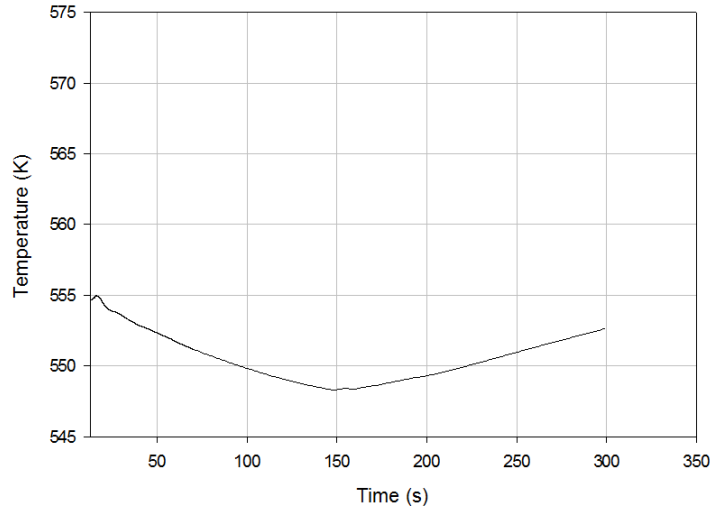


Figure 8-86: Averaged liquid temperature

Liquid Mass Flow Through Break

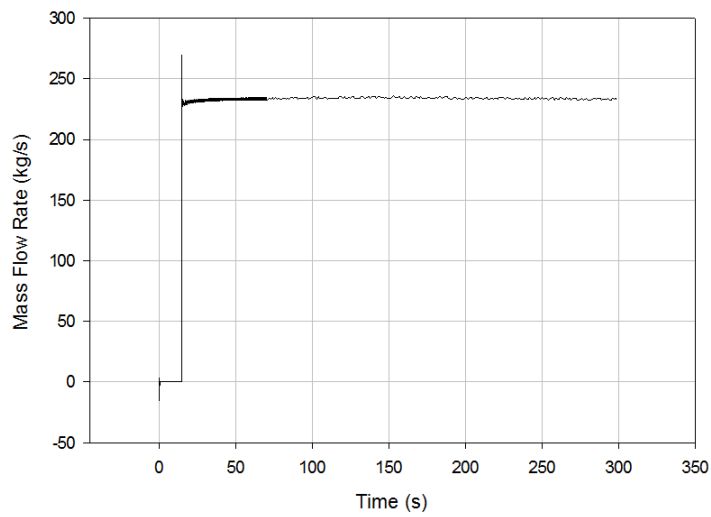


Figure 8-87: Mass flow through the break

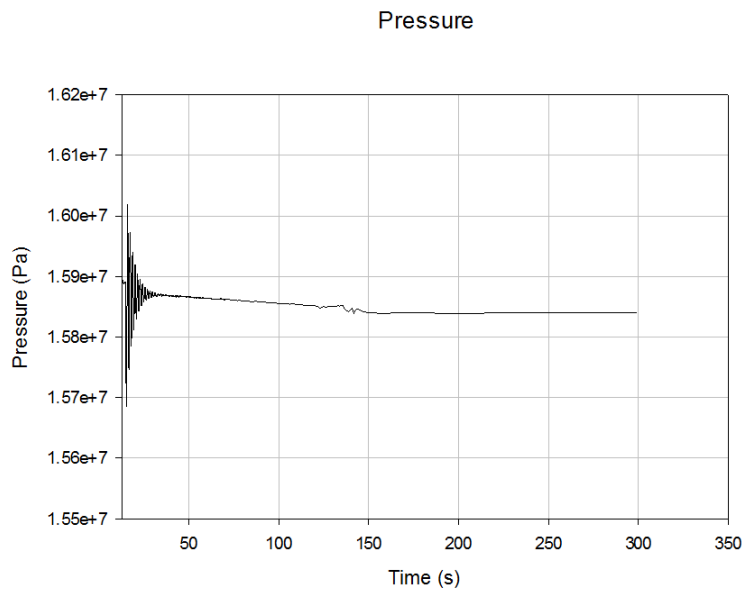


Figure 8-88: System Pressure

8.8.4 Rod Ejection without SCRAM, SERPENT 2

The general impression of the SERPENT 2 model is that the cross sections are less powerful, when compared to SCALE. The power is rising much more slowly and peaks at lower power, then SCALE model. In general the SERPENT models seem slower in comparison to SCALE, which also may be because even though the initial total reactivity is equivalent, the reactivity peak is only 0.56 \$, which is significantly lower, then with SCALE (0.98 \$). There is a rather more sluggish increase of the moderator temperature, alongside with a slow increase of fuel temperature, subsequently decreasing as the reactivity decreases.

The issue of low power will require deeper understanding of SERPENT 2 and running more sensitivity calculations while testing the results on coupled model. However this process is extremely time consuming, since each full procedure (stand alone, coupled steady state, coupled transient) takes five to seven days, without taking account of the time needed for data analysis. The cross-sections themselves are very similar, however when it comes to macroscopic XS, even the 4th or 5th digit makes a significant difference. This is because the microscopic XS are of power fo -25 and when these are converted to macroscopic XS, the order of magnitude changes to a centimetre to -1 . Nevertheless the general trend of the transient is in an agreement with the expectations. The following step will be benchmarking with experimental data to determine precision of either calculation, since the results presented in this thesis can be compared only to literature and judged by expert opinions of the CVR research staff.

Table 8.5: Chronological sequence of the events

Time (s)	Event Category	Parameter	Value or cause	Unit
-5.00	Value	Primary Pressure	1.59E+07	Pa
-5.00	Value	Power	3.12E+06	W
-5.00	Value	Max hot rod temperature	5.58E+02	K
-5.00	Value	Liquid Density	7.60E+02	kg/m3
-5.00	Value	Liquid Temperature	5.56E+02	K
-5.00	Value	Total reactivity	1.92E-01	\$
0.00	Event	Rod Ejection	Initiated event	-
0.00	Event	SB LOCA	Time triggered	-
1.00	Value	Primary Pressure	1.60E+07	Pa
1.00	Value	Power	1.23E+07	W
1.00	Value	Max hot rod temperature	5.56E+02	K
1.00	Value	Liquid Density	7.62E+02	kg/m3
1.00	Value	Liquid Temperature	5.55E+02	K
1.00	Value	Total reactivity	5.67E-01	\$
1.01	Event	SCRAM	NO	-
5.00	Value	Primary Pressure	1.59E+07	Pa
5.00	Value	Power	4.69E+07	W
5.00	Value	Max hot rod temperature	5.56E+02	K
5.00	Value	Liquid Density	7.62E+02	kg/m3
5.00	Value	Liquid Temperature	5.55E+02	K
5.00	Value	Total reactivity	5.87E-01	\$
10.00	Value	Primary Pressure	1.59E+07	Pa
10.00	Value	Power	1.77E+08	W
10.00	Value	Max hot rod temperature	5.59E+02	K
10.00	Value	Liquid Density	7.63E+02	kg/m3
10.00	Value	Liquid Temperature	5.54E+02	K
10.00	Value	Total reactivity	5.33E-01	\$
100.00	Value	Primary Pressure	1.59E+07	Pa
100.00	Value	Power	3.48E+08	W
100.00	Value	Max hot rod temperature	5.74E+02	K
100.00	Value	Liquid Density	7.48E+02	kg/m3
100.00	Value	Liquid Temperature	5.63E+02	K
100.00	Value	Total reactivity	-4.10E-02	\$

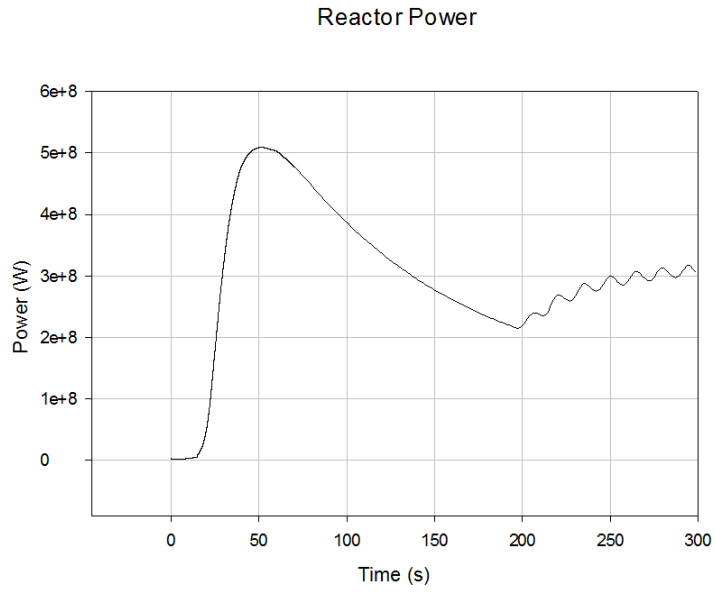


Figure 8-89: Core power

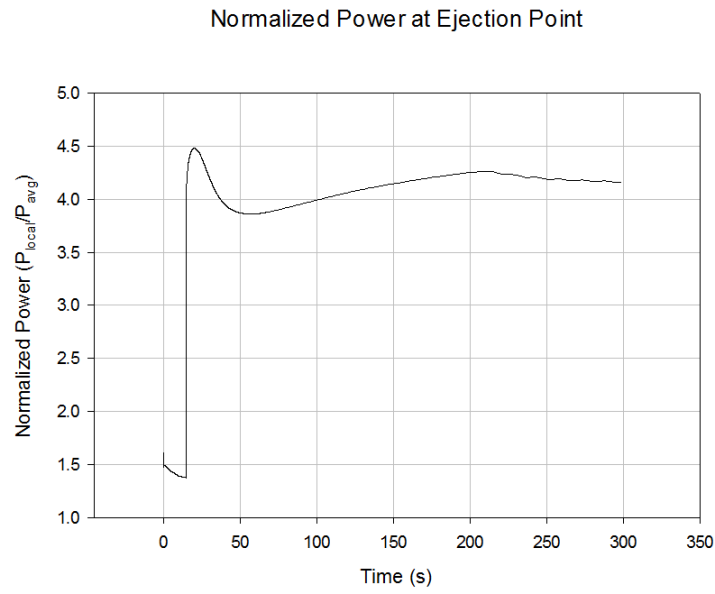


Figure 8-90: Normalized power at ejection point

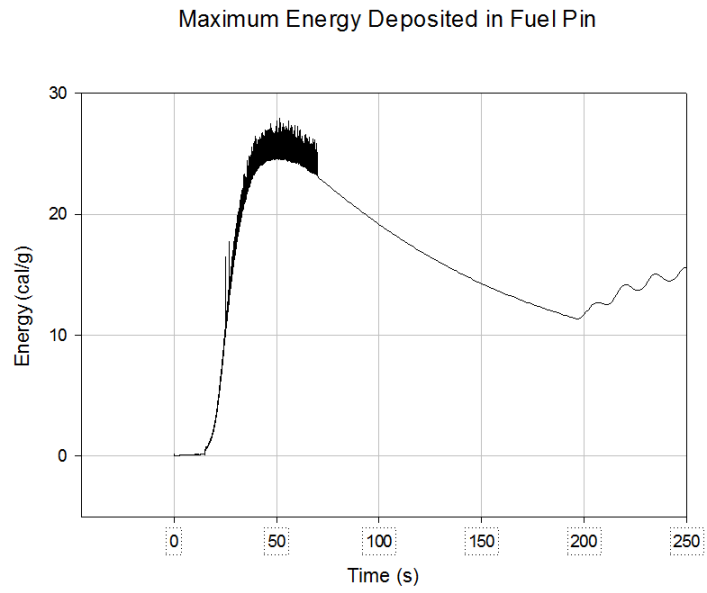


Figure 8-91: Maximum energy deposited in fuel pin

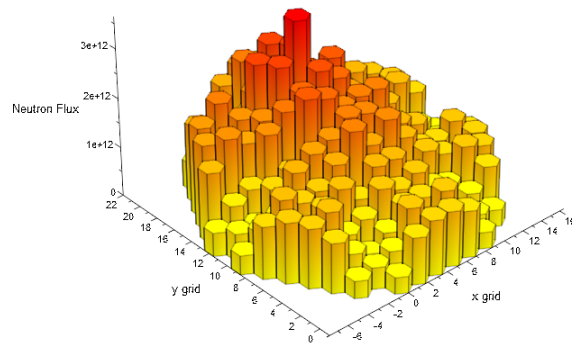


Figure 8-92: Averaged fast flux

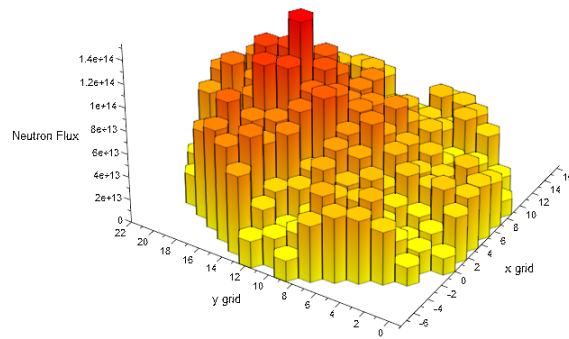


Figure 8-93: Averaged fast flux after 100 s

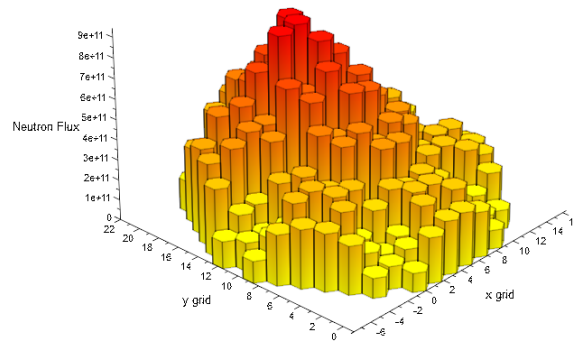


Figure 8-94: Averaged thermal flux

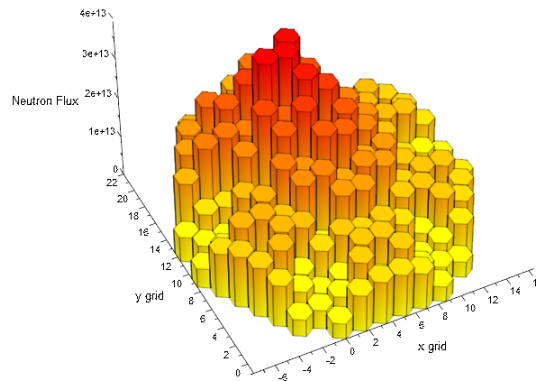


Figure 8-95: Averaged thermal flux after 100 s

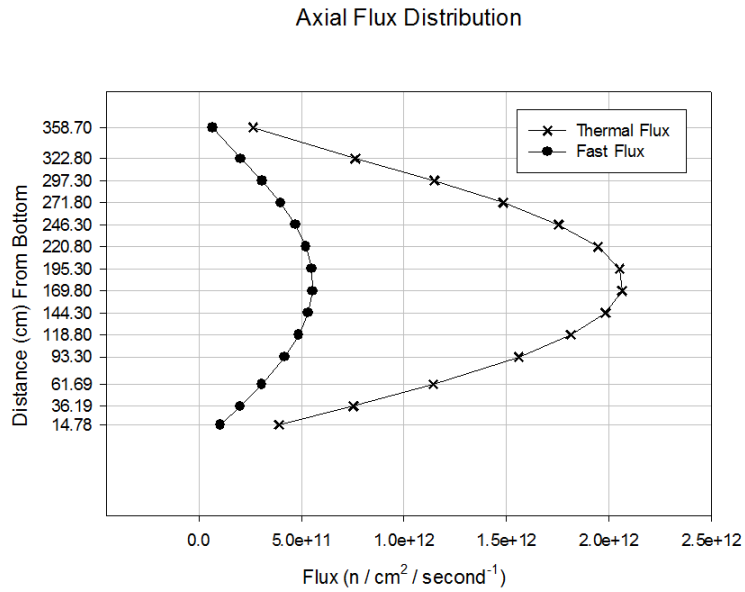


Figure 8-96: Axial flux profile

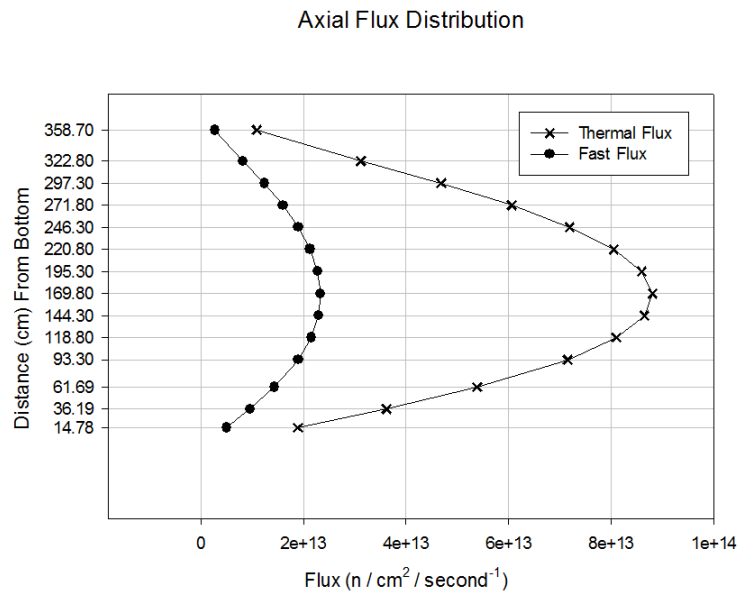


Figure 8-97: Axial flux profile after 100 s

Central Flux Cross Section

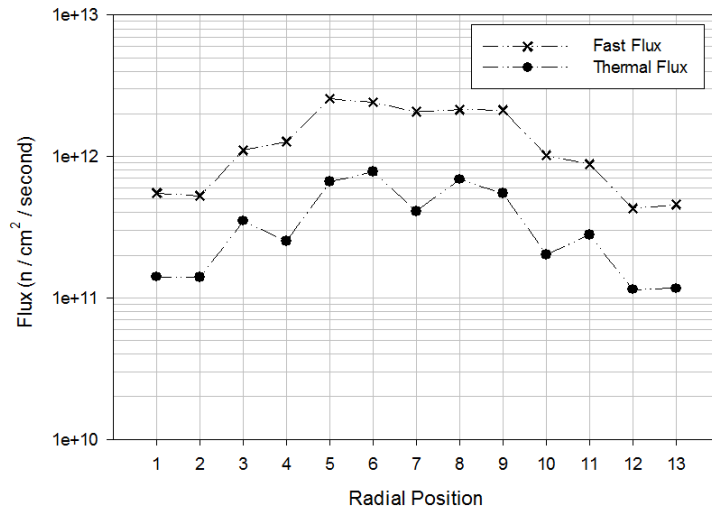


Figure 8-98: Flux profile central cross section

Central Flux Cross Section

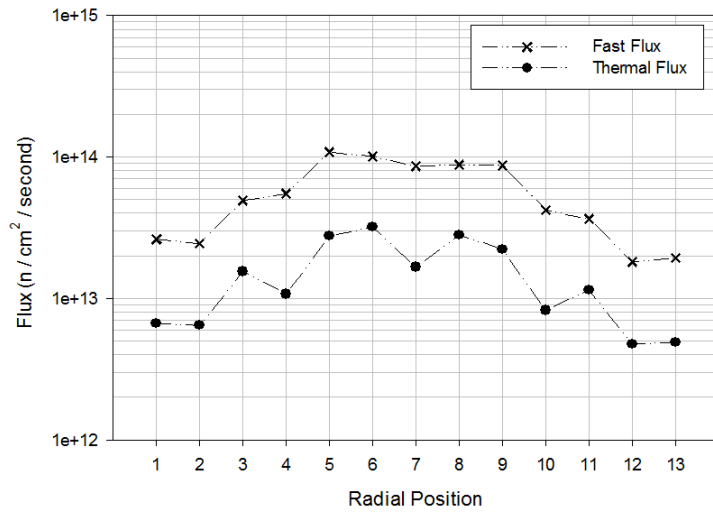


Figure 8-99: Flux profile central cross section after 100 s

Flux Cross Section at Ejection Point

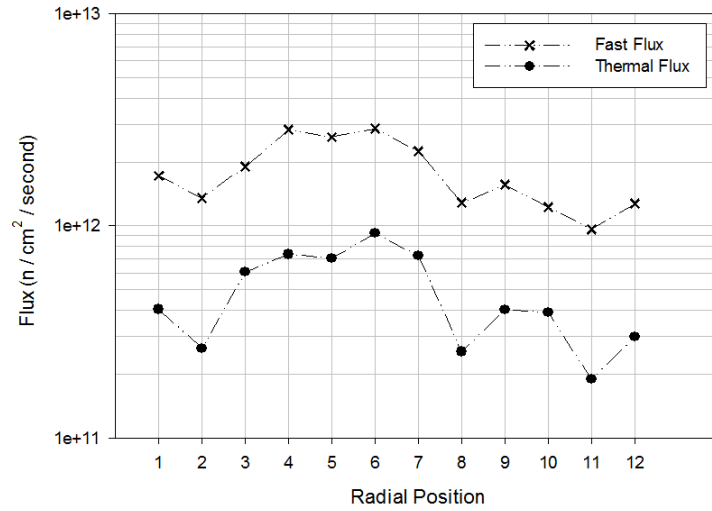


Figure 8-100: Flux profile cross section at ejection point

Flux Cross Section at Ejection Point

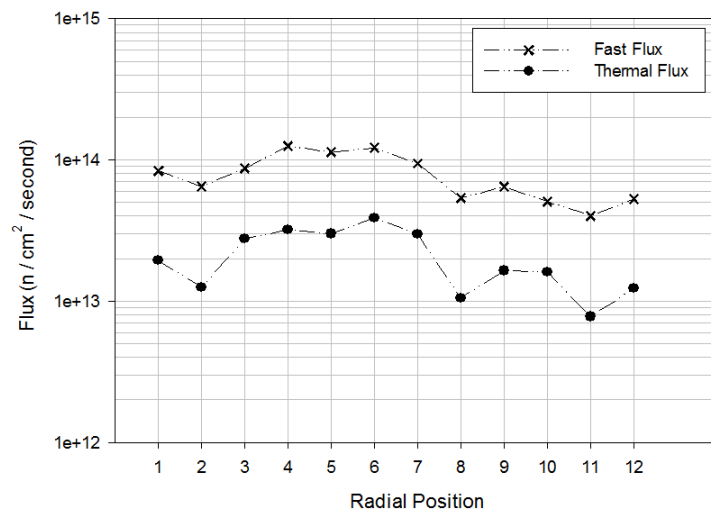


Figure 8-101: Flux profile cross section at ejection point after 100 s

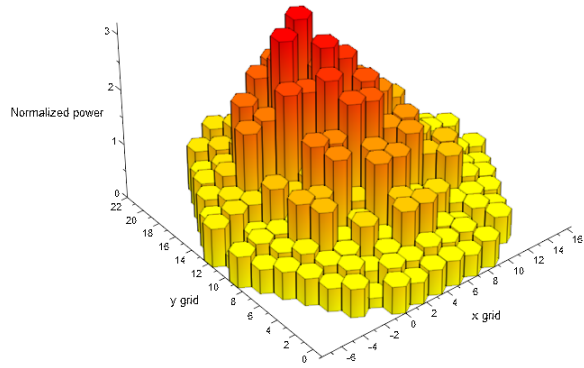


Figure 8-102: Averaged radial normalized power profile

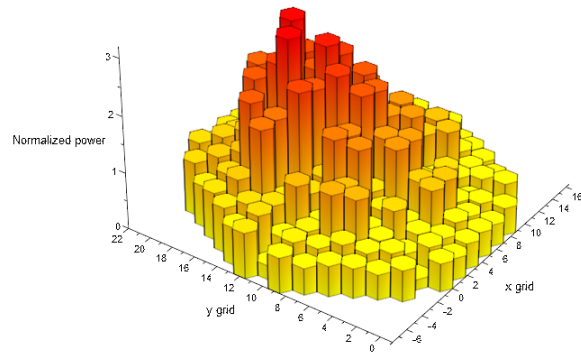


Figure 8-103: Averaged radial normalized power profile after 100 s

Axial Power Distribution

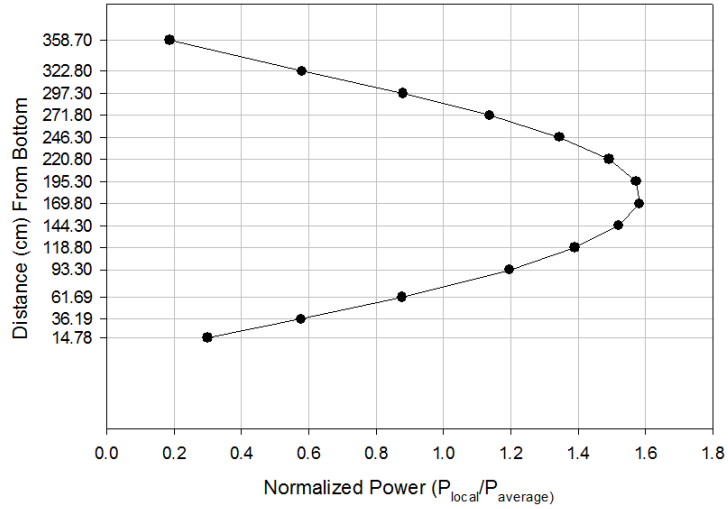


Figure 8-104: Axial normalized power

Axial Power Distribution

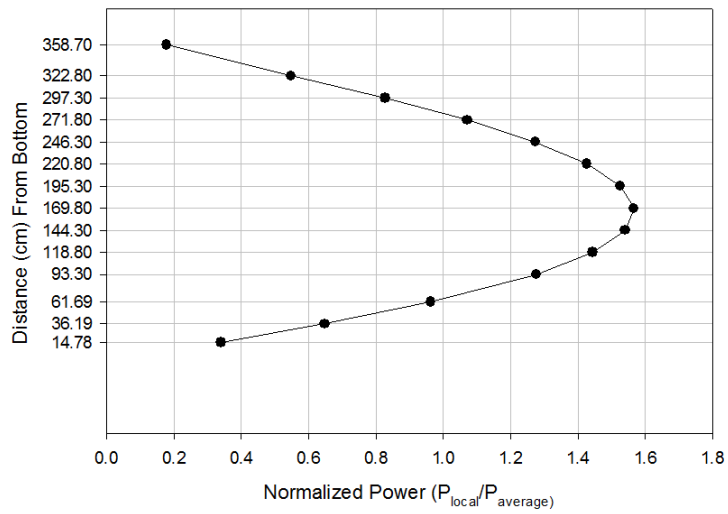


Figure 8-105: Axial normalized power after 100 s

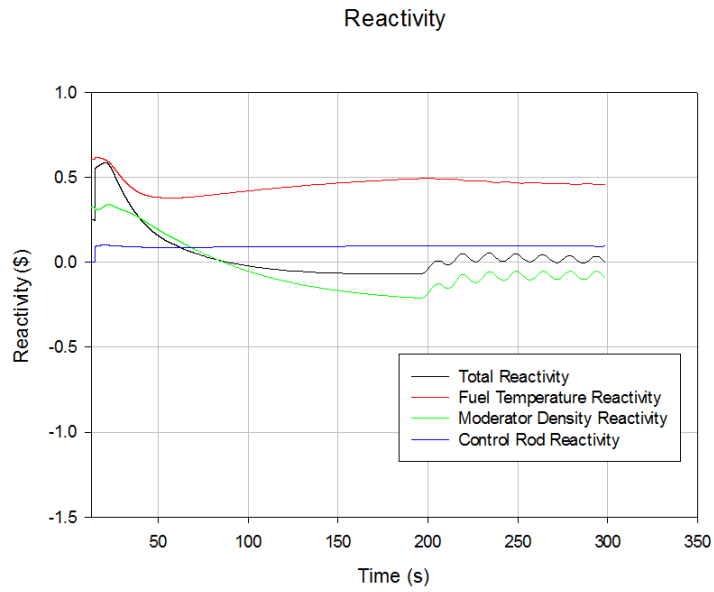


Figure 8-106: Reactivity

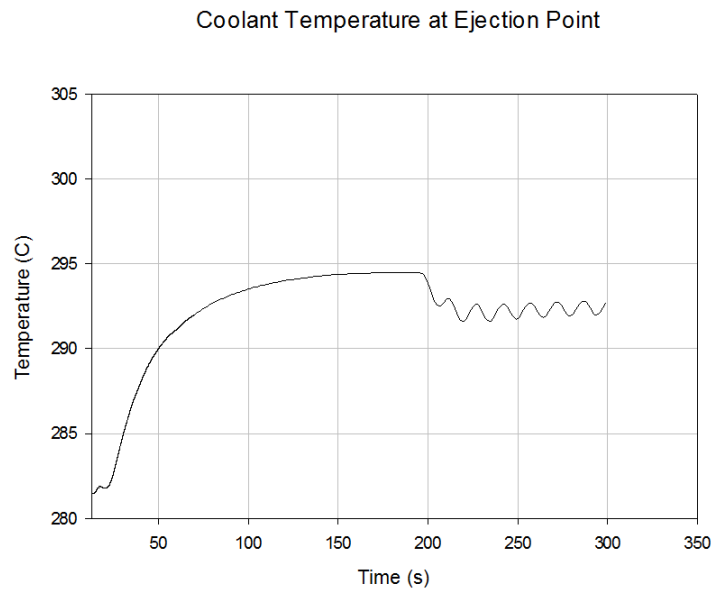


Figure 8-107: Coolant temperature at ejection point

Fuel Temperature at Ejection Point

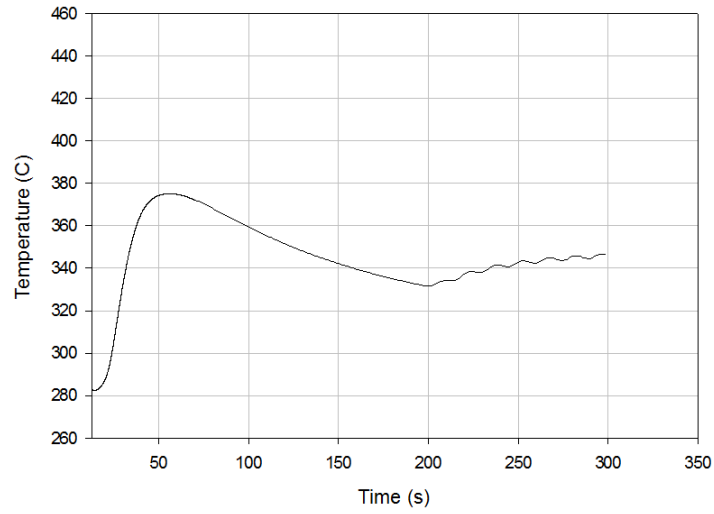


Figure 8-108: Fuel temperature at ejection point

Maximum Hot Rod Temperature

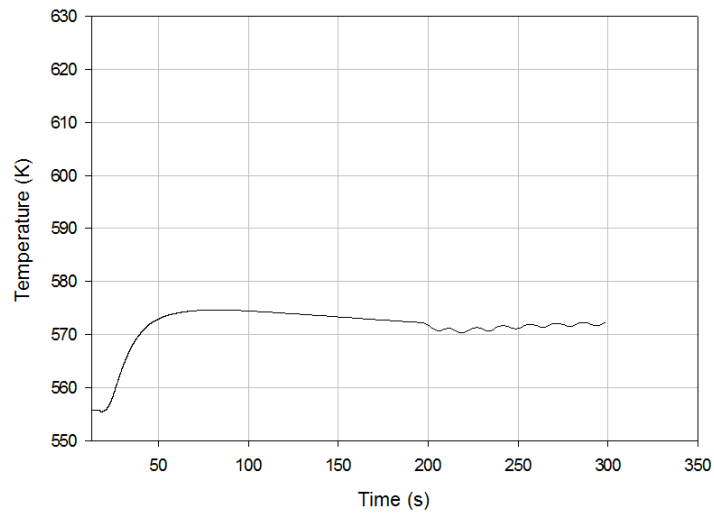


Figure 8-109: Maximal hot rod temperature

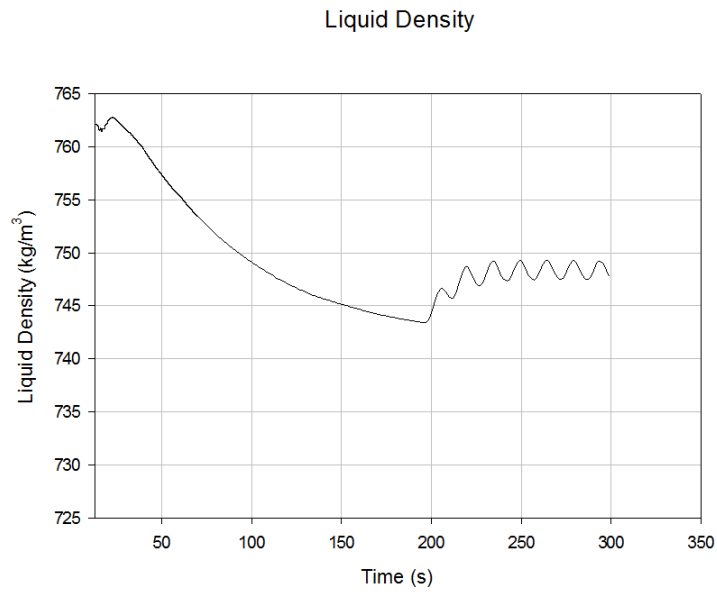


Figure 8-110: Averaged liquid density

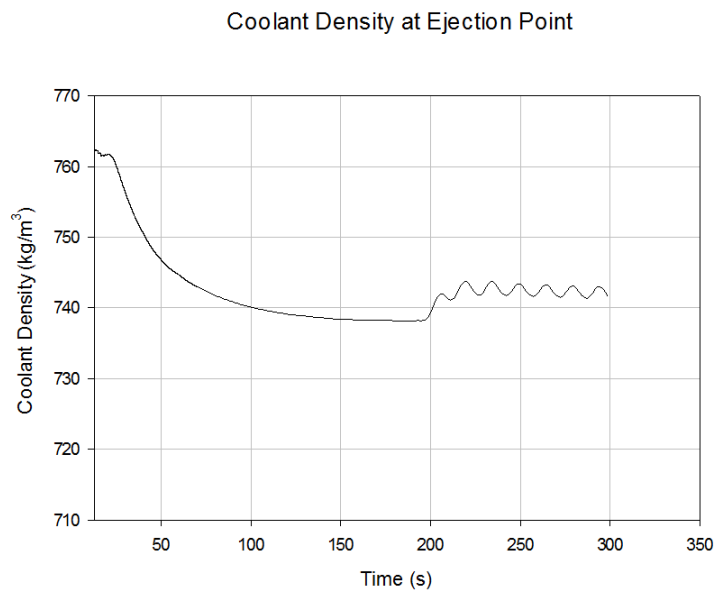


Figure 8-111: Coolant density at ejection point

Liquid Temperature

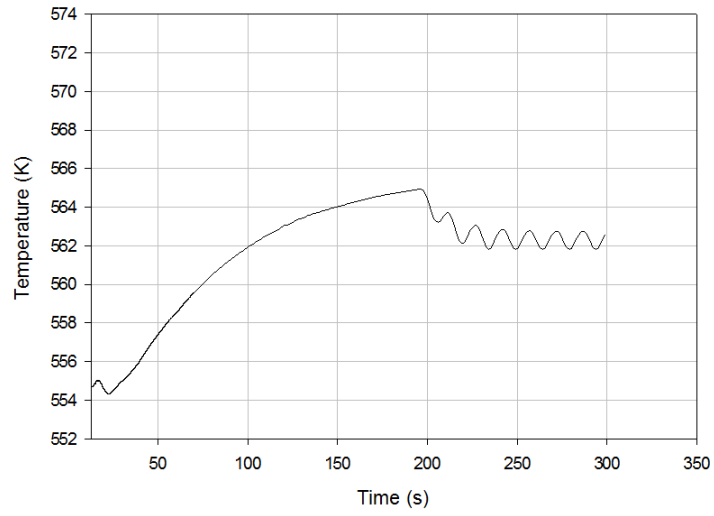


Figure 8-112: Averaged liquid temperature

Liquid Mass Flow Through Break

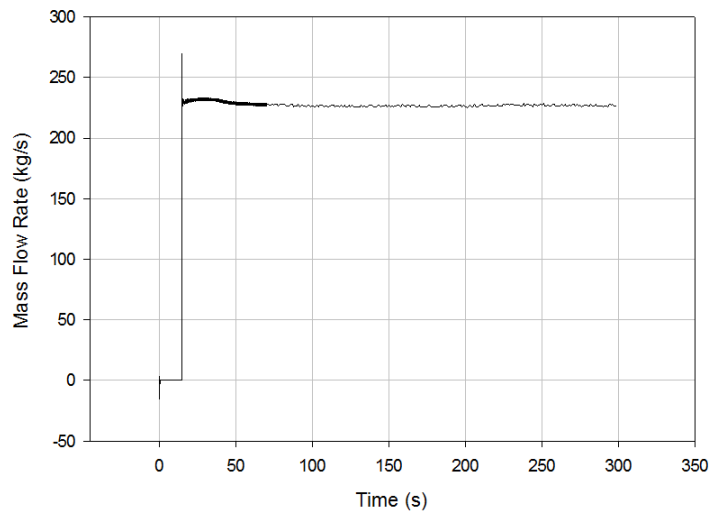


Figure 8-113: Mass flow through the break

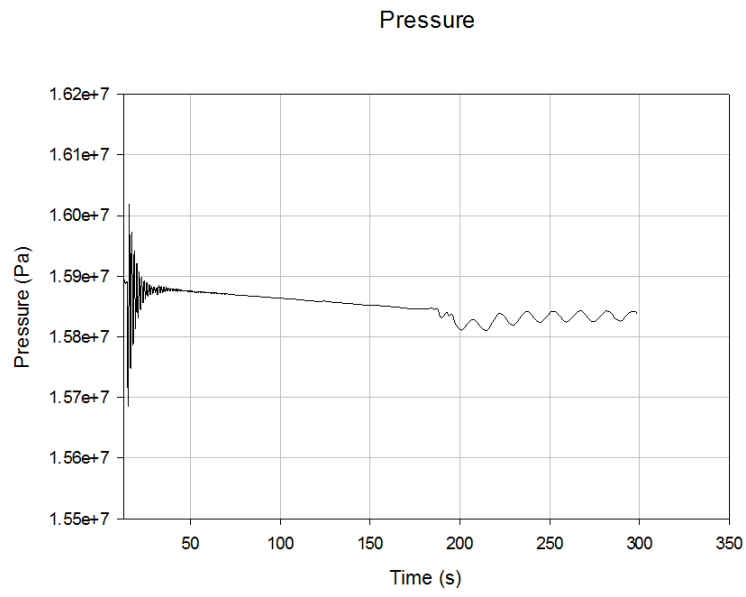


Figure 8-114: System Pressure

8.8.5 Rod Ejection with SCRAM, SERPENT 2

In this scenario using SERPENT 2 cross sections, SCRAM occurs one second after the ejection. Same logic applies as in the SCALE-SCRAM scenario, therefore all the progress up to SCRAM is the same as before. SCRAM introduces about 5 \$ of negative reactivity, virtually stopping the reactor, as shown on the power progression in figure 8-115 on page 144. Because SCRAM occurs only one second after the ejection, neither fuel or coolant temperature rises, however because there is no pin power model for models with hexagonal lattice, the temperatures within each assembly is averaged, therefore it is difficult to tell the actual highest temperature in the hot pin. In this case, the calculated increase is even lower, because the cross sections are most likely lower. This scenario therefore has lower impact on the system, then the non-SCRAM one, however it is more realistic, which is why it is analysed in this thesis.

An important issue is the lack of Assembly Discontinuity Factors (ADF) in the output of SERPENT 2 and a difficulty to set-up of albedos. Most likely due to missing ADFs, the 3D radial plots are more discrete-like, instead of the continuous impression that was visible in the SCALE model.

Table 8.6: Chronological sequence of the events

Time (s)	Event Category	Parameter	Value or cause	Unit
-5.00	Value	Primary Pressure	1.59E+07	Pa
-5.00	Value	Power	3.12E+06	W
-5.00	Value	Max hot rod temperature	5.58E+02	K
-5.00	Value	Liquid Density	7.60E+02	kg/m3
-5.00	Value	Liquid Temperature	5.56E+02	K
-5.00	Value	Total reactivity	1.92E-01	\$
0.00	Event	Rod Ejection	Initiated event	-
0.00	Event	SB LOCA	Time triggered	-
1.00	Value	Primary Pressure	1.60E+07	Pa
1.00	Value	Power	1.22E+07	W
1.00	Value	Max hot rod temperature	5.56E+02	K
1.00	Value	Liquid Density	7.62E+02	kg/m3
1.00	Value	Liquid Temperature	5.55E+02	K
1.00	Value	Total reactivity	5.67E-01	\$
1.01	Event	SCRAM	YES	-
5.00	Value	Primary Pressure	1.59E+07	Pa
5.00	Value	Power	3.79E+05	W
5.00	Value	Max hot rod temperature	5.55E+02	K
5.00	Value	Liquid Density	7.63E+02	kg/m3
5.00	Value	Liquid Temperature	5.54E+02	K
5.00	Value	Total reactivity	-4.24E+00	\$
10.00	Value	Primary Pressure	1.59E+07	Pa
10.00	Value	Power	2.15E+05	W
10.00	Value	Max hot rod temperature	5.54E+02	K
10.00	Value	Liquid Density	7.64E+02	kg/m3
10.00	Value	Liquid Temperature	5.54E+02	K
10.00	Value	Total reactivity	-4.21E+00	\$
100.00	Value	Primary Pressure	1.59E+07	Pa
100.00	Value	Power	1.44E+04	W
100.00	Value	Max hot rod temperature	5.51E+02	K
100.00	Value	Liquid Density	7.71E+02	kg/m3
100.00	Value	Liquid Temperature	5.49E+02	K
100.00	Value	Total reactivity	-3.95E+00	\$

Reactor Power

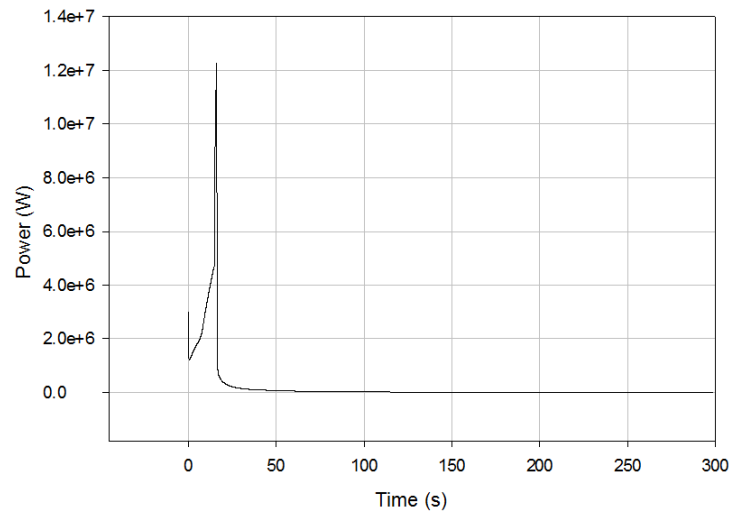


Figure 8-115: Core power

Normalized Power at Ejection Point

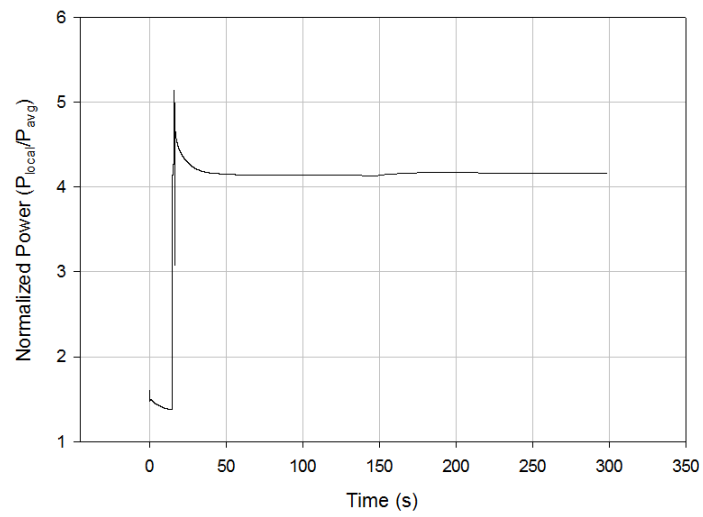


Figure 8-116: Normalized power at ejection point

Maximum Energy Deposited in Fuel Pin

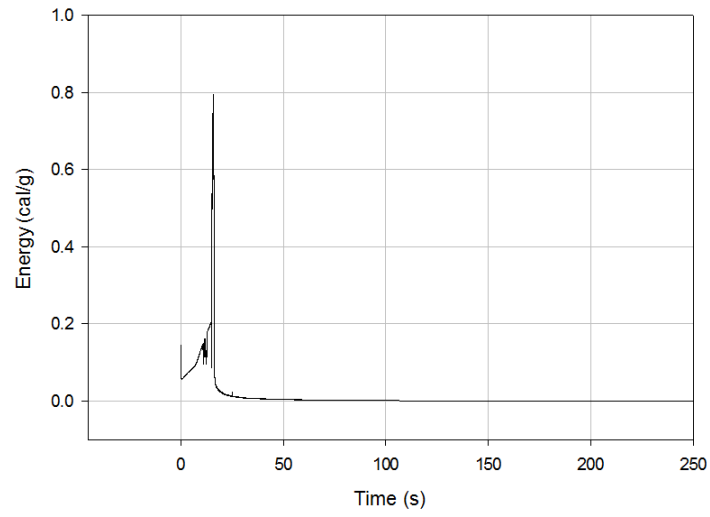


Figure 8-117: Maximum energy deposited in fuel pin

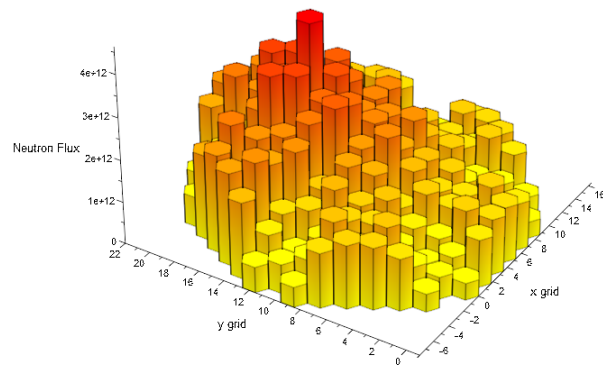


Figure 8-118: Averaged fast flux

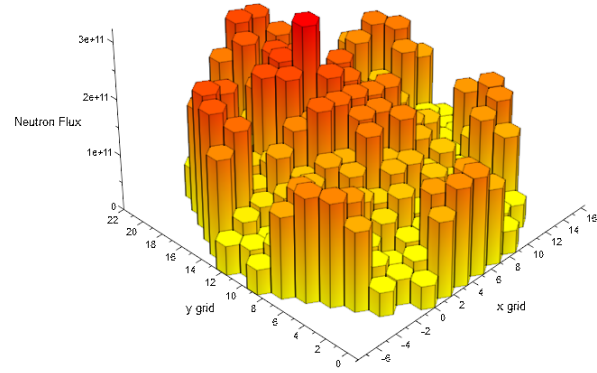


Figure 8-119: Averaged fast flux after SCRAM

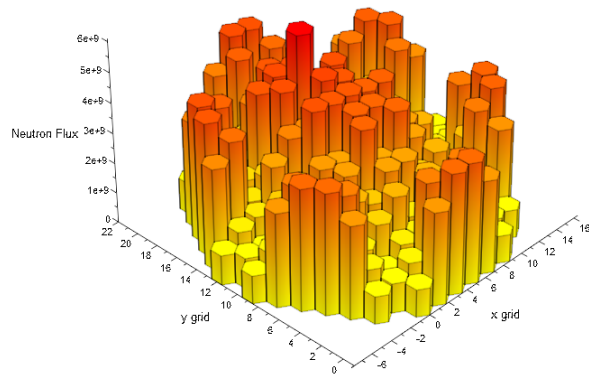


Figure 8-120: Averaged fast flux after SCRAM after 100 s

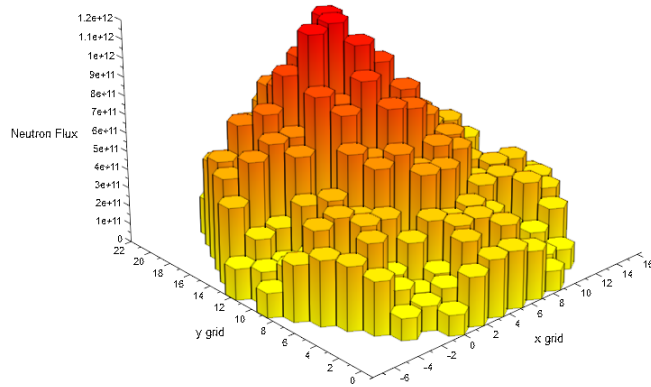


Figure 8-121: Averaged thermal flux

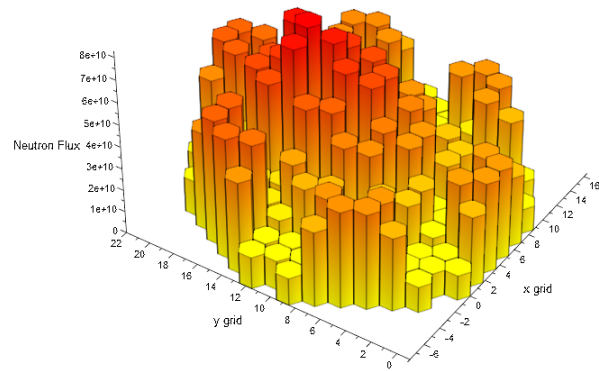


Figure 8-122: Averaged thermal flux after SCRAM

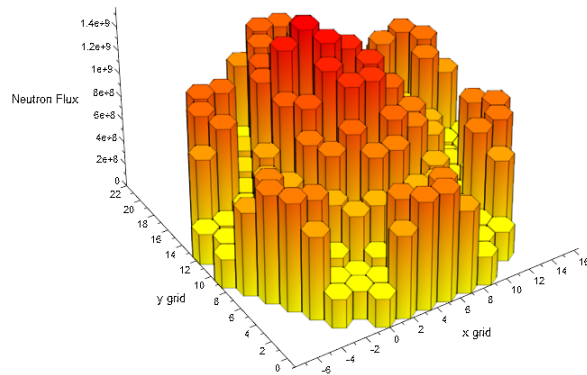


Figure 8-123: Averaged thermal flux after SCRAM after 100 s

Axial Flux Distribution

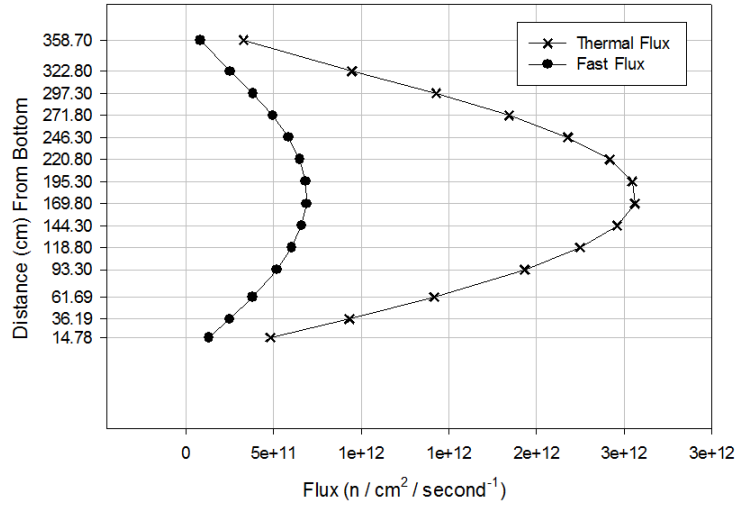


Figure 8-124: Axial flux profile

Axial Flux Distribution

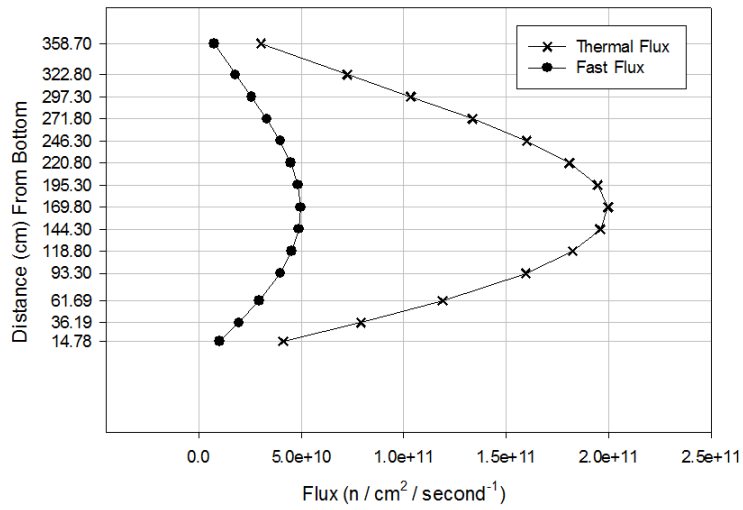


Figure 8-125: Axial flux profile after SCRAM

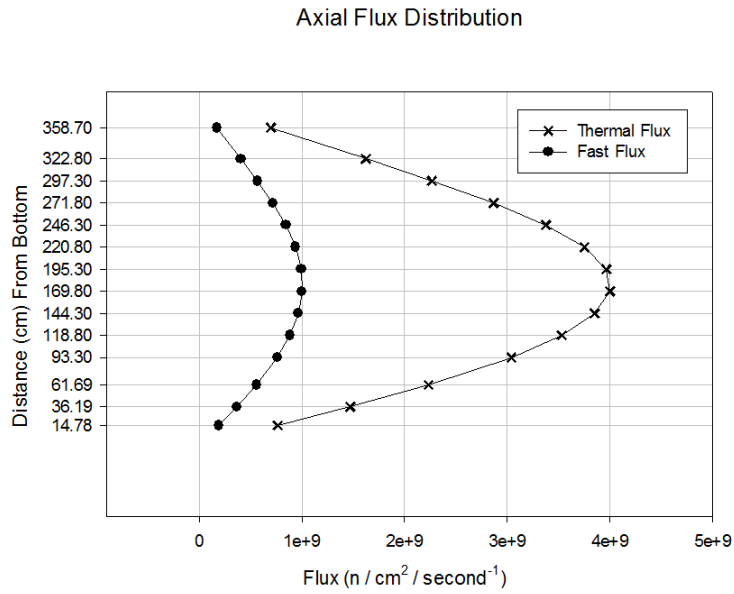


Figure 8-126: Axial flux profile after SCRAM after 100 s

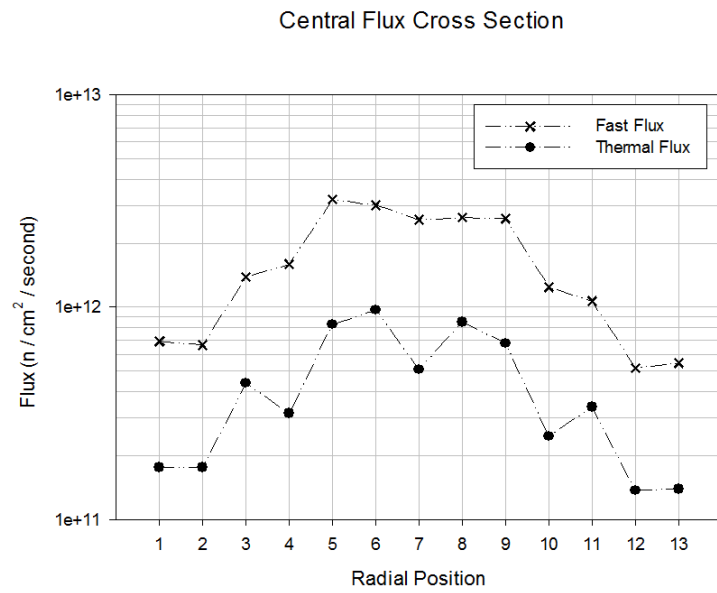


Figure 8-127: Flux profile central cross section

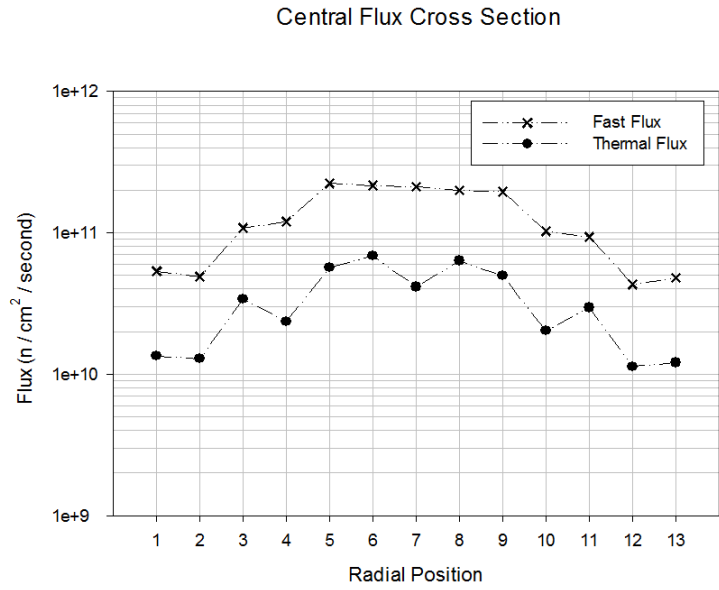


Figure 8-128: Flux profile central cross section after SCRAM

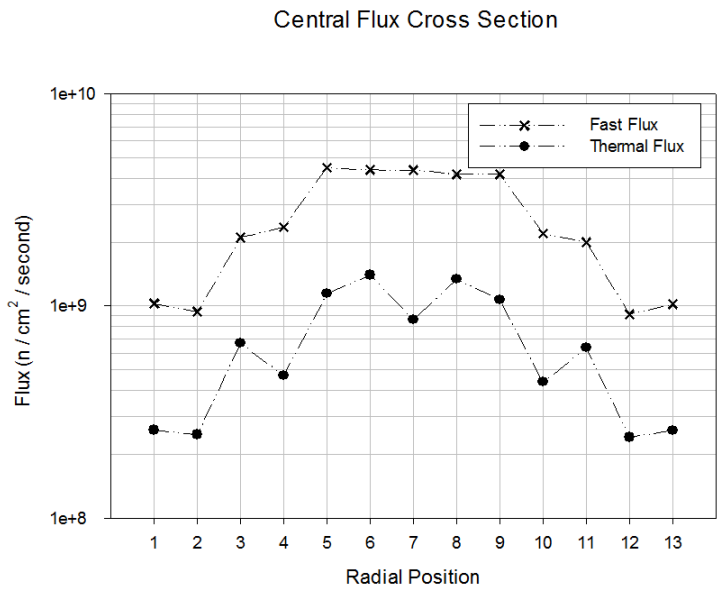


Figure 8-129: Flux profile central cross section after SCRAM after 100 s

Flux Cross Section at Ejection Point

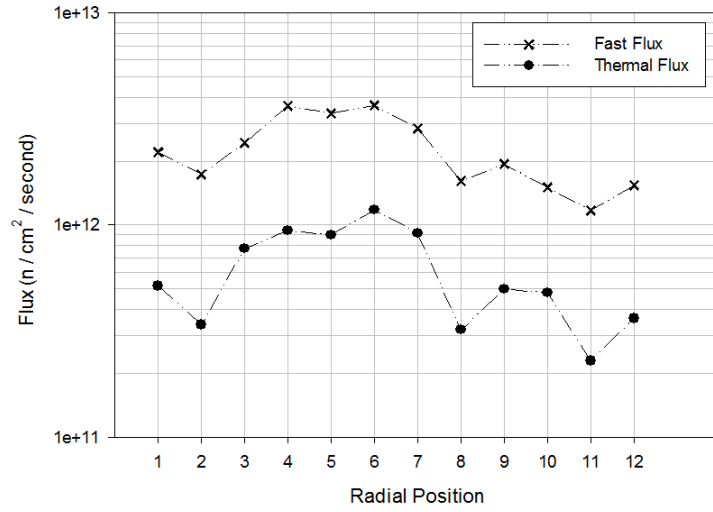


Figure 8-130: Flux profile cross section at ejection point

Flux Cross Section at Ejection Point

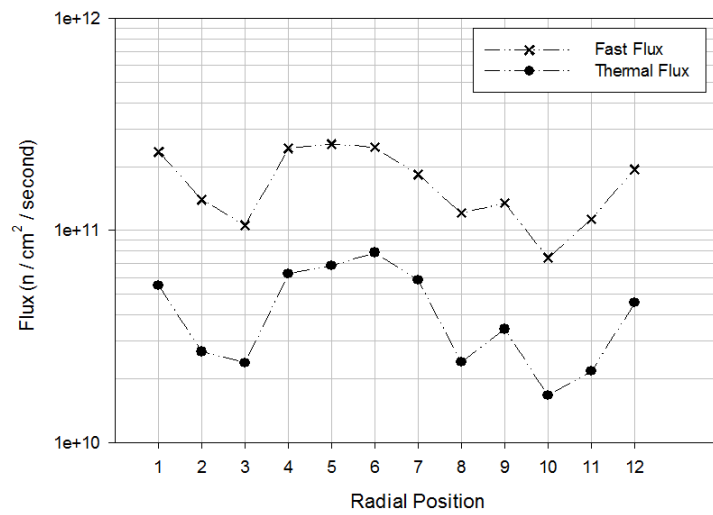


Figure 8-131: Flux profile cross section at ejection point after SCRAM

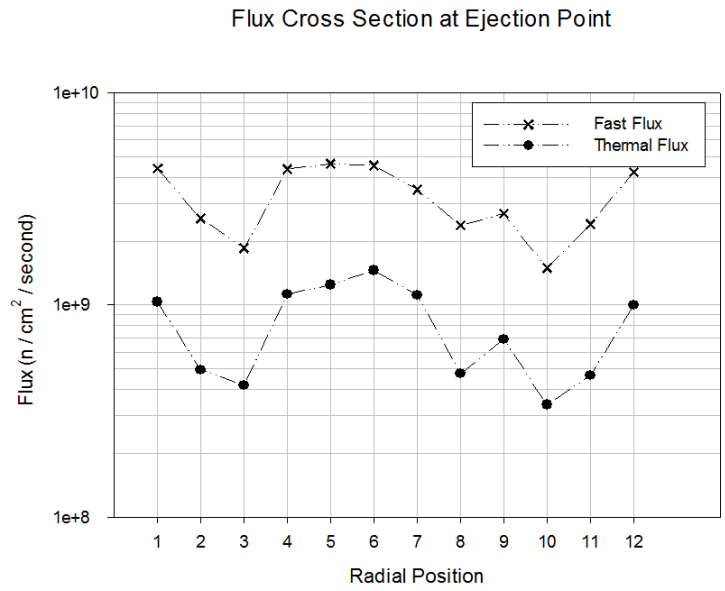


Figure 8-132: Flux profile cross section at ejection point after SCRAM after 100 s

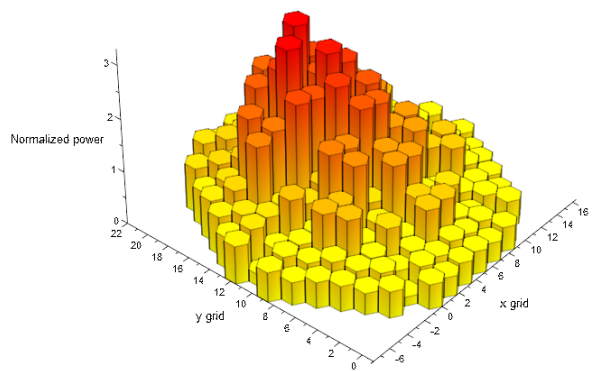


Figure 8-133: Averaged radial normalized power profile

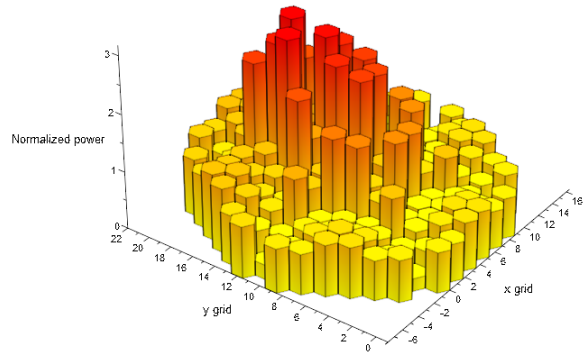


Figure 8-134: Averaged radial normalized power profile after SCRAM

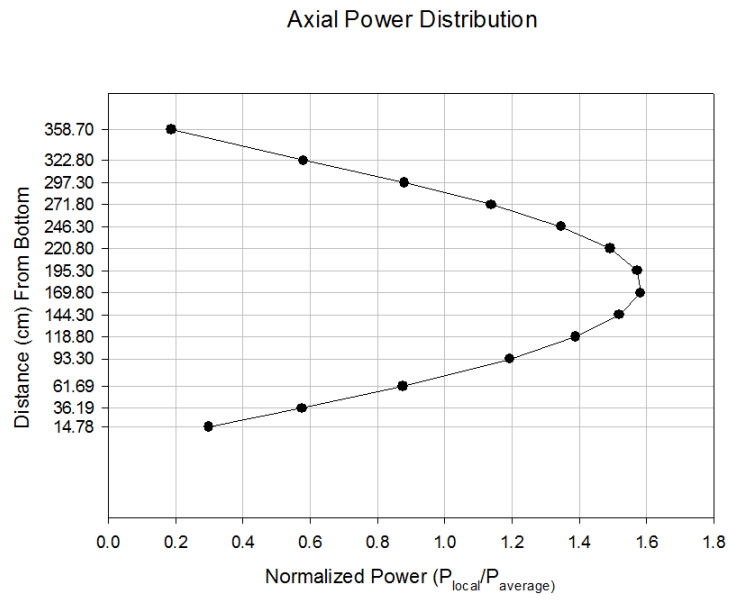


Figure 8-135: Axial normalized power

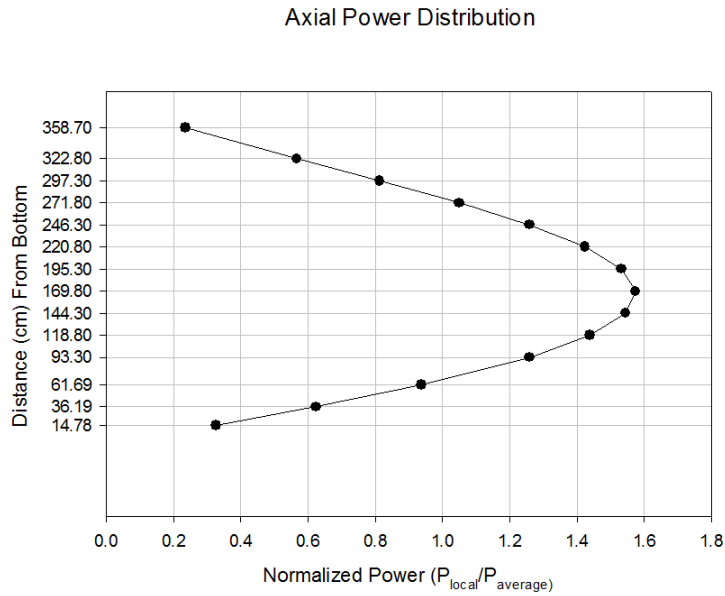


Figure 8-136: Axial normalized power after SCRAM

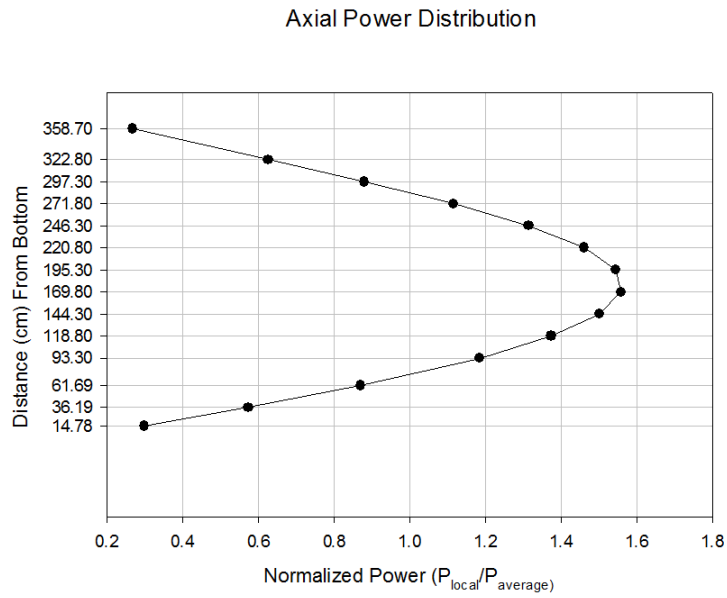


Figure 8-137: Axial normalized power after SCRAM after 100 s

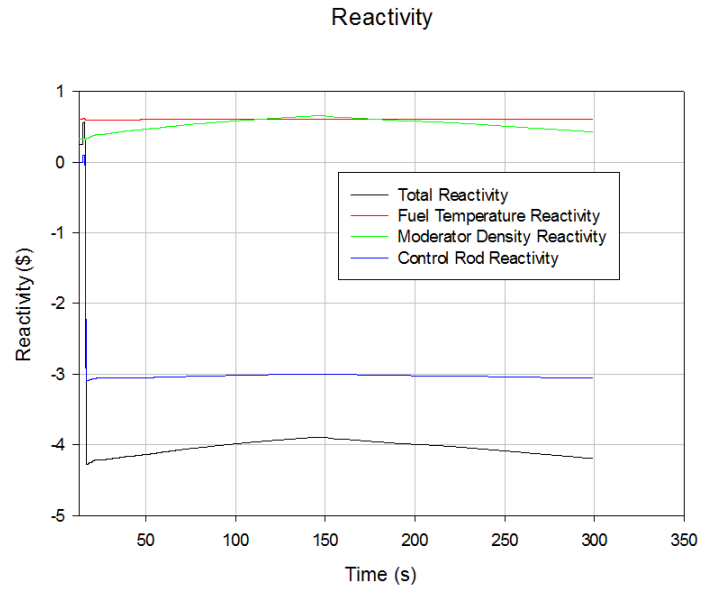


Figure 8-138: Reactivity

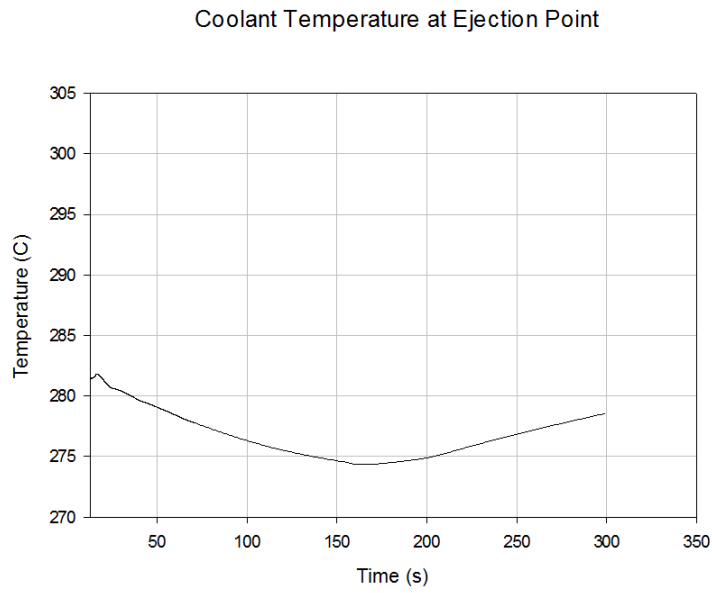


Figure 8-139: Coolant temperature at ejection point

Fuel Temperature at Ejection Point

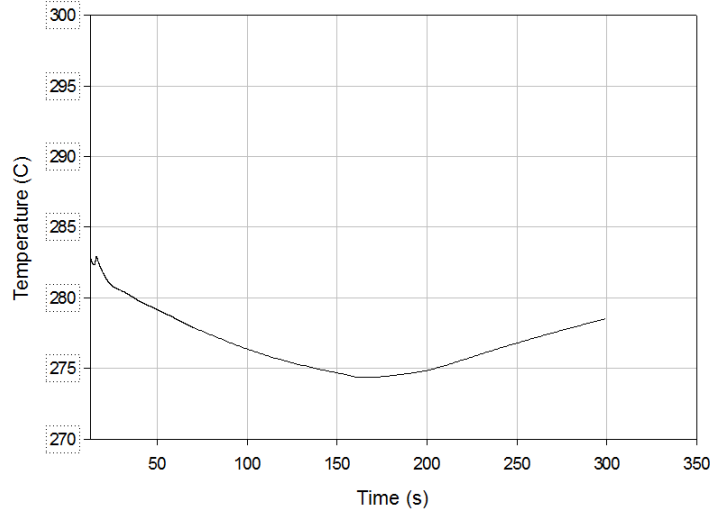


Figure 8-140: Fuel temperature at ejection point

Maximum Hot Rod Temperature

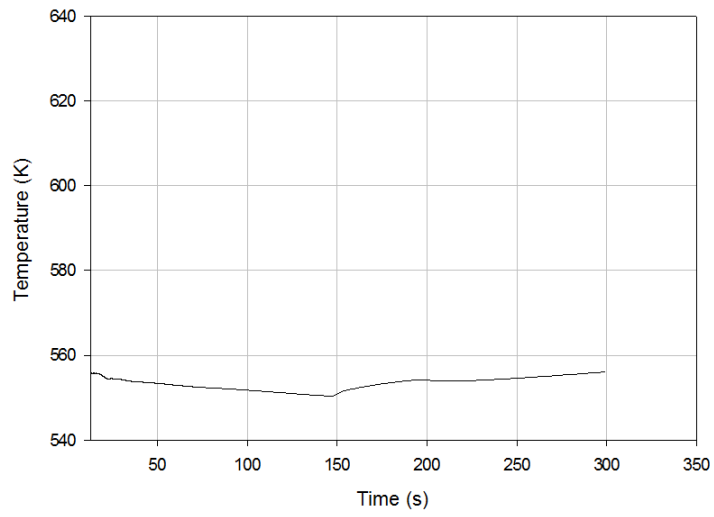


Figure 8-141: Maximal hot rod temperature

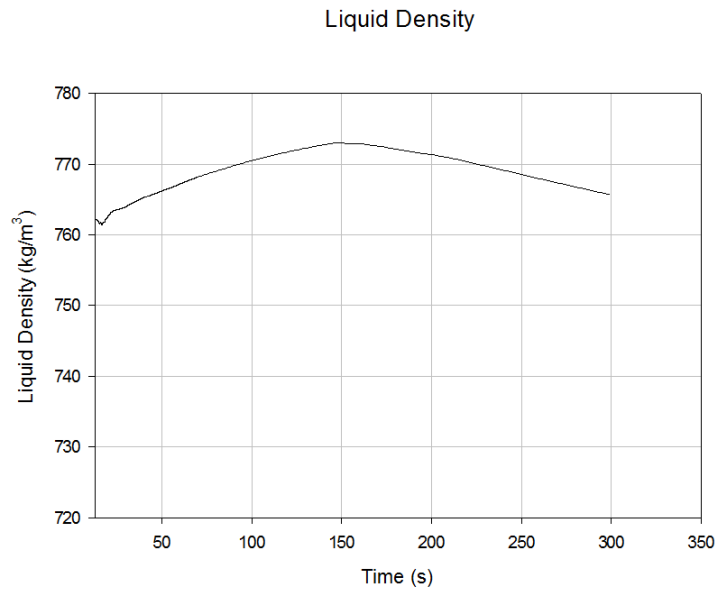


Figure 8-142: Averaged liquid density

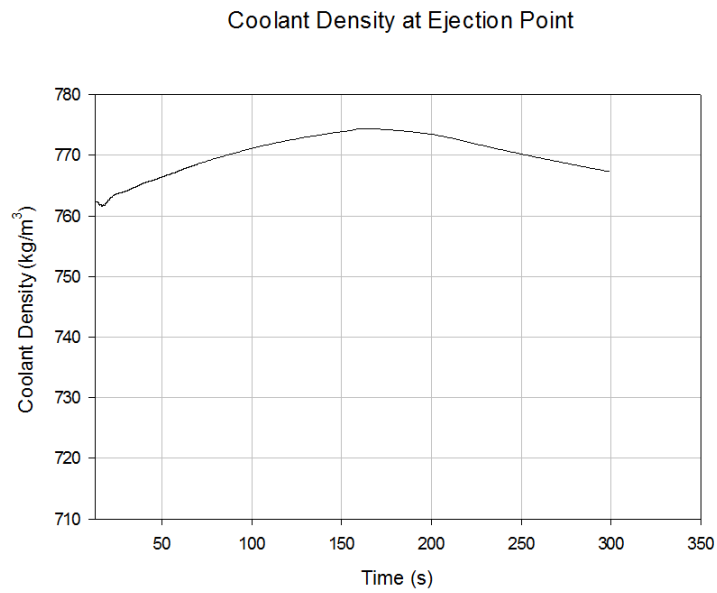


Figure 8-143: Coolant density at ejection point

Liquid Temperature

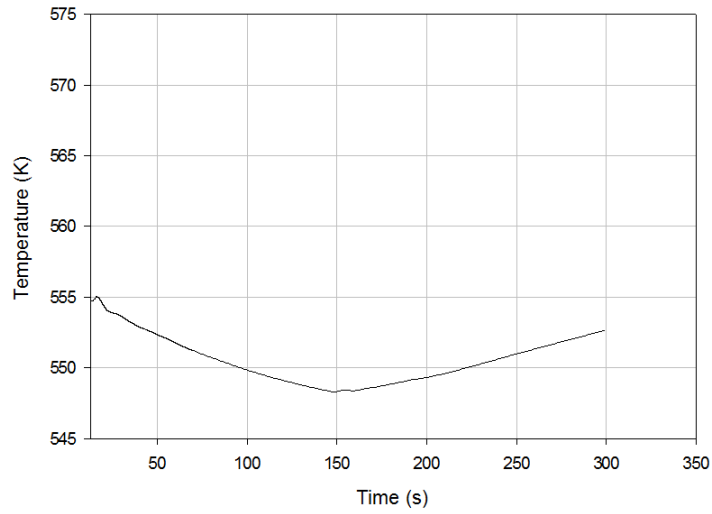


Figure 8-144: Averaged liquid temperature

Liquid Mass Flow Through Break

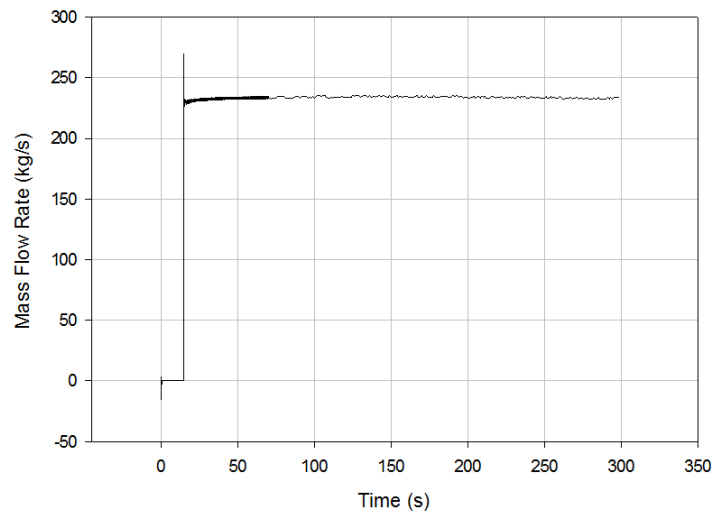


Figure 8-145: Mass flow through the break

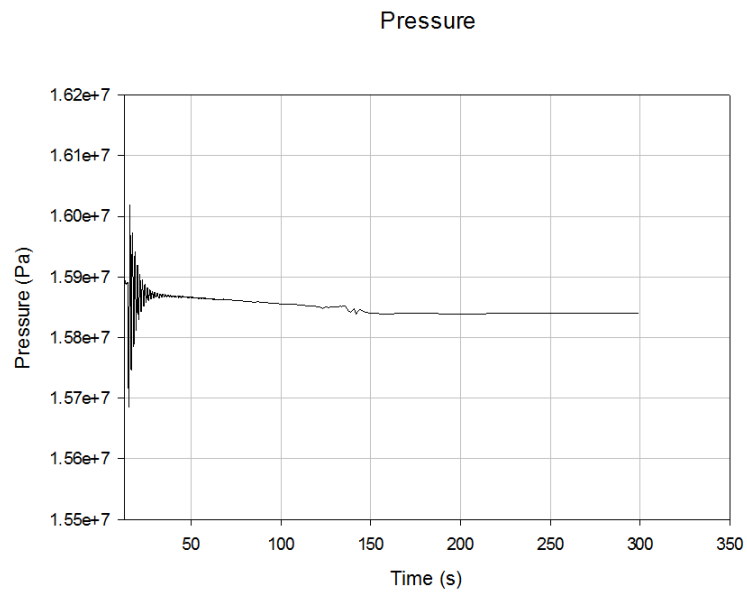


Figure 8-146: System Pressure

Chapter 9

Conclusions

The rod ejection accident scenario is labelled as a Reactivity Initiated Accident and is also considered a Design Basis Accident (DBA). The general approach is to improve the existing models and methodologies in order to increase the precision of results. This goal is being approached from two sides, first to couple different codes (neutronics with thermal-hydraulics and also with material codes) together and second to transition from 1D calculations to 3D. This is increasingly possible with the increase in computer power, which allows to run much more complex calculations.

There were two main goals to this thesis. First, to establish a methodology for coupling PARCS with TRACE for reactor with hexagonal lattice and second to run a rod ejection scenario on this coupled model. Because there are no existing analyses done on VVER 1000 reactor with coupled PARCS/TRACE, the verification of the model had to be done by comparison to similar published models. The general process was to create homogenized macroscopic cross sections for six different fuel assembly types, specifications of which were provided by the Research Centre Rez and are considered confidential. Because the cross sections are the core part of a PARCS

input, a separate verification process was chosen in order to check the cross sections. To do this, two lattice codes were used, deterministic code SCALE/TRITON and a Monte Carlo code SERPENT 2. After the cross sections were implemented into the PARCS models, the PARCS geometry definition had to be mapped with the one of TRACE. After that, a reference steady state coupled calculation was performed for each scenario separately. When the individual steady state calculations were done, the resulting restart data were inserted into the transient models. Four scenarios were considered, those were with and without SCRAM for models using either SCALE or SERPENT generated cross sections. These scenarios are a result of extensive sensitivity analysis varying several cross-section parameters such as albedo or cross sections themselves and benchmarking to the safety report of NPP Temelin, which is a VVER 100.

After comparing the results, in both stand alone steady state and coupled steady state, the results were fairly similar. However when running the transient calculation, the model using SERPENT 2 cross sections was underpowered, most likely due to the cross sections them-selves. The SCALE based model showed reasonable results with comparison with [9], however in this case the comparison is between a VVER 1000 reactor type and a generic 3-loop PWR, witch is square lattice.

There were several challenges when coupling these codes for hexagonal lattice. The major one, which costed the most time is a lack of proper guide on how to perform coupling without using graphical interface SNAP, which does not support hexagonal lattice. This issue is currently being solved with the authors of the code and hopefully a better user guide will be available in next years. Second difficulty was the absence of auto-mapping function for hexagonal lattice, which had to be substituted by a MATLAB script. This can also be a source of uncertainty, because it is difficult to be sure, the mapping was done correctly. Lastly the code itself has a significant

setback for the rod ejection calculation, which is a lack of pin power calculation for hexagonal lattice. Because of this, the power is averaged over the whole assembly and therefore is lower, than the actual value. This can be however corrected using the peak factor as done in this thesis. Currently there are alternative neutronic codes, that can be coupled with TRACE, for example DYN3D, which can be coupled not only to TRACE, but also with RELAP and ATHLET codes.

In the end, the future work to be done is firstly to improve the user guide for coupling PARCS with TRACE for hexagonal lattice. The work done in this thesis will undergo further tuning and a number of sensitivity analyses will be performed to achieve better results. Firstly a database of cross sections will be created for multiple steps in the burnup cycle and secondly the TRACE model will have to be further modified for coupling.

Bibliography

- [1] U.S. NUCLEAR REGULATORY COMMISSION. *10-CFR*,.
- [2] U.S. NUCLEAR REGULATORY COMMISSION. *NUREG-0800*,.
- [3] U.S. NUCLEAR REGULATORY COMMISSION. *TRACE V5.840*. Division of Safety Analysis, Office of Nuclear Regulatory Research, U. S. Nuclear Regulatory Commission, Washington, DC, 3.2 edition, AprilDecemberMay 2014. This is a full MANUAL entry.
- [4] T. Downar, Y. Xu, and V. Seker. *PARCS v3.2, U.S. NRC Core Neutronics Simulator*. U.S. NUCLEAR REGULATORY COMMISSION, Ann Arbor, MI, 3.2 edition, AprilDecemberMay 2014. This is a full MANUAL entry.
- [5] Yuri Chugui et. all. 3d optical measuring technologies for industrial applications. *Research Gate*, 2011.
- [6] ČEZ, 2016.
- [7] gidropress.podolsk.ru, 2016.
- [8] Marek Ruscak Guido Mazzini, Mylos Kyncl. Analyses of feed water trip with sbo sequence of vver1000 reactor. *Journal of Nuclear Engineering and Radiation Science*, 2015.
- [9] Jesus Vincente Javier Riverola, Tomas Nunez. Realistic and conservative rod ejection simulation in a pwr core at hzp, eoc with coupled parcs and relap.
- [10] Jaakko Leppanen. *SERPENT User Manual*. VTT, jun 2015.
- [11] Ph.D. Mgr. DAGMAR AUTERSKÁ. Provoz jaderneho reaktoru. University of West Bohemia, 2016.

- [12] Bruno Miglierini, Guido Mazzini, and Marek Ruscak. 3d neutronic analysis of vver1000/v-320 using parcs code. IEEE, 2014.
- [13] Bruno Miglierini, Marek Ruscak, and Guido Mazzini. Practical acquiring of the parcs code for 3D analyses of neutronic behavior of VVER1000/V320. VVER 2013 Conference, 2013.
- [14] Multiple. Bezpečnostní zpráva je temelin, safety report of NPP temelin. Internal document, 2007.
- [15] Marek Ruscak. Simulation of reactor kinetics in nuclear power plant using simulator parcs., jun 2014. Bachelor Thesis at University of Hradec Kralove.
- [16] Nuclear Tourist, 2016.

Appendix A

Glossary

Design Basis Accident A postulated accident that a nuclear facility must be designed and built to withstand without loss to the systems, structures, and components necessary to ensure public health and safety.

Design Basis Condition The range of conditions and events taken explicitly into account in the design of a facility, according to established criteria, such that the facility can withstand them without exceeding authorized limits by the planned operation of safety systems. Used as a noun, with the definition above. Also often used as an adjective, applied to specific categories of conditions or events to mean ‘included in the design basis’; as, for example, in design basis accident, design basis external events, design basis, earthquake etc.

Fuel temperature coefficient of reactivity The change in reactivity per degree of change in the temperature of nuclear fuel. The physical property of fuel pellet material (uranium-238) that causes the uranium to absorb more neutrons away from the fission process as fuel pellet temperature increases. This acts to stabilize power reactor operations. This coefficient is also known as the Doppler coefficient.